Università degli Studi di Trieste
Dipartimento di Ingegneria ed Architettura

Scienza e tecnologia dei materiali ceramici

Prof. Valter Sergo

Contributi di:
Federico Antonelli
Elisa Favero
Silvia Dalla marta

Taxonomy of Ceramics

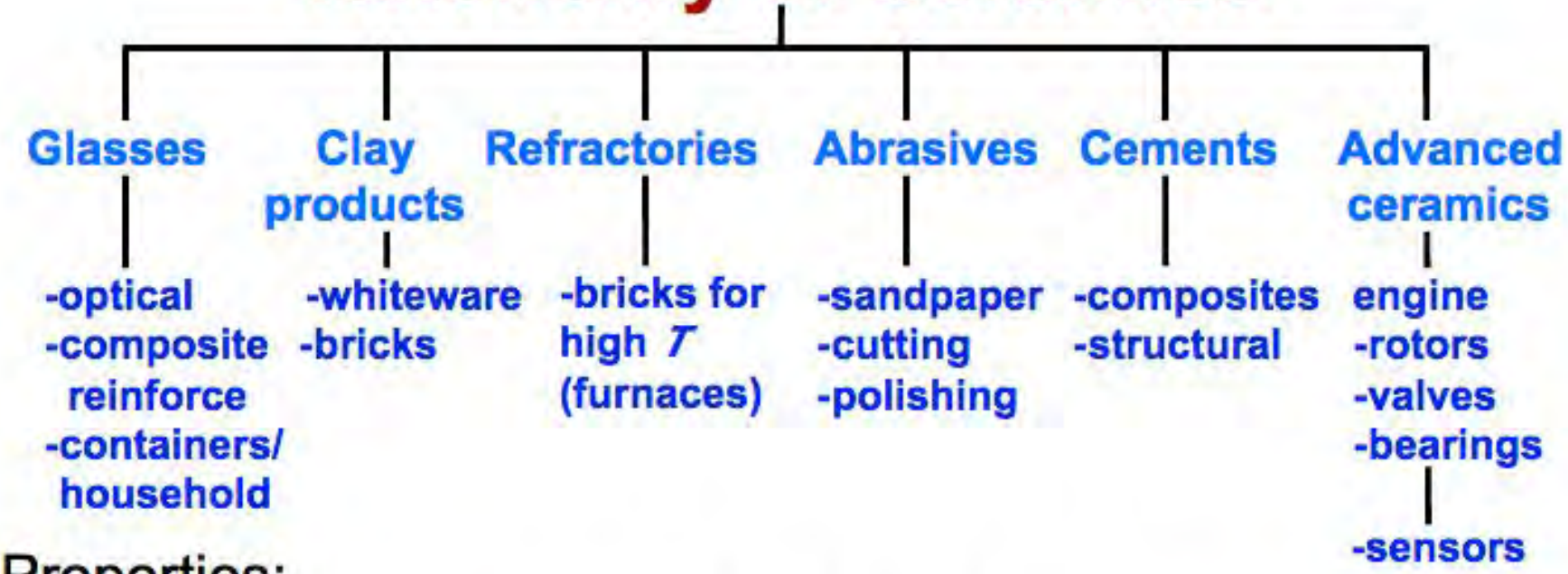

- Properties:
  -- T_m for glass is moderate, but large for other ceramics.
  -- Small toughness, ductility; large moduli & creep resist.
- Applications:
  -- High T, wear resistant, novel uses from charge neutrality.
- Fabrication
  -- some glasses can be easily formed
  -- other ceramics can not be formed or cast.

hexagonal closed-packed structure

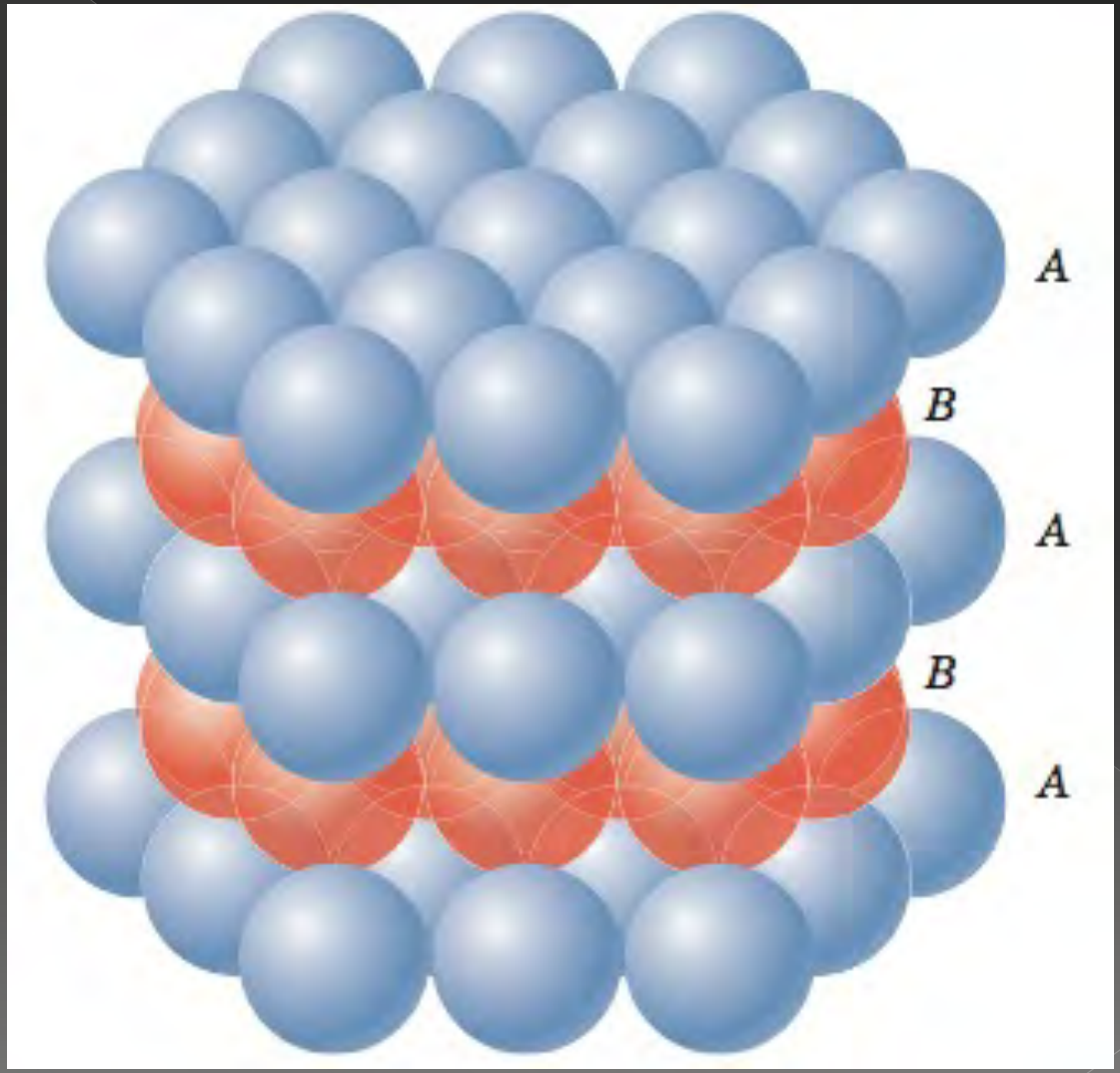

Cubic Closed-packed Structure (FCC)

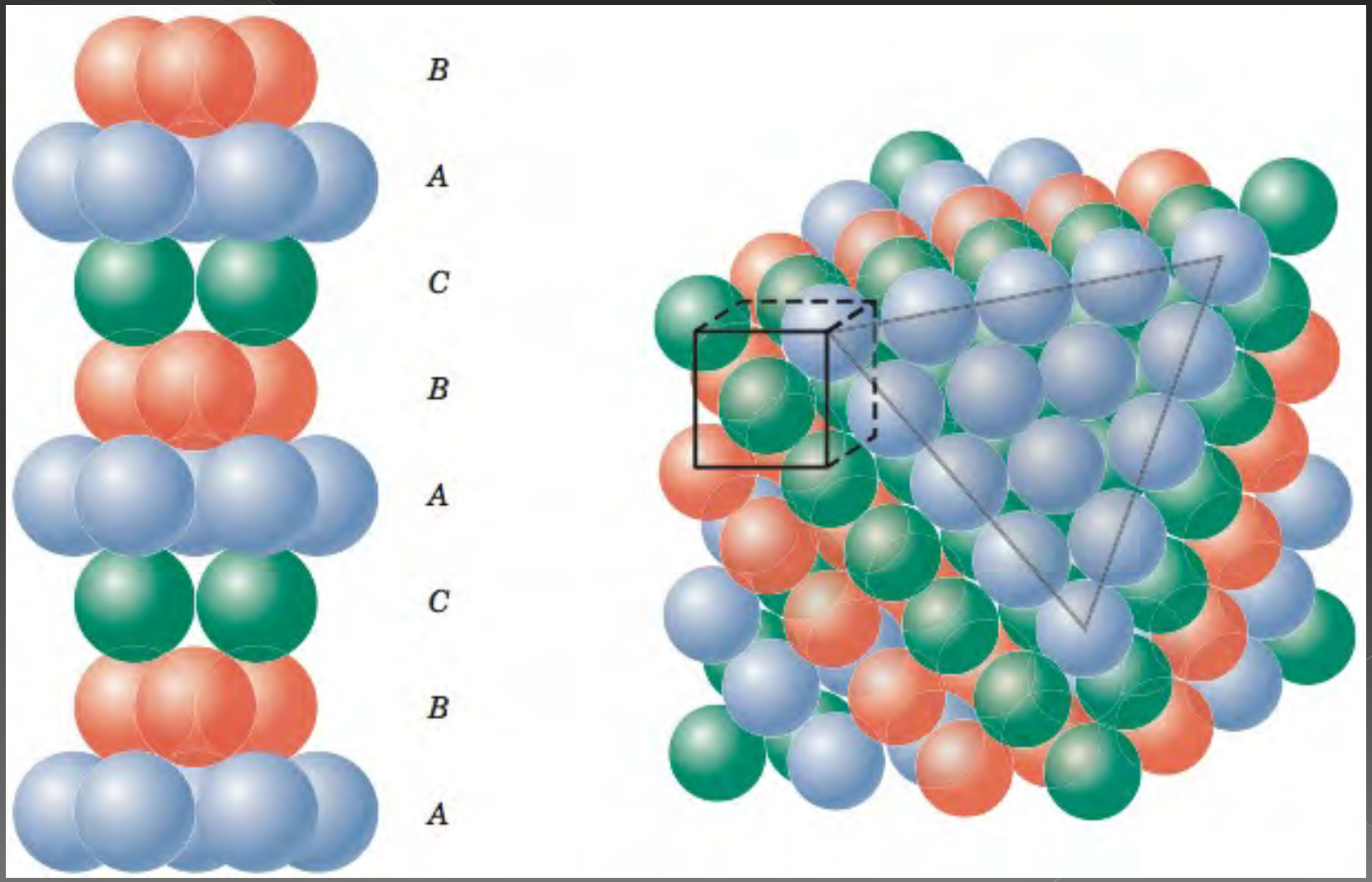

Packing of atoms determines structures

- Packing efficiency can be characterized by coordination number which depends on cation-anion radius ratio (r_c/r_a)

Cation-anion radius ratio (r_c/r_a)	< 0.155	0.155 – 0.225	0.225 – 0.414	0.414 – 0.732	0.732 – 1.000	> 1.000
Coordination number	2	3	4	6	8	12

Simple cubic

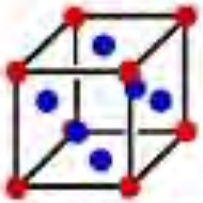

Face-centered cubic

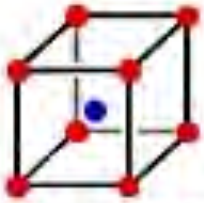

Body-centered cubic

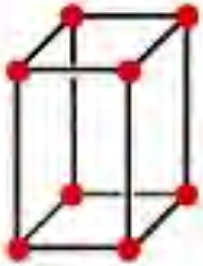

Simple tetragonal

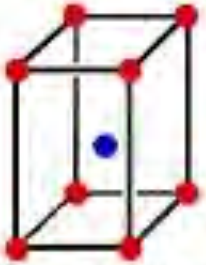

Body-centered tetragonal

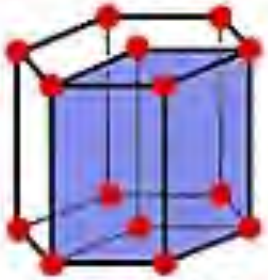

Hexagonal

Simple orthorhombic

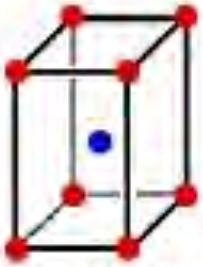

Body-centered orthorhombic

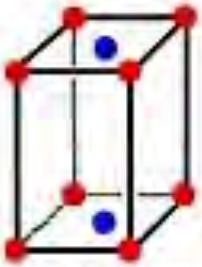

Base-centered orthorhombic

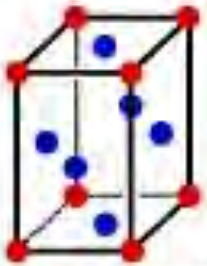

Face-centered orthorhombic

Rhombohedral

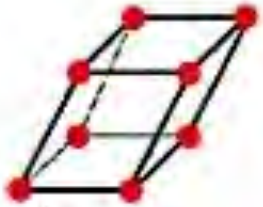

Simple Monoclinic

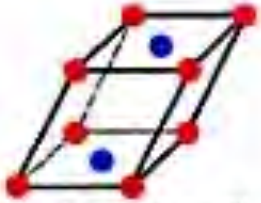

Base-centered monoclinic

Triclinic

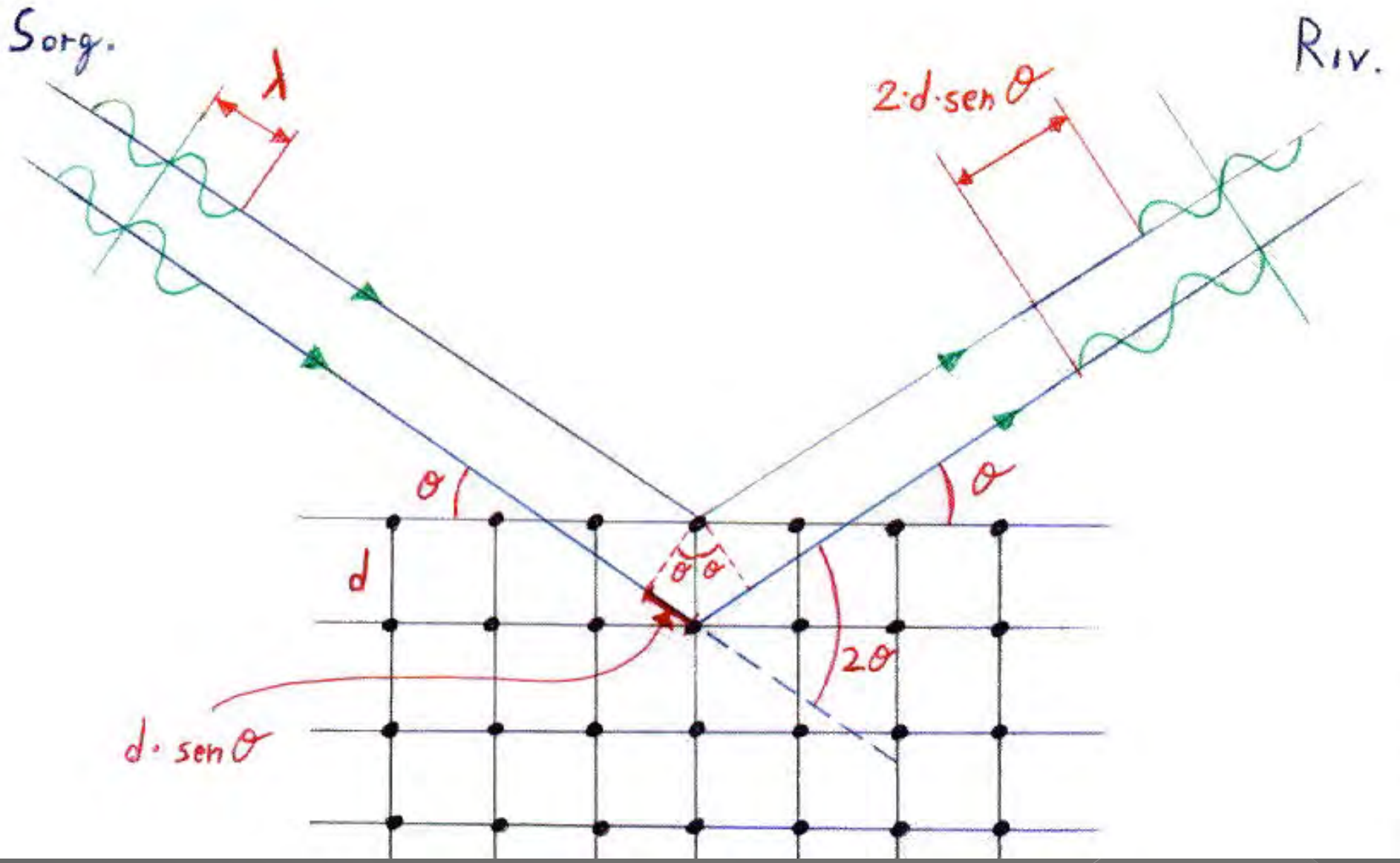
Sorg.
λ
Riv.
2·d·sen θ
θ
θ
d
θ θ
2θ
d · sen θ

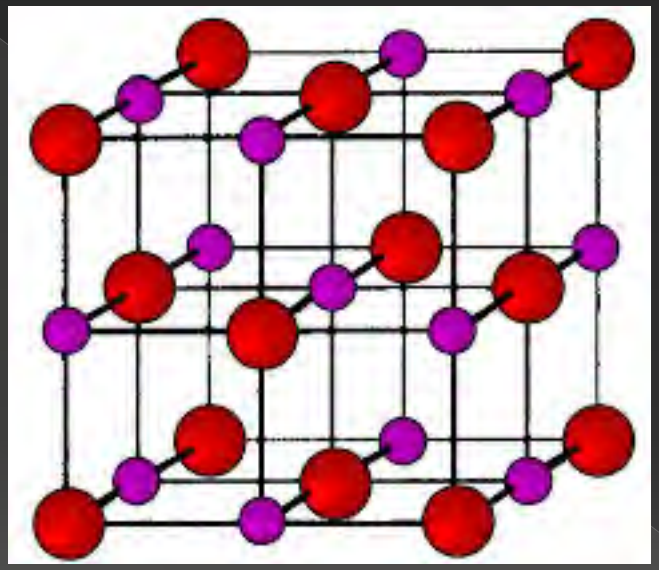

Rock Salt: MgO, CaO, NiO

ROCKSALT (NaCl)

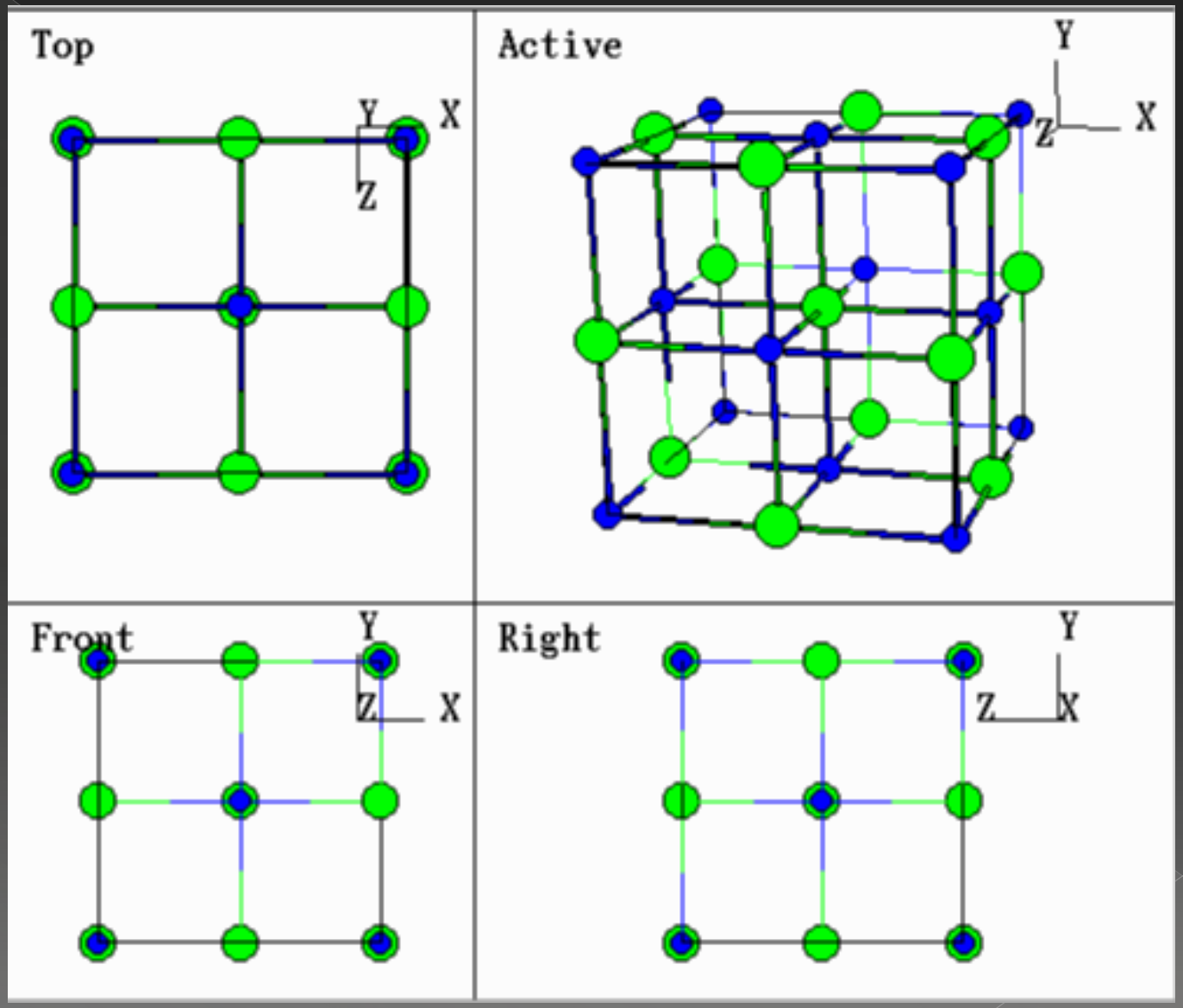

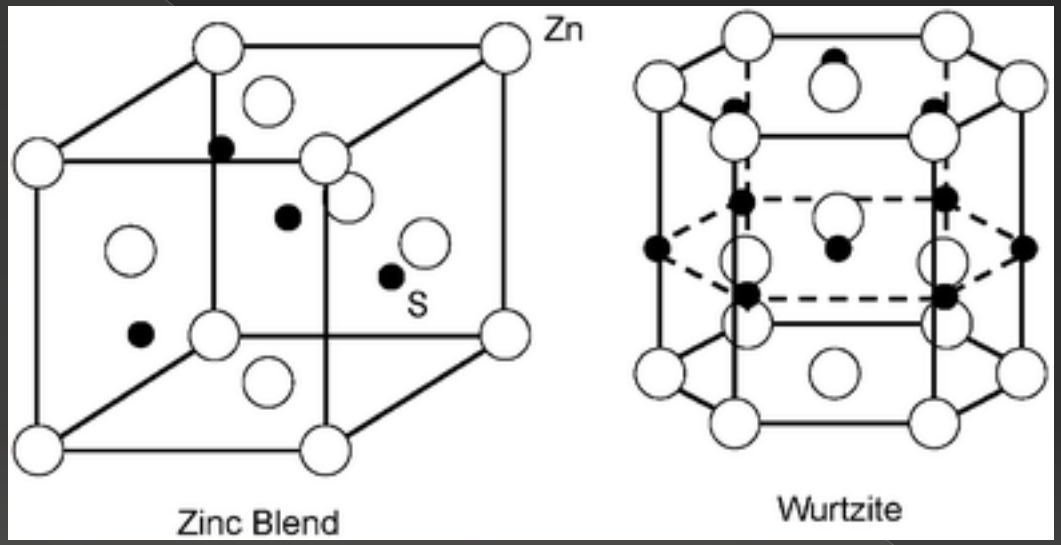

Zinc Blend and wurtzite: ZnO, SiC, BeO

WURTZITE [(Zn,Fe)S]

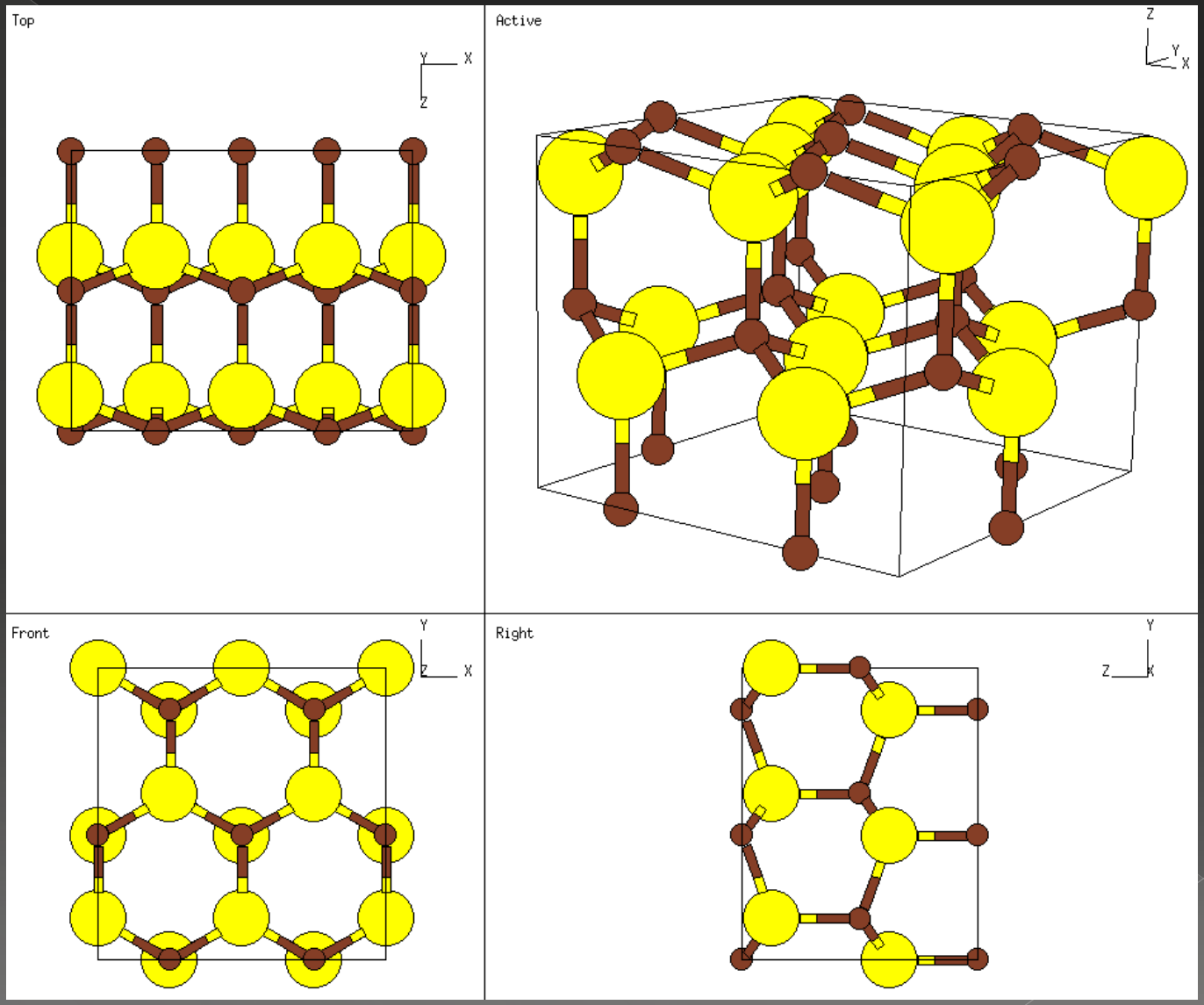

SPHALERITE [(Zn,Fe)s]

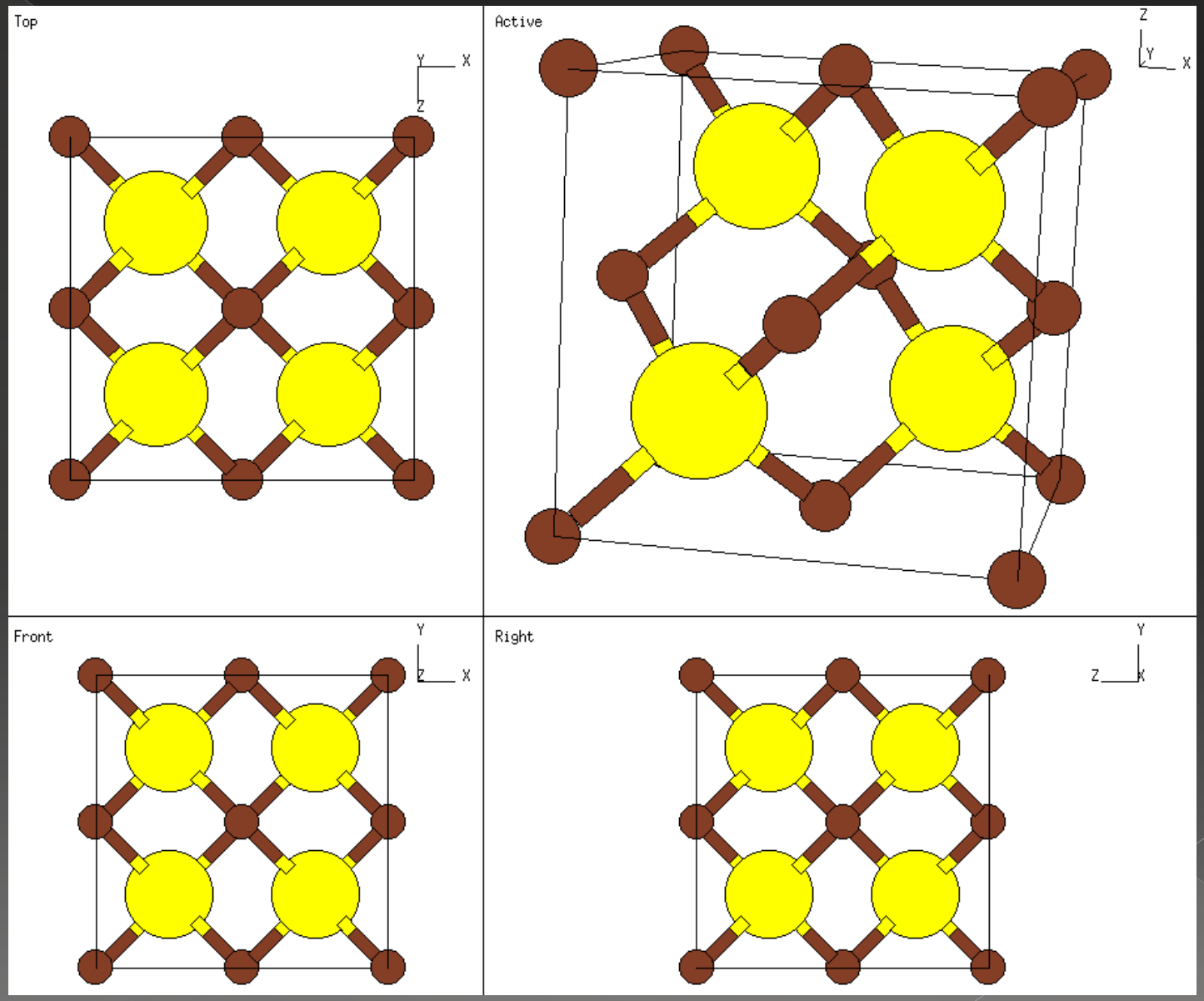

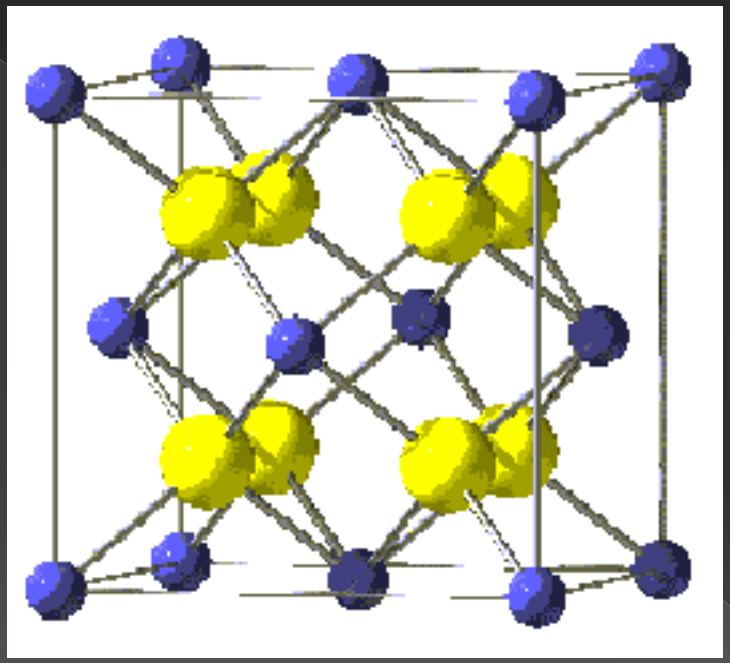

Fluoride struture: ZrO_2, CeO_2, UO_2

FLUORITE (CaF_2)

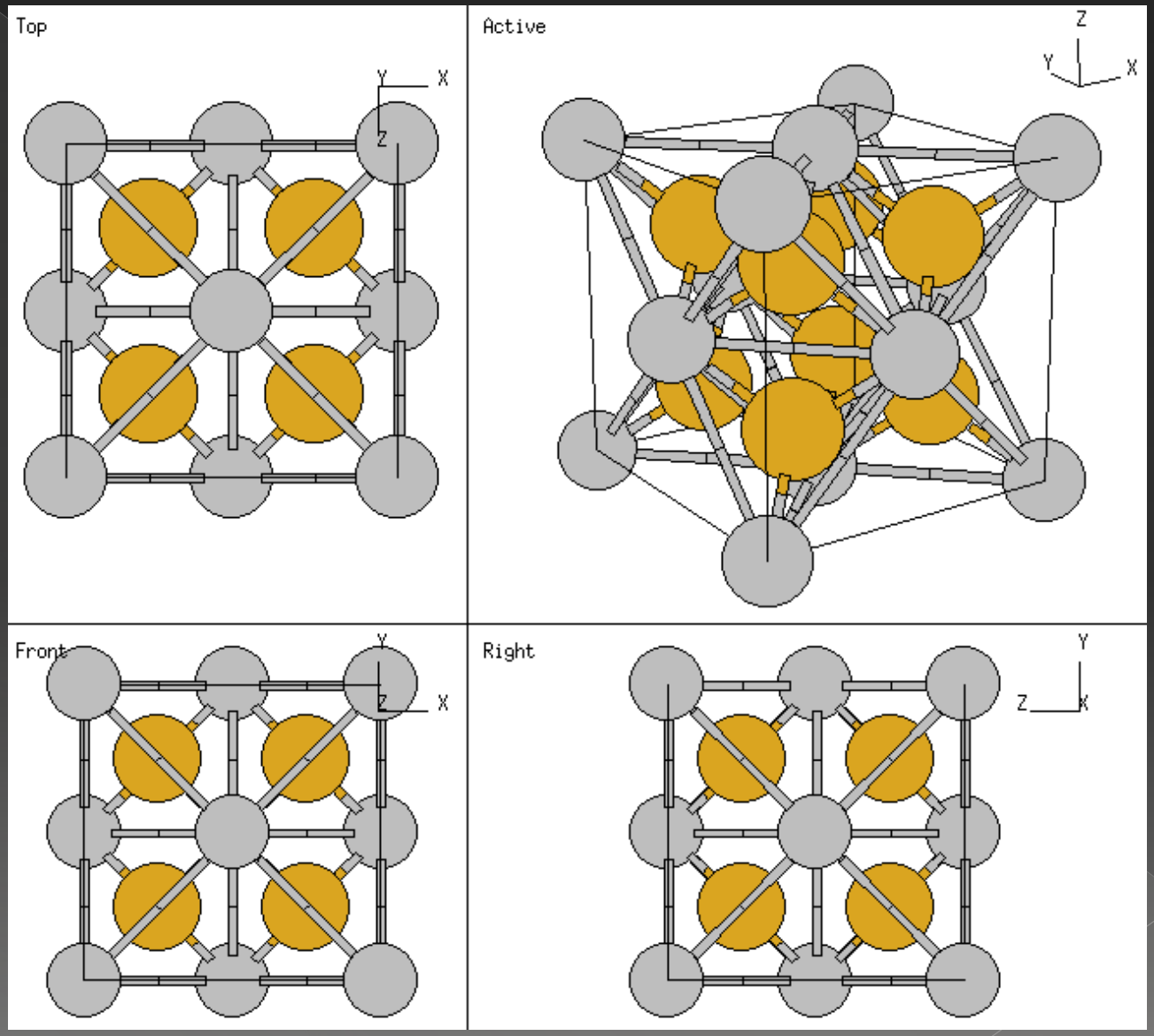

CORUNDUM (Al_2O_3 - α)

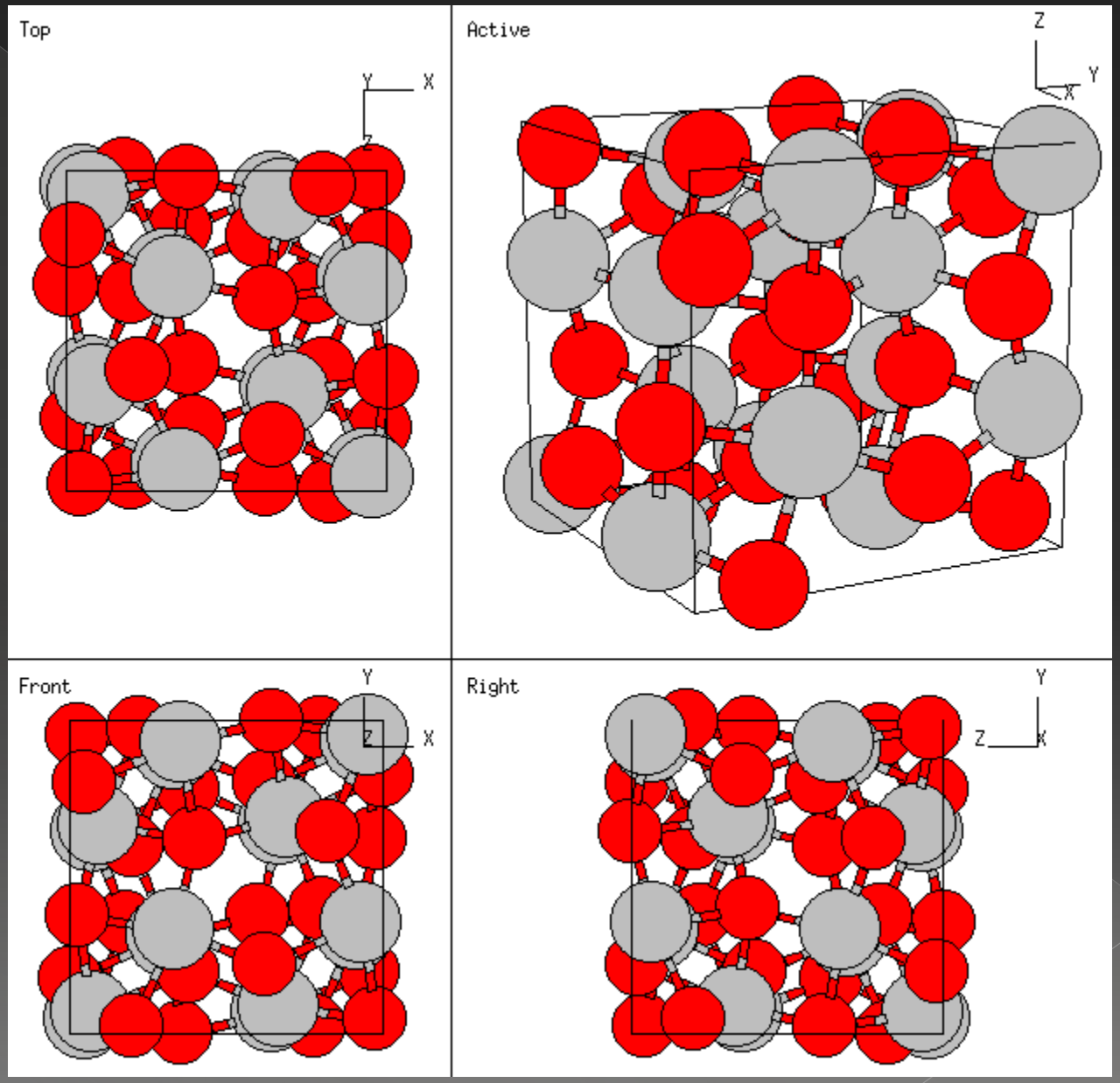

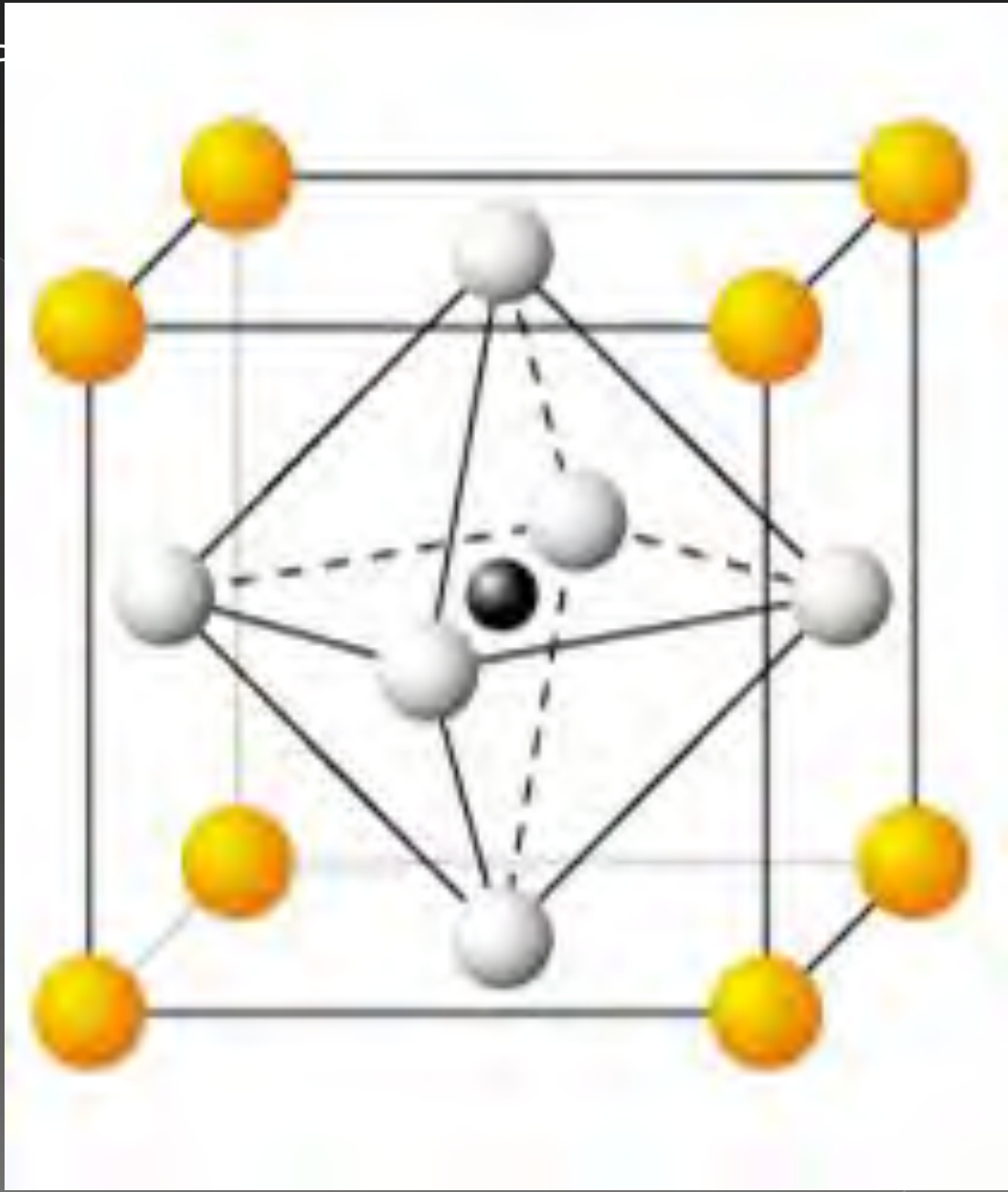

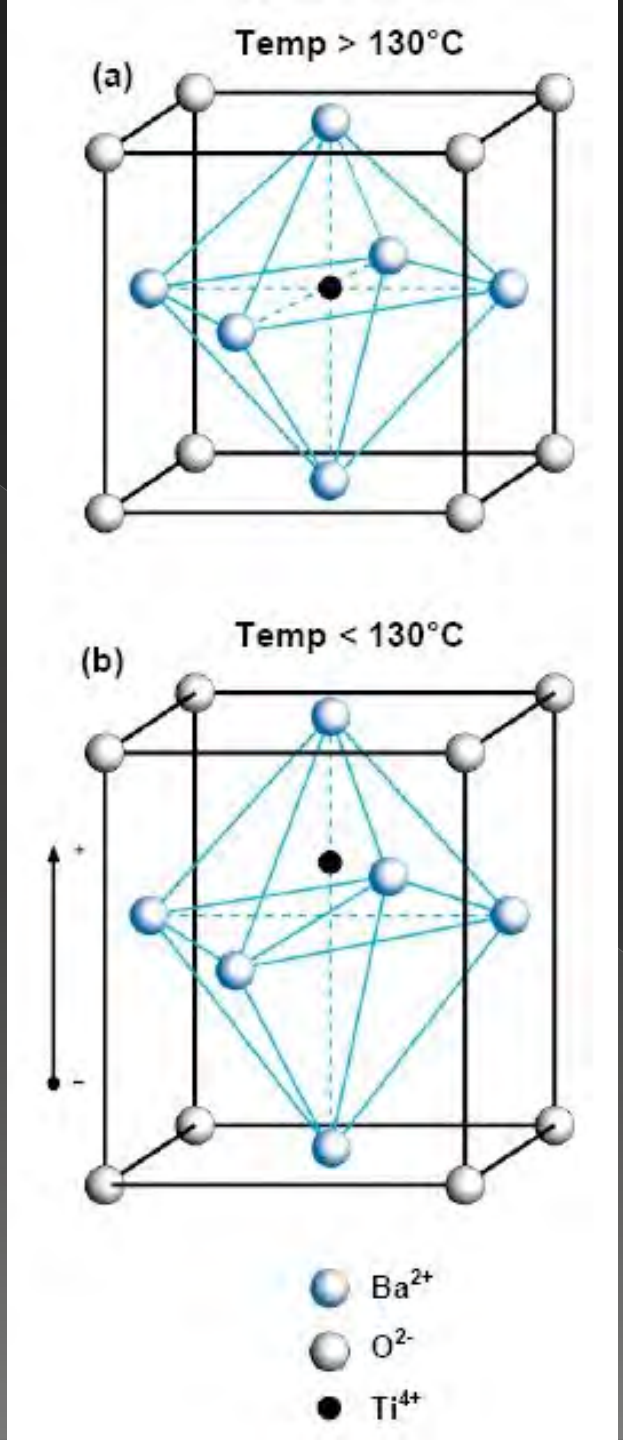
Temp > 130°C
(a)
Temp < 130°C
(b)
+
-
Ba^{2+}
O^{2-}
Ti^{4+}

Cubic Body Centered

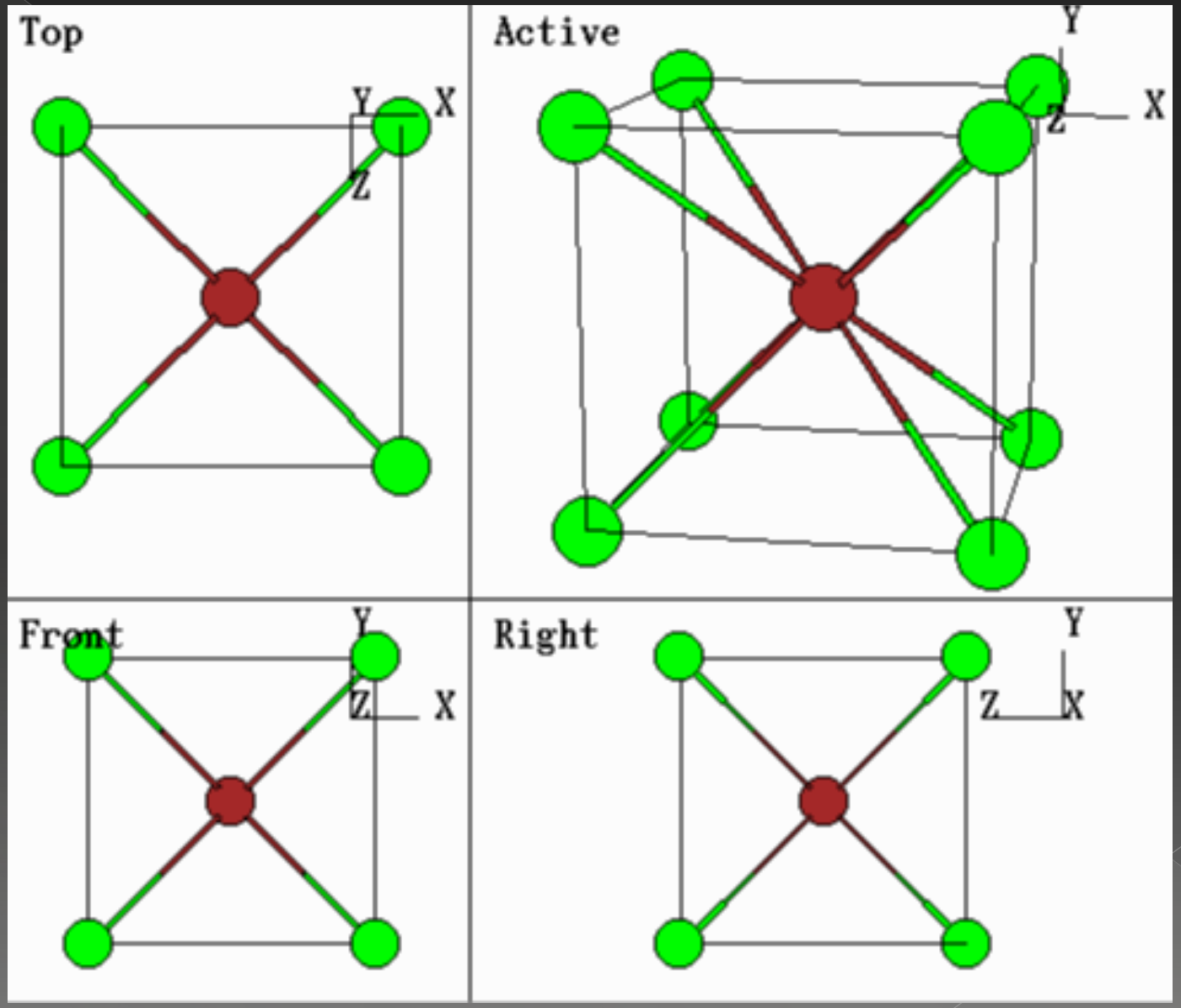

PEROVSKITE ($CaTiO_3$)

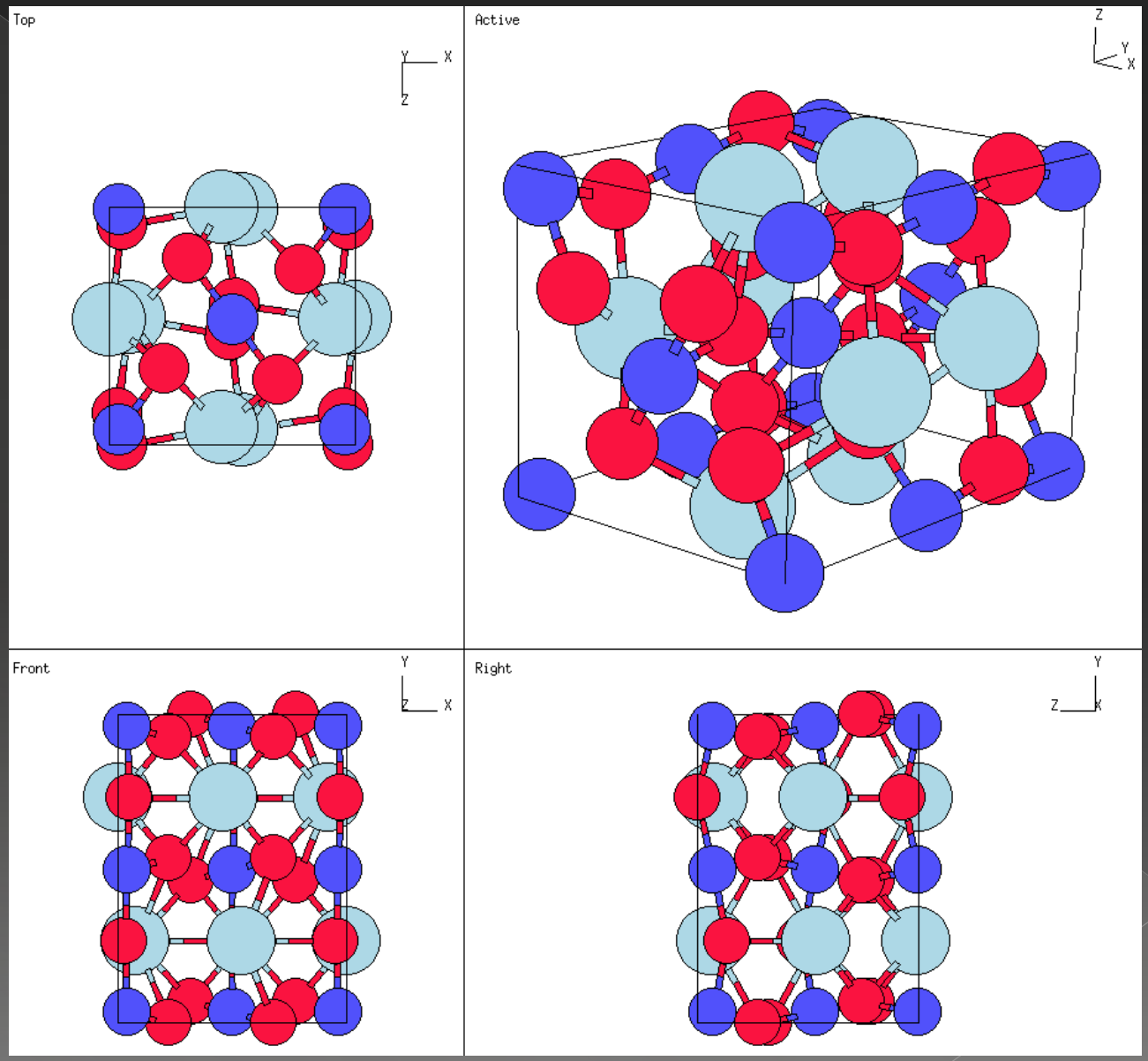

Kröger – Vink Notation

- Proposed in 1956 by F.A. Kröger and H.J. Vink in the journal *Solid State Physics* (*F.A. Kröger, H.J. Vink, Relations between the Concentrations of Imperfections in Crystalline Solids, Solid State Physics, Volume 3, 1956, 307-435*)
- Set of conventions used to describe lattice position and electric charge for point defects in crystalline structures
- The key concept is the crystal lattice to consist of POSITIONS and ATOMS

Vacancy

- There can be <u>unoccupied</u> positions :

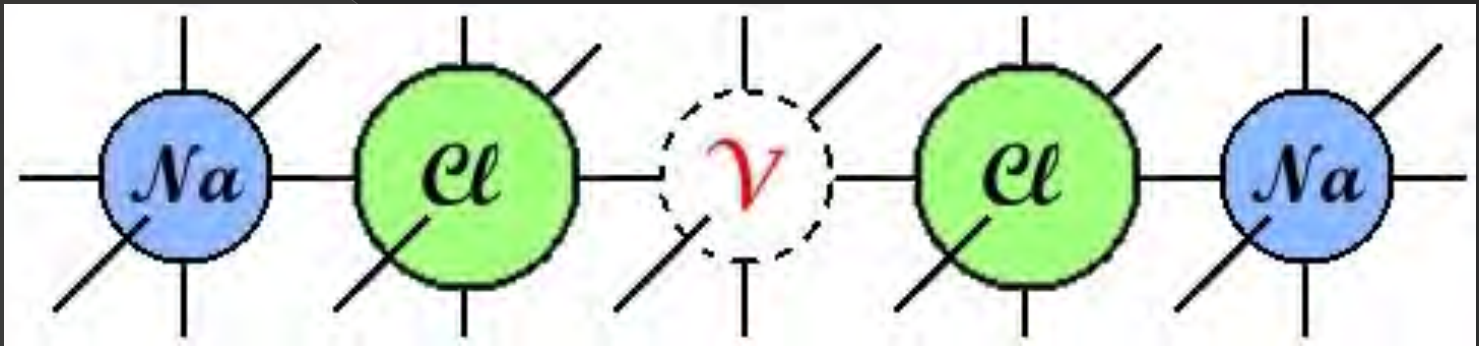

these empty positions are called **VACANCIES**

- In the picture, there is a Na vacancy, which is symbolized by:

$$V_{Na}$$

Vacancy & Charge

- However, like ions, also vacancies have charge:
  e.g. proceeding with the previous example, the absence of a ion Na^+ leads to a lack of positive charge, meaning a *negative charge* concentration!

- **Vacancies have always OPPOSITE CHARGE to the missing ion**

Charge

- $'$ → negative charge e.g. $V_{Na}^{'}$
- $\bullet$ → positive charge e.g. $V_O^{\bullet\bullet}$ [Oxygen vacancy with 2 (+) charges]
- $\times$ → neutrality e.g. $Cl_{Cl}^{\times}$

(neutrality may be unexpressed)

Substitutional defect

- An atom or a ion can be replaced by another:

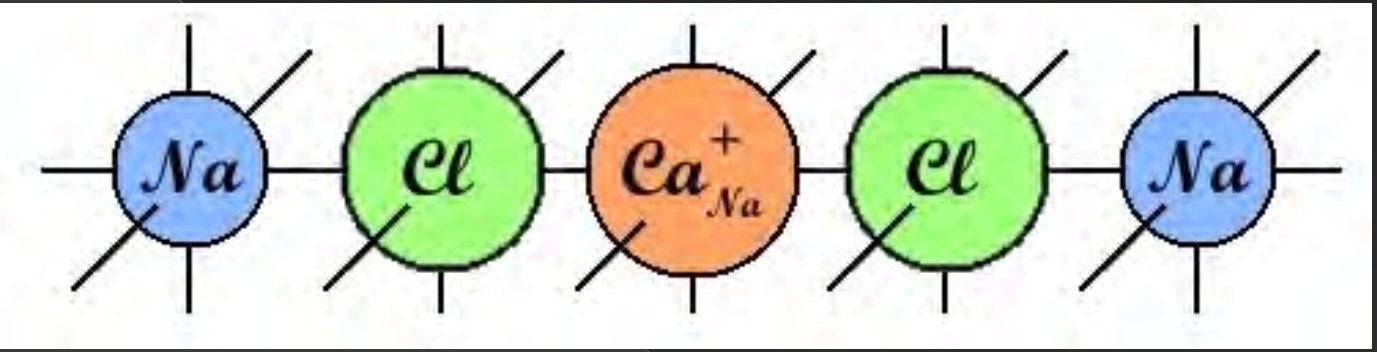

- The Ca ion took the place of the Na ion, which is symbolized by:

$$Ca_{Na}$$

- As Ca ion has 2 (+) charges, while Na ion has only 1 (+) charge, there is a total 1 (+) charge, so:

$$Ca_{Na}^{\bullet}$$

Interstitial defect

- An atom or a ion can be present on any site that would be unoccupied in a perfect crystal, as is typical for H^+ ions in metallic lattice:

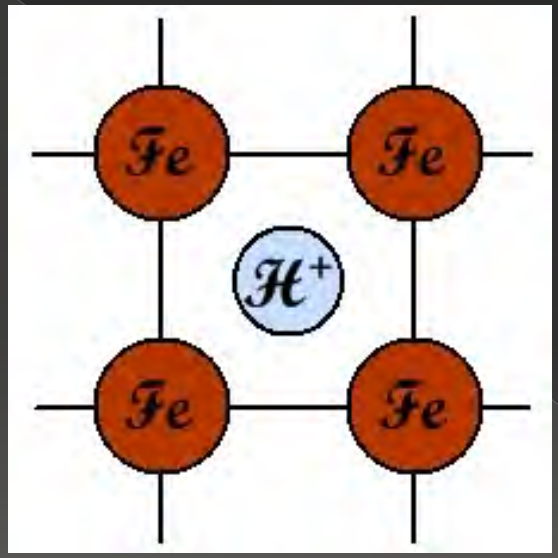

- Interstitial H^+ ion in Fe lattice is symbolized by:

$$H_i^{\bullet}$$

Pure electric charge

pure electric charges

- electrons
- "holes"

- electron: $e^{|}$
- hole: $h^{\bullet}$

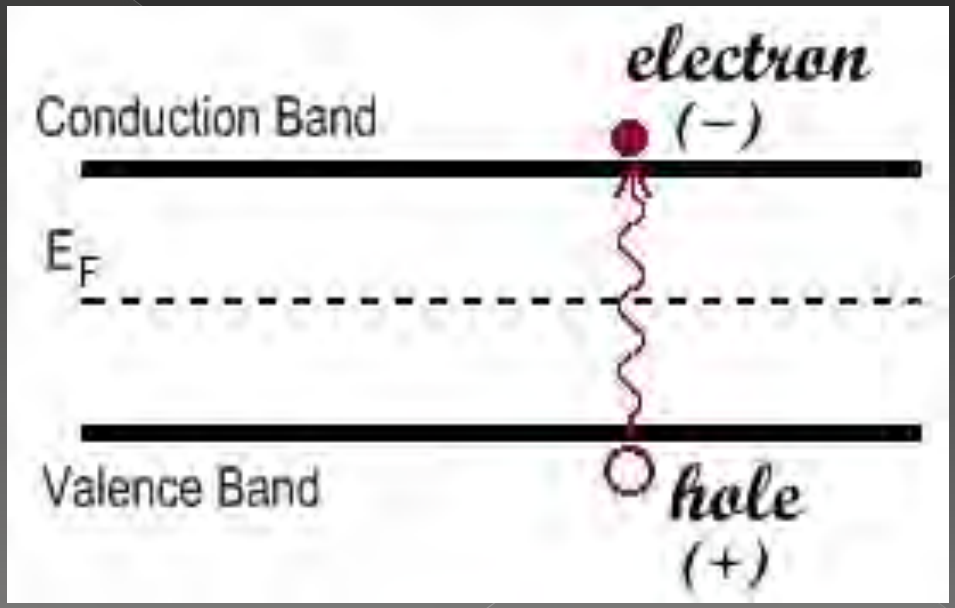

Quasi – Chemical Approach

to defect formation

- Apply Chemical Equilibrium concepts to solid dissolutions of a substance into another
- In order to be able to describe (hence with predictive purposes also) defects formation "reactions"

RULES for defect formation "reactions"

1) **SITE BALANCE,**

2) **MASS BALANCE,**

3) **CHARGE BALANCE.**

Given a generic compound $M_A X_B$:

- **SITE BALANCE**: at equilibrium the ratio of #M SITES (NOT actual atoms) to #X SITES must always be preserved
  - So, creating anionic sites must lead to the creation of cationic sites as well (and vice versa) **IN THE RIGHT RATIO**
- **MASS BALANCE**: defect formation reactions can't create nor destroy mass
- **CHARGE BALANCE** (Electro Neutrality Condition): preservation of crystal global neutrality
  - So, there can't be reactions which leave the crystal charged
  - So, the total sum of negative electric charges must be equal to total sum of positive charges

Defects

Perfect Crystal

- Crystal which has a completely ordered structure with atoms at rest and electrons distributed in the lowest possible energy states.
- But *REAL* crystals contain a variety of imperfections, or *defects*.
- In crystalline ceramics the structure and chemistry of the material will be determined by the kinetics of defect movement.

Defects

- What is special about ceramic defects is that they can be *charged*, while metals cannot.
- *DEFECT HIERARCHY*: defects are often classified in terms of a dimensionality: 0D, 1D, 2D, or 3D.

"Dimension"	Defect
0	Point defects
1	Line defects
2	Surfaces Grain boundaries Phase boundaries
3	Volume defects

- NB: In spite of the classification, ALL these defects are three-dimensional!

Point defects

- Point defects are particularly important in ceramics because of the role they can play in determining the properties of a material.

  e.g. the entire semiconductor industry is possible because of minute concentrations of point defects that are added to Si (dopants determine the whole material electrical properties: if it's n-type, p-type, or semi-insulating).

Point defects

- Types of point defects:
  - ***Misplaced atoms*** & ***Solute atoms*** (*substitutional defects*: atoms or ions are replaced by others),
  - ***Vacancies*** (empty positions),
  - ***Interstitials*** (atoms or ions present on any site that would be unoccupied in a perfect crystal),
  - ***Electronic defects*** (electrons and holes),
  - ***Associated centers*** (two point defects which interact so that they can be considered as a single defect; if more atoms are involved, they would be called a *defect cluster* or a *defect complex*).

Solid Solutions

- If a material crystallizes in the presence of foreign atoms, their inclusion in the main crystalline structure could:
  - *Increase* significantly system's energy ⇒ foreign atoms would be almost completely *excluded* from forming crystalline structure
  - *Decrease* considerably system's energy ⇒ there would be the development of a *new crystalline form*
  - In intermediate cases, foreign atoms would fit in a random way in the forming crystalline structure ⇒ *SS*
- SS are stable, of course, when the mixed crystal has a lower $\Delta G_{formation}$ than the other 2 alternatives.

Let's try to apply Quasi – Chemical Approach rules to 2 real instances:

SS of calcium chloride ($CaCl_2$) in sodium chloride ($NaCl$), which we would assume as a perfect crystal:

- First of all, SS of $CaCl_2$ in $NaCl$ is indicated as follows:

$$CaCl_2 \xrightarrow{NaCl}$$

- MASS BALANCE:

$$CaCl_2 \xrightarrow{NaCl} Ca_{Na} + 2Cl_{Cl}$$

- CHARGE BALANCE: being Ca^{++} the cation, it would probably substitute host Na^{+} cations, leading to an exceeding (+) charge $\Rightarrow$ adding charges to previous equation:

$$CaCl_2 \xrightarrow{NaCl} Ca_{Na}^{\bullet} + 2Cl_{Cl}^{\times}$$

but this equation doesn't balance charges!! So…

- SITE BALANCE: in this example the right ratio anionic/cationic sites is 1:1: our equation doesn't balance lattice sites neither! So…

$$CaCl_2 \xrightarrow{NaCl} Ca_{Na}^{\bullet} + 2Cl_{Cl}^{\times} + V_{Na}^{|}$$

REMARKS:

- All balances are related to a *perfect*, *neutral* crystal.
- Having charge separation, we expect the new crystal to be a better conductor…
- The equation we wrote gives us a better knowledge of the system in an atomic scale:

  e.g. we could represent it as:

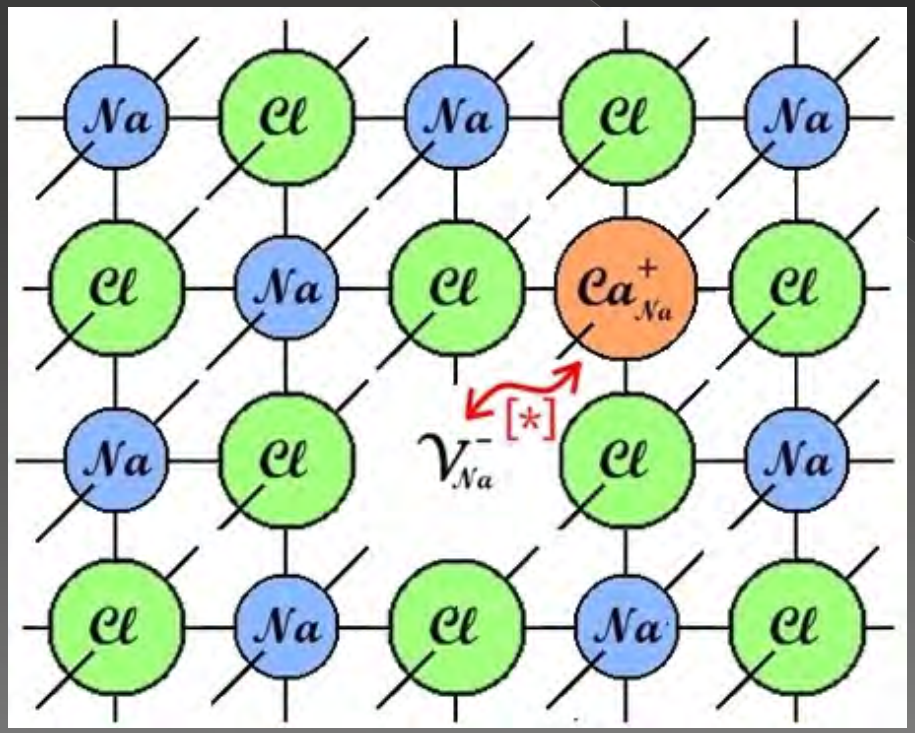

[*] close enough to balance charges!

SS of titania (TiO_2) in magnesia (MgO), which we would still assume a perfect crystal

- Mg has a double valence, while Ti has 4 (+) charges…

$$TiO_2 \xrightarrow{MgO} Ti_{Mg}^{\bullet\bullet} + 2O_O^{\times} + V_{Mg}^{''}$$

Schottky Disorder

- Simultaneous anionic and cationic vacancies.
- Total stoichiometry of the solid isn't compromised by Schottky disorders, because the number of empty M and X sites is balanced as to preserve local electro neutrality.
- Opposite charged vacancies tend to associate (they carry an *effective* charge), so they'd never be too far-away from one another.
- Schottky disorder formation "reaction":

$$\varnothing \xrightarrow{MgO} V_{Mg}^{''} + V_{O}^{\bullet\bullet}$$

Schottky Disorder

- This is a common defect in *alkali halides* at high T.
- In oxides vacancies $\Delta G_{formation}$ is 2x-3x $\Delta G_{formation}$(alkali halides), so at equilibrium the number of S. disorders in not relevant until very high T.

Frenkel Disorder

- Auto-interstitial defect: there is the same number of reticular vacancies and interstitial atoms, cause reticular atoms migrate in interstitial positions.

$$Ti_{Ti} \xrightarrow{TiO_2} V_{Ti}^{''''} + Ti_i^{\bullet\bullet\bullet\bullet}$$

- e.g. halide: $AgBr$ $\quad Ag_{Ag} \xrightarrow{AgBr} V_{Ag}^{'} + Ag_i^{\bullet}$

- e.g. oxide: Y_2O_3 $\quad O_O \xrightarrow{Y_2O_3} V_O^{''} + O_i^{\bullet\bullet}$

Frenkel Disorder

- This is a common defect in:
  - Crystals with *fluorite structure*, which has large interstitial sites.
  - Crystals with high polarizable ions, which can in an easier way set up in interstitial sites.
- The energy change for F. disorder formation depends strongly on reticular structure and ion characteristics.

Some more examples

SS of TiO_2 in MgO

- We wrote

$$TiO_2 \xrightarrow{MgO} Ti_{Mg}^{\bullet\bullet} + 2O_O^{\times} + V_{Mg}^{''}$$

for substitutional SS, but it could be also an interstitial SS:

$$TiO_2 \xrightarrow{MgO} Ti_{Mg}^{\bullet\bullet} + O_i^{''} + O_O^{\times}$$

- Which one is better?

- Evaluate ΔG° and choose the favorite!
- Usually it is $\Delta G_i >> \Delta G_V \Rightarrow$ easier formation of vacancies than interstitials.

SS of TiO_2 in MgO

- This specific instance follows that general rule, too, as the passage of atoms to interstitial positions requires quite high energies:

$$\Delta H_i >> \Delta H_V$$

- $\Rightarrow$ almost the entire part of defects will be substitutional:

$$TiO_2 \xrightarrow{MgO} Ti_{Mg}^{\bullet\bullet} + 2O_O^{\times} + V_{Mg}^{\prime\prime}$$ ✓

$$TiO_2 \xrightarrow{MgO} Ti_{Mg}^{\bullet\bullet} + O_i^{\prime\prime} + O_O^{\times}$$ ✗

Zirconia doped with calcia

- There are, again, 2 possibilities:

① $2CaO \xrightarrow{ZrO_2} Ca_{Zr}^{''} + 2O_O^{\times} + Ca_i^{\bullet\bullet}$

to mantain constant the ratio anionic/cationic sites in zirconia's reticulum
(of course interstitial is *not* considered to this aim)

② $CaO \xrightarrow{ZrO_2} Ca_{Zr}^{''} + O_O^{\times} + V_O^{\bullet\bullet}$

- Zirconia has a Fluorite structure ⇒ lots of empty space inside ⇒ interstitials are *not* automatically privileged…
- So??

Zirconia doped with calcia

- Let's consider the profiles of density in function of mole % of CaO in ZrO_2 (at T_{amb}):

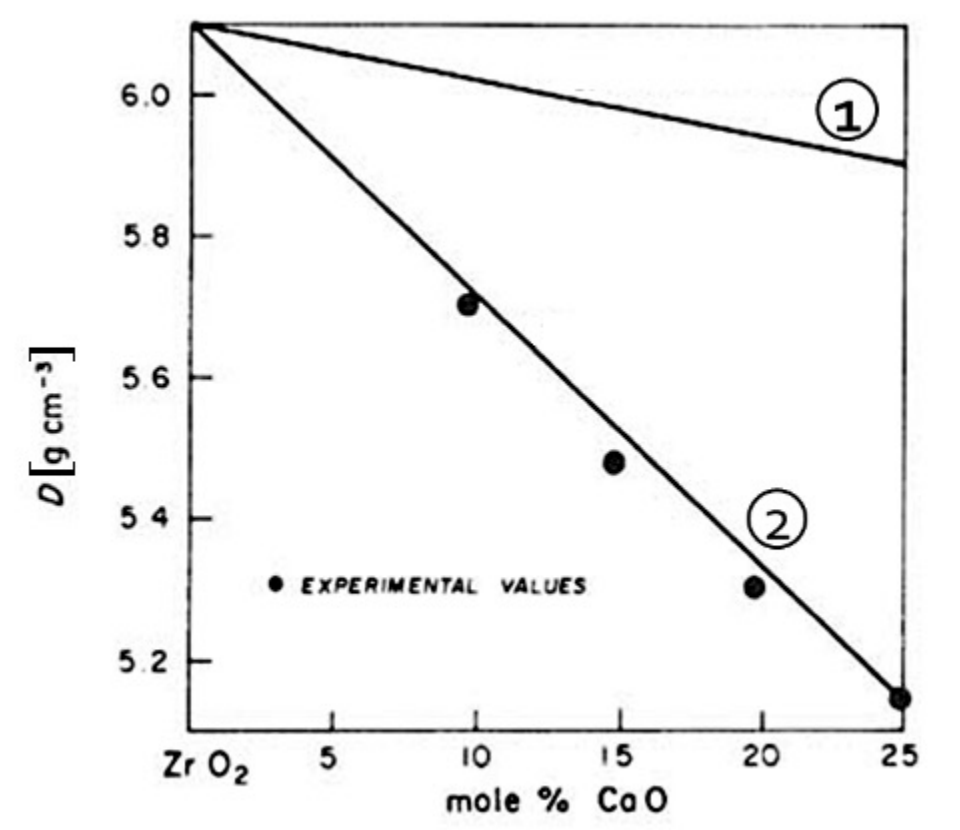

- Experimentally, reaction ② is the favourite.

Lambda sensor (or oxygen sensor)

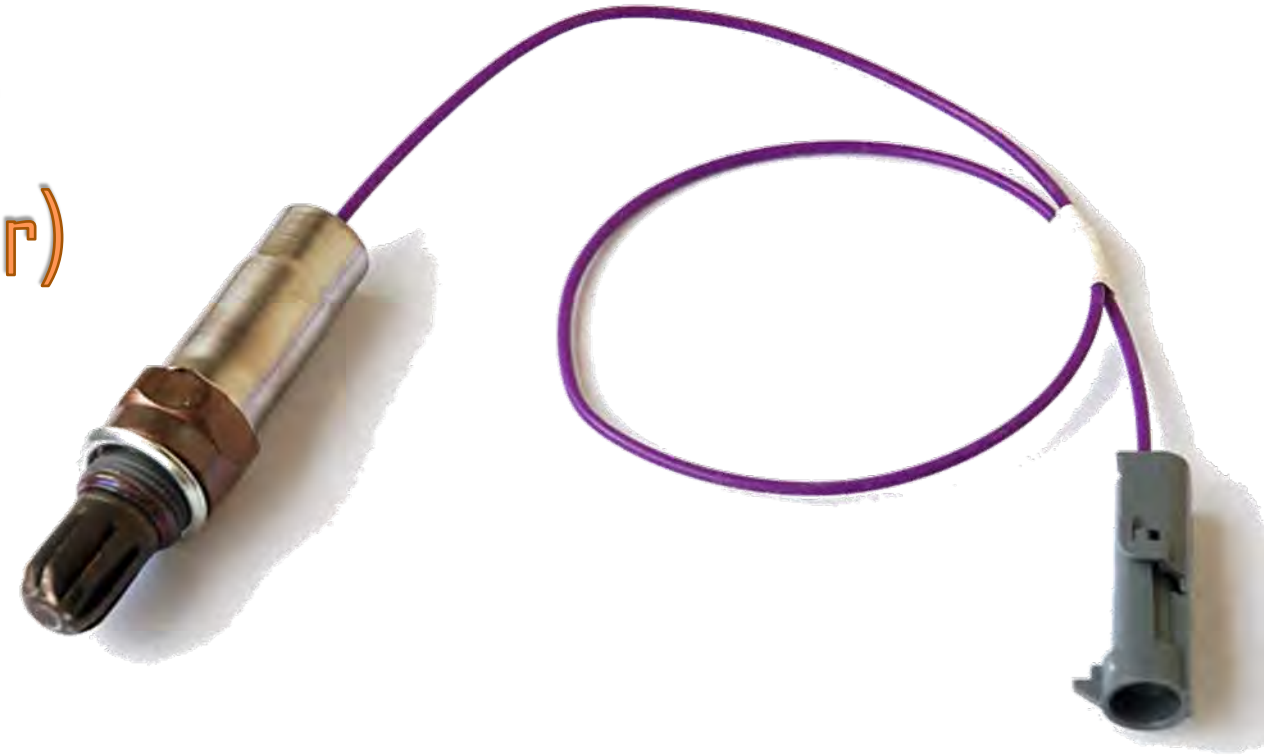

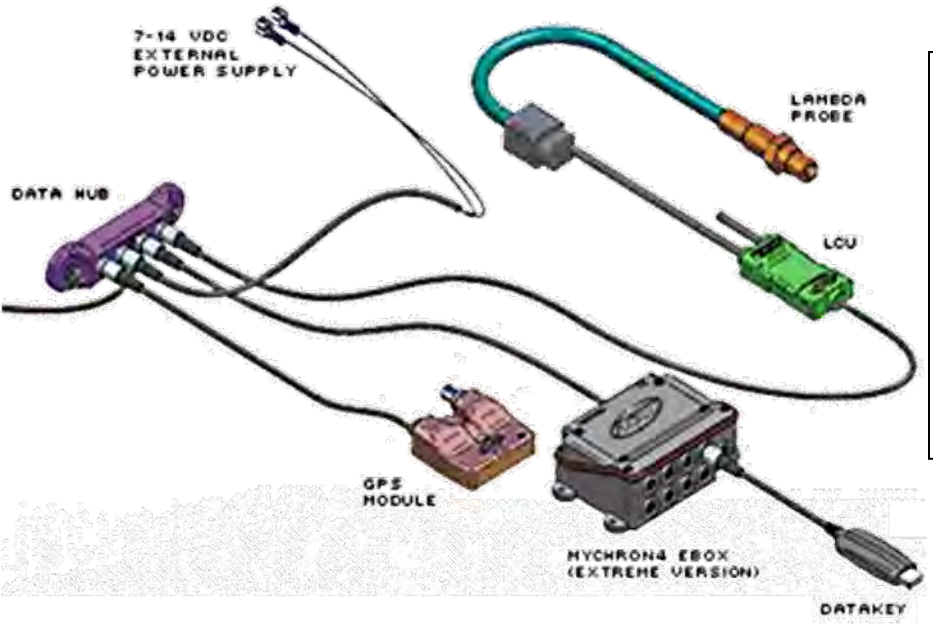

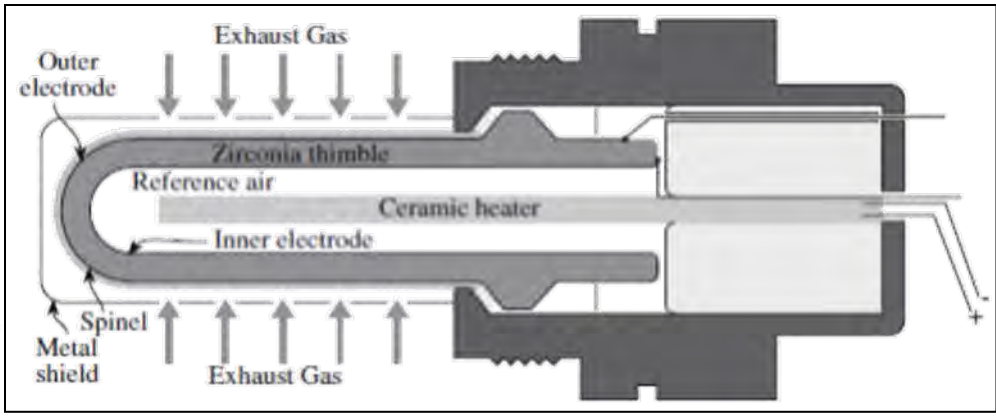

Zirconia doped with yttria

$$Y_2O_3 \xrightarrow{ZrO_2} 2Y_{Zr}^{'} + V_O^{\bullet\bullet} + 3O_O^{\times}$$

- Applications of *pure* zirconia are restricted because it shows *polymorphism*:
  - It is ***monoclinic*** at room temperature
  - Changes to the denser ***tetragonal*** phase from circa 1000 °C.
- The phase change t-ZrO_2 ⇆ m-ZrO_2 shows a large change in volume (ΔV=5%) which causes *extensive cracking*.
- The addition of some oxides (like CaO, Y_2O_3) results in (meta)stabilizing the t-phase (or c-phase) at room temperature.

Yttria-stabilized Zirconia

Cubic zirconia (or CZ) : hard, optically flawless and usually colorless (but may be made in a variety of different colors).
Single crystals of the cubic phase of zirconia are commonly used as diamond simulant in jewellery.

Magnesia doped with lithium fluoride

$$LiF \xrightarrow{MgO} Li_{Mg}^{'} + F_O^{\bullet}$$

Magnesia doped with alumina

$$Al_2O_3 \xrightarrow{MgO} 2Al_{Mg}^{\bullet} + V_{Mg}^{''} + 3O_O^{\times}$$

Quasi – Chemical Approach

Constant of Reaction

- There's a need of a more immediate way to estimate defect concentration in crystals.
- Applying:
  - Kröger – Vink notation
  - Quasi – Chemical approach

  to equations that represent defect formation's processes
- A "*constant of reaction*" for those equation can be defined.

With e.g. : $TiO_2 \xrightarrow{MgO} Ti_{Mg}^{\bullet\bullet} + 2O_O^{\times} + V_{Mg}^{''}$

Defining: $n_Y = \#\ \underline{sites}\ for\ species\ Y$

$[M_X] =$ *fraction of X species' reticular sites which have been occupied by M atoms*

$$\left[Ti_{Mg}^{\bullet\bullet}\right] = \frac{\#Ti^{4+}/cm^3}{\#Mg^{2+}/cm^3} = \frac{n_{Ti_{Mg}^{\bullet\bullet}}}{n_{Mg}}$$

$$\left[O_O^{\times}\right] = \frac{\#O/cm^3}{\#O/cm^3} = 1$$

$\Rightarrow$

$$\left[V_{Mg}^{''}\right] = \frac{\#V_{Mg}^{''}/cm^3}{\#Mg/cm^3} = \frac{n_{V_{Mg}^{''}}}{n_{Mg}}$$

So:

$$K_r = \frac{\left[Ti_{Mg}^{\bullet\bullet}\right]\left[V_{Mg}^{''}\right]\left[O_O^{\times}\right]^2}{a_{TiO_2}}$$

(where activity of solute specie is at the denominator)

And, going on with the "Quasi – Chemical" approach:

$$K_r = e^{-\frac{\Delta G^\circ}{RT}}$$

Where ΔG° is energy change associated with the dissolution process of TiO_2 in MgO

$\Rightarrow$

$$\frac{\left[Ti_{Mg}^{\bullet\bullet}\right]\left[V_{Mg}^{''}\right]\left[O_O^{\times}\right]^{\cancel{2}\,1}}{a_{TiO_2}} = e^{-\frac{\Delta G^\circ}{RT}} \qquad (1)$$

ENC (Electro Neutrality Condition):

$$2en_{Ti_{Mg}}^{\bullet\bullet} = 2en_{V_{Mg}}^{''}$$

$$\Rightarrow \quad \frac{n_{Ti_{Mg}}^{\bullet\bullet}}{n_{Mg}} = \frac{n_{V_{Mg}}^{''}}{n_{Mg}} \quad \Rightarrow \quad \left[Ti_{Mg}^{\bullet\bullet}\right] = \left[V_{Mg}^{''}\right]$$

Finally, the (1) becomes:

$$\left[Ti_{Mg}^{\bullet\bullet}\right] = \left(a_{TiO_2}\right)^{1/2} e^{-\frac{\Delta G^\circ}{2RT}} \qquad (2)$$

which permit to *ESTIMATE DEFECTS CONCENTRATION*

NOTE: $0 < \left[Ti_{Mg}^{\bullet\bullet}\right] < 1$

Phase Diagram

In the phase diagram:

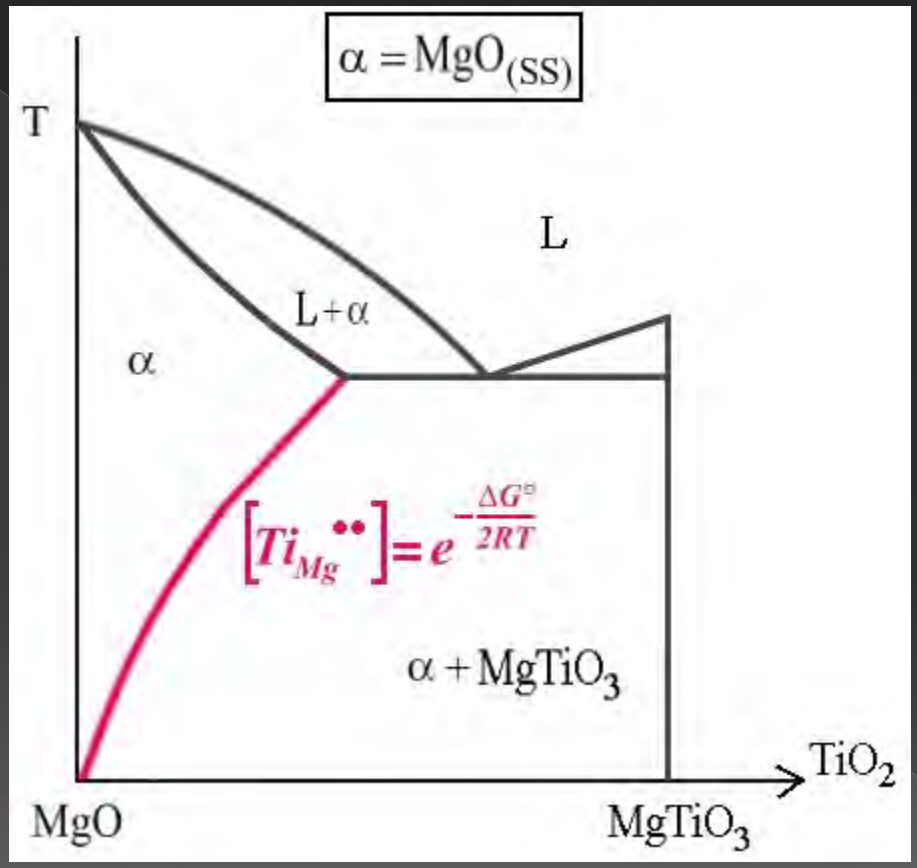

From equation [2] we can also obtain an expression for the SOLVUS LINE (remembering that, for solids, at equilibrium activity is *1*).

Phase Diagram

So, when you come down on a composition line:

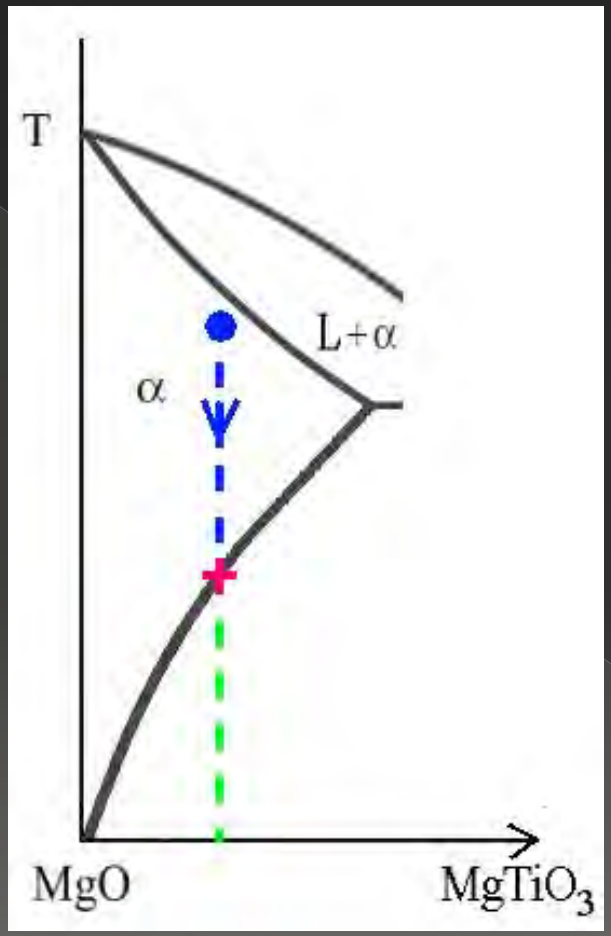

activity changes till when you reach the *solvus line* → then in the microstructure you'll have precipitation of TiO_2.

Some examples

Schottky Disorder in magnesia

$$\emptyset \xrightarrow{MgO} V_{Mg}^{''} + V_O^{\bullet\bullet}$$

$$\Rightarrow \left[V_{Mg}^{''}\right]\left[V_O^{\bullet\bullet}\right] = K_r = e^{-\frac{\Delta H_S}{RT}}$$

With: $\Delta H_S = 7.5\, eV/mol\,\mathcal{V}$

Schottky Disorder in magnesia

$$n_O = n_{Mg} = n_{MgO}$$

$$ENC: \quad 2en_{V_O^{\bullet\bullet}} = 2en_{V_{Mg}^{''}}$$

$$\left[V_{Mg}^{''}\right] = \left[V_O^{\bullet\bullet}\right] = e^{-\frac{\Delta H_S}{2RT}}$$

- So, at T = 2,000 K $\Rightarrow$ [V] $\approx 10^{-9}$
- $\Rightarrow$ in 1 *mol* there'll be $\approx 10^{+14}$ defects. $\left(n_V = [V] \cdot n_{MgO} \right)$
- NB: in a *real* crystal, there'll be, in any case, <u>*AT LEAST*</u> $10^{16} - 10^{17}$ defects/mol
- $\Rightarrow$ [V] $\approx 10^{-6} - 10^{-7}$

Schottky Disorder in alumina

$$\emptyset \xrightarrow{Al_2O_3} 2V_{Al}^{'''} + 3V_O^{\bullet\bullet}$$

$$\left[V_O^{\bullet\bullet}\right]^3\left[V_{Al}^{'''}\right]^2 = e^{-\frac{\Delta H_S}{RT}}$$

With: $\Delta H_S = 25eV$

Schottky Disorder in alumina

$$ENC: \quad 2en_{V_O^{\bullet\bullet}} = 3en_{V_{Al}^{'''}}$$

$$n_{Al} = 2n_{Al_2O_3}$$

$$n_O = 3n_{Al_2O_3}$$

$$2n_O\left[V_O^{\bullet\bullet}\right] = 3n_{Al}\left[V_{Al}^{'''}\right]$$

$$2\left(3n_{Al_2O_3}\right)\left[V_O^{\bullet\bullet}\right] = 3\left(2n_{Al_2O_3}\right)\left[V_{Al}^{'''}\right]$$

$$\Rightarrow \left[V_O^{\bullet\bullet}\right] = \left[V_{Al}^{'''}\right]$$

$$\Rightarrow \left[V_O^{\bullet\bullet}\right] = \left[V_{Al}^{'''}\right] = e^{-\frac{\Delta H_S}{5RT}}$$

Schottky Disorder in alumina

$$\Rightarrow \left[V_O^{\bullet\bullet}\right] = \left[V_{Al}^{'''}\right] = e^{-\frac{\Delta H_S}{5RT}}$$

ΔH_S is sort of "medium E per defect"

- So:
  - 1 Schottky disorder in alumina disarranges **5** points in crystal structure (3 V_O and 2 V_{Al})
  - 1 Schottky disorder in magnesia (previous example) disarranges **2** points in crystal structure (1 V_O and 1 V_{Mg})

Schottky disorder's energy of formation

SPECIE	ΔH_S [eV]	$\Rightarrow$ E/defect [eV]
Al_2O_3	25	~5
MgO	7.5	3.75
CaO	6.1	3.05
NaCl	2.30	1.65
KCl	2.26	1.1
LiF	2.34	1.17
LiCl	2.12	1.1
LiBr	1.80	0.9
LiI	1.30	0.7

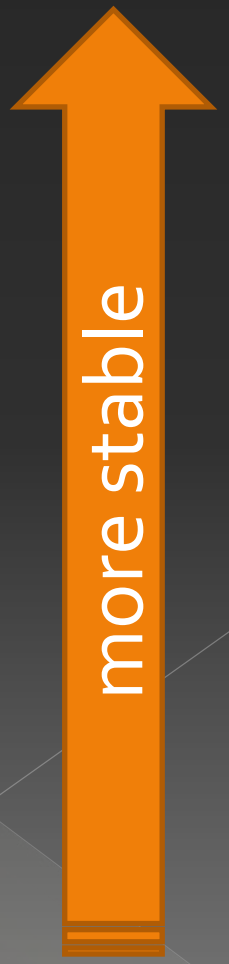

Frenkel Disorder in urania

$$U_U^{\times} \xrightarrow{UO_2} U_i^{\bullet\bullet\bullet\bullet} + V_U^{\prime\prime\prime\prime}$$

$$\frac{\left[U_i^{\bullet\bullet\bullet\bullet}\right]\left[V_U^{\prime\prime\prime\prime}\right]}{\left[U_U^{\times}\right]} = e^{-\frac{\Delta H_F}{RT}}$$

- NB: thank to the low defect concentration, $[U_U]$ is SUBSTANTIALLY 1.

Frenkel Disorder in urania

$$ENC: \quad 4en_{U_i^{\bullet\bullet\bullet\bullet}} = 4en_{V_U^{\prime\prime\prime\prime}}$$

As urania has a fluorite structure it is: $n_i = \frac{1}{4} n_U$

$$n_U = n_{UO_2}$$

$$\Rightarrow \quad \frac{n_{U_i^{\bullet\bullet\bullet\bullet}}}{n_i} = 4\frac{n_{U_i^{\bullet\bullet\bullet\bullet}}}{n_U} = 4\frac{n_{V_U^{\prime\prime\prime\prime}}}{n_U} \quad \Rightarrow \quad \left[U_i^{\bullet\bullet\bullet\bullet}\right] = 4\left[V_U^{\prime\prime\prime\prime}\right]$$

$$\Rightarrow \quad \left[U_i^{\bullet\bullet\bullet\bullet}\right]^2 = 4e^{-\frac{\Delta H_F}{RT}}$$

$$\Rightarrow \quad \left[U_i^{\bullet\bullet\bullet\bullet}\right] = 4e^{-\frac{\Delta H_F}{2RT}}$$

Fuel rods for nuclear reactors

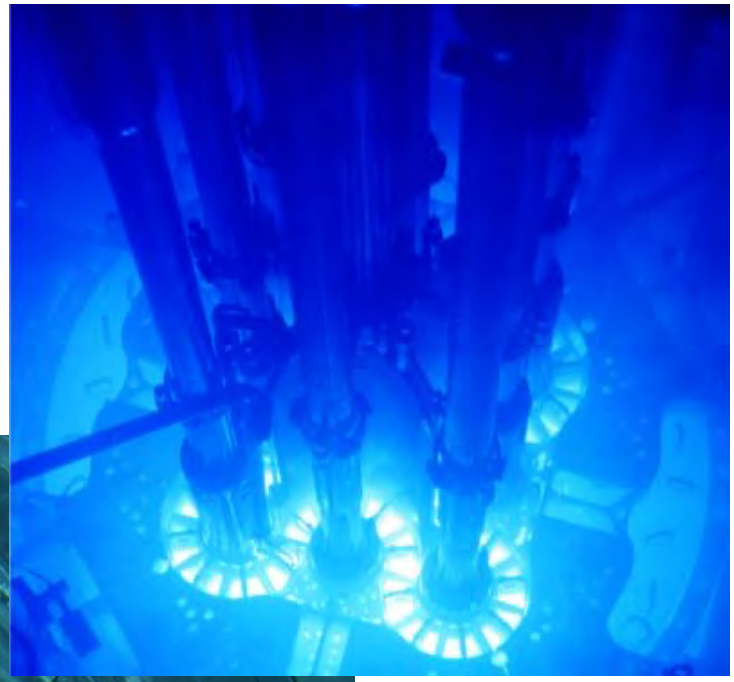

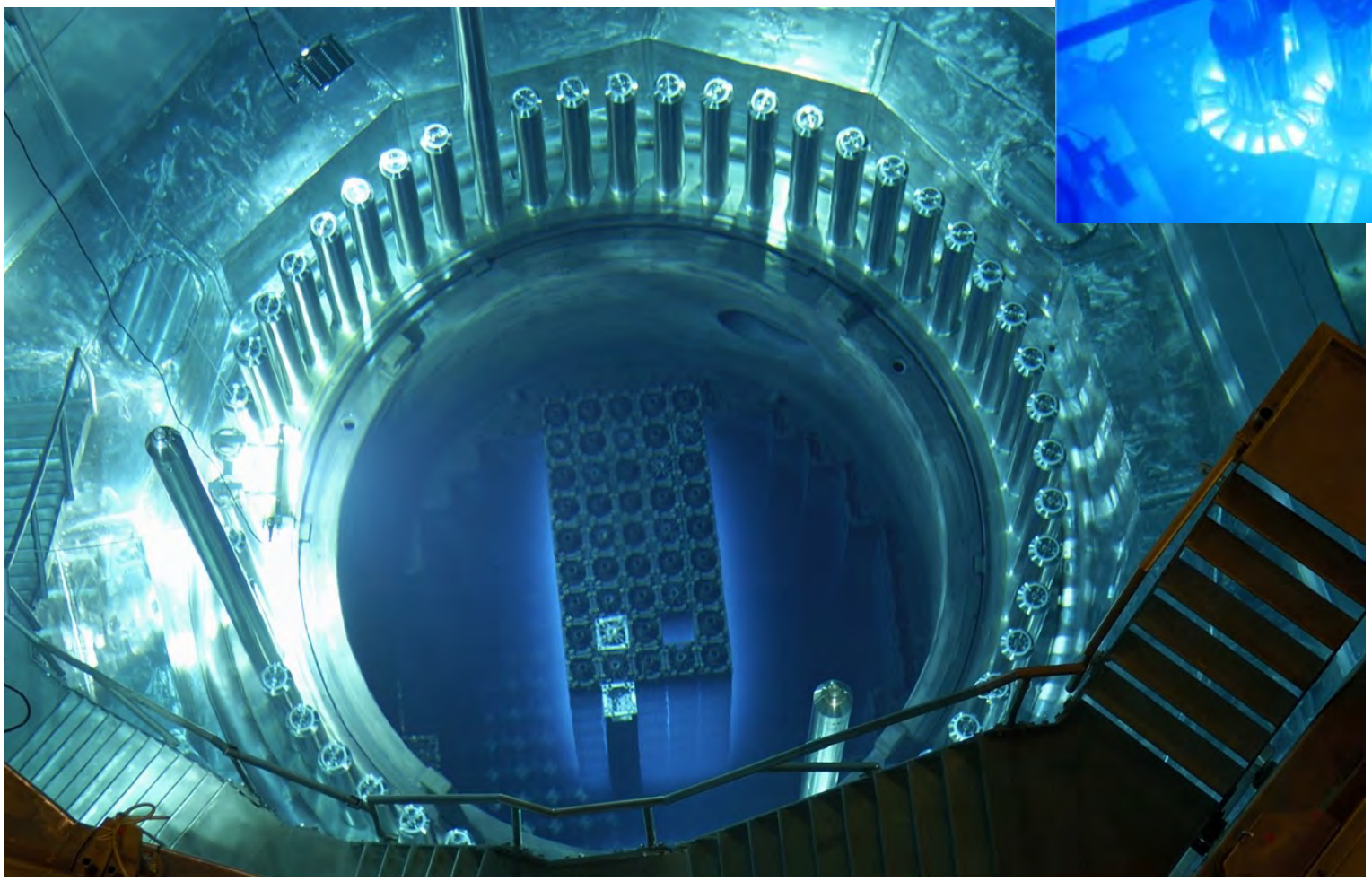

Frenkel disorder's energy of formation

STRUCTURE	MATERIAL – interstitial	ΔG [eV]
Rocksalt str.	MgO – Mg	13.5
	MgO – O	17.6
Corundum	Al_2O_3 – Al	14
	Al_2O_3 – O	16.5
Fluorite str.	UO_2 – U	3.4
Fluorite	CaF_2 – Ca	2.8
till 147 °C: wurtzite (over 147 °C: CBC and there is also a metastable form, with sphalerite str.)	AgI – Ag	0.75

Oxygen has also a bigger steric effect

Concentrations of charge carriers (electrons and holes)

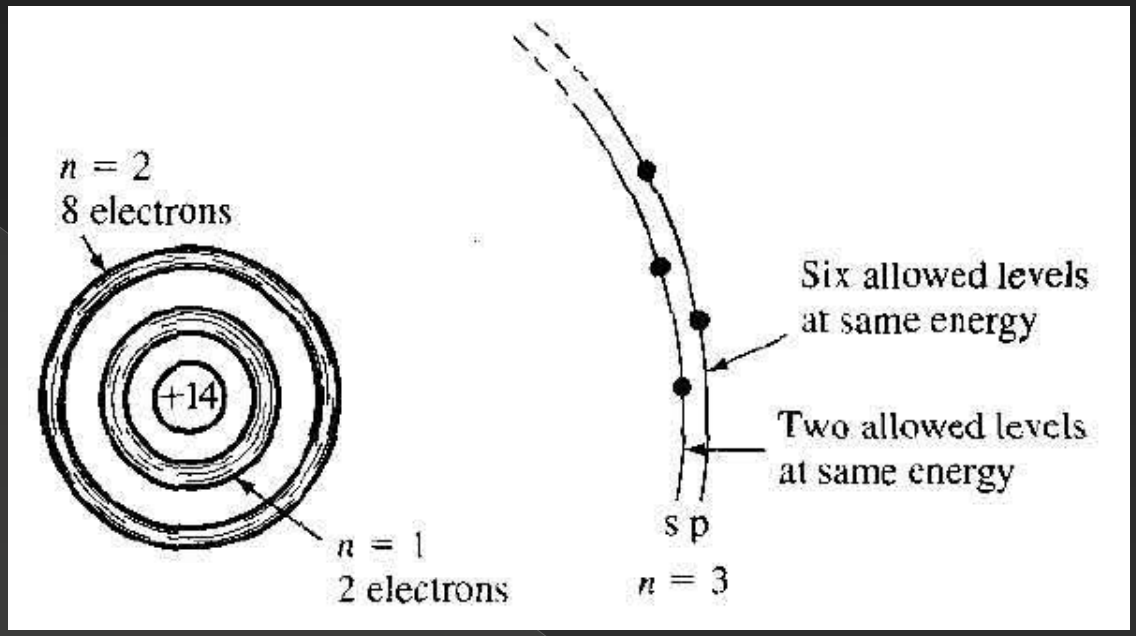

Schematic of an isolated Si atom

- Consider a regular periodic arrangement of atoms in which each atom contains more than one electron (eg Si).
- Suppose the atom in this imaginary crystal contains e^- up through the n=3 energy level.
- If the atoms are initially very far apart , the e^- in adjacent atoms will not interact and will occupy the discrete energy levels.

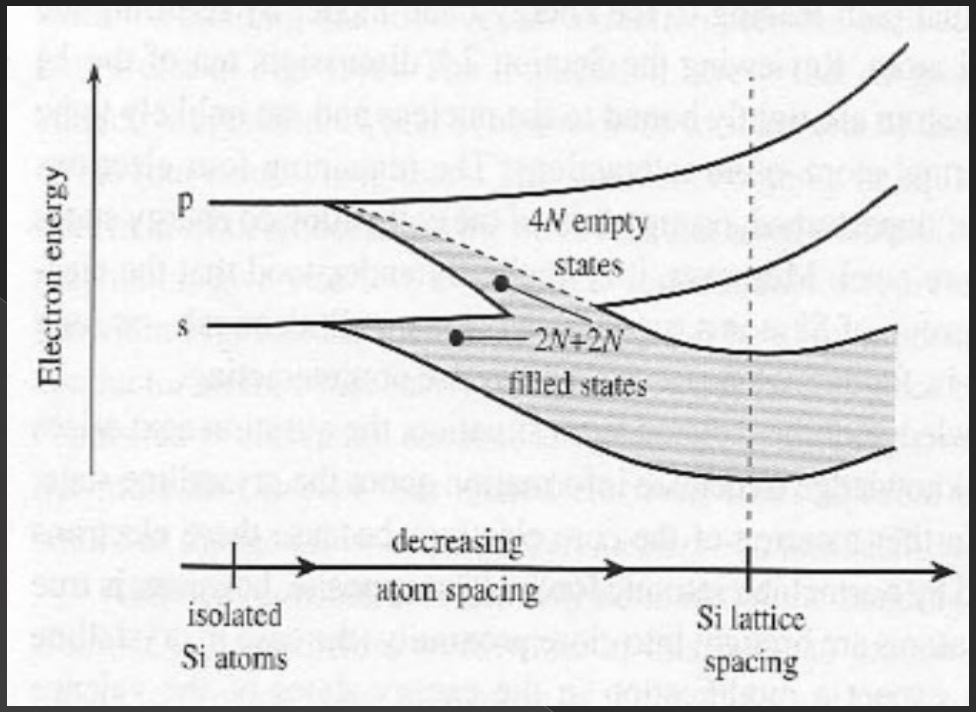

Splitting of the s and p states of Si into the allowed and forbidden energy bands

- If these atoms are brought closer together, somehow (quantum mechanics), their quantized energy levels split and turn into many states grouped in "energy bands" (see diagrams)
- Conduction only happens if electrons have empty "states" available at nearby energy

- Considering an intrinsic semiconductor we have:

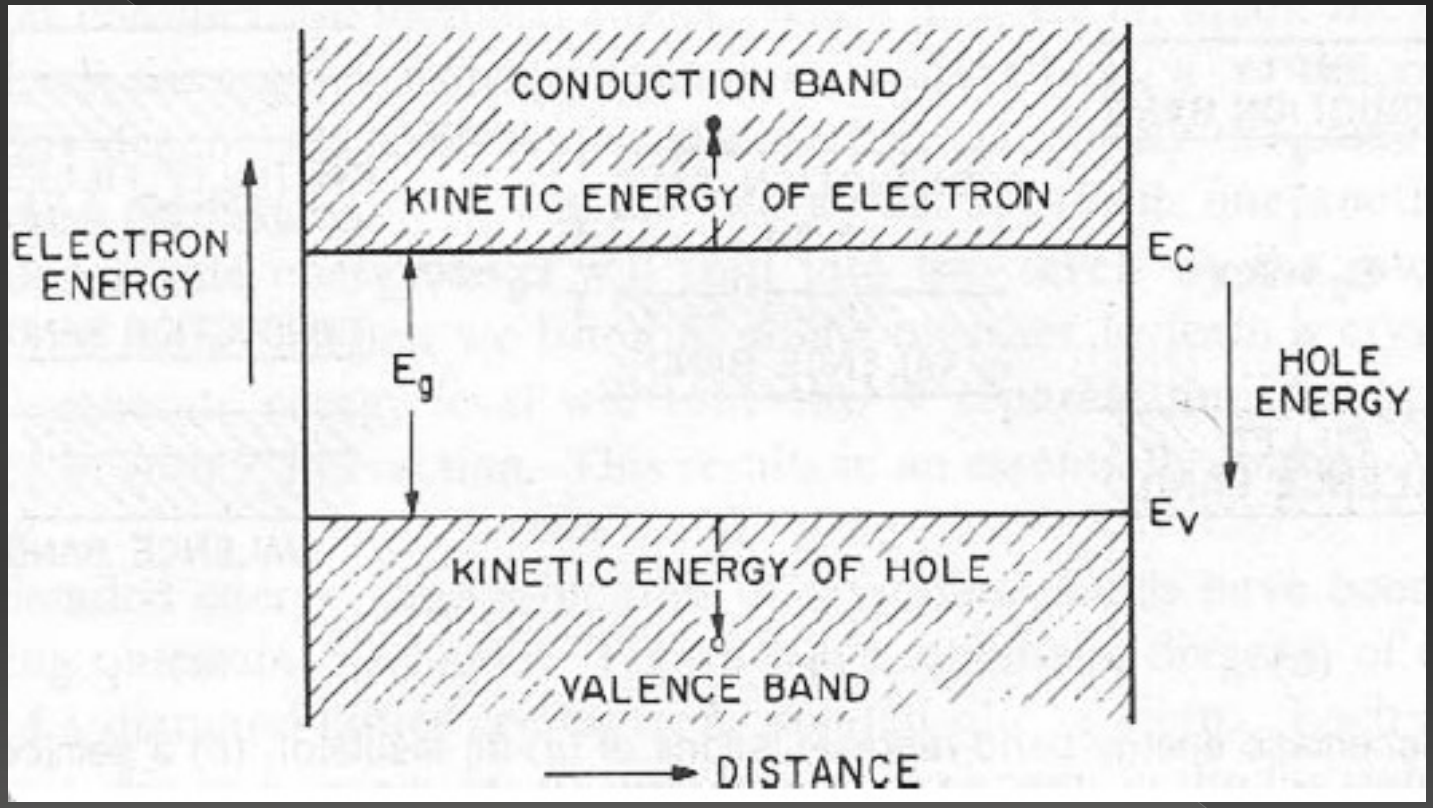

- When an e^- springs from VB to CB, it leaves a hole in VB

- According to Quasi – Chemical approach it's possible to represent this process as:

$$\emptyset \longrightarrow e^{|} + h^{\bullet}$$

$$\Rightarrow \qquad \left[e^{|}\right]\left[h^{\bullet}\right] = e^{-\frac{E_{GAP}}{RT}}$$

$$\left[e^{|}\right] = \frac{n}{N_C} \qquad \left[h^{\bullet}\right] = \frac{p}{N_V}$$

where:

$$n = \frac{\#e^{-}}{CC}$$

$$p = \frac{\#holes}{CC}$$

$$N_C = \#available \;\; states \;\; (= electron \; E \; levels) \; in \; CB$$

$$N_V = \#available \;\; states \;\; (= electron \; E \; levels) \; in \; VB$$

$$\Rightarrow \qquad \frac{n}{N_C}\frac{p}{N_V} = e^{-\frac{E_{GAP}}{RT}}$$

- We have that

$$N_C \cong N_V \cong 2.5 \cdot 10^{19} \frac{\#}{CC}$$

- This is a number little lower than the number of atoms in 1 CC
- So almost every atom contributes with one state

- If, as supposed, the S.C. is intrinsic, we can obtain the concentrations of charge carriers equation:

$$n = p = n_i$$

$$\Rightarrow \quad np = n_i^{\,2} = N_C N_V e^{-\frac{E_{GAP}}{RT}}$$

$$\Rightarrow \quad \boxed{n_i = \sqrt{N_C N_V}\, e^{-\frac{E_{GAP}}{2RT}}}$$

- Some E_{GAP} values for ceramics:

Ceramic	Energy gap [eV]
Al_2O_3	7
Si	1.1
Single crystal ZnO	3.2
Cd doped ZnO	~3.0
Mg doped ZnO	~4.0
Single crystal TiO_2	3.23

(Ceramics Science and Technology: Properties; Volume 2; Ralf Riedel, I-Wei Chen)

- ***Pay attention!!*** There are direct and indirect S.C.s, which means they may have respectively a direct or indirect transition…

Direct transition

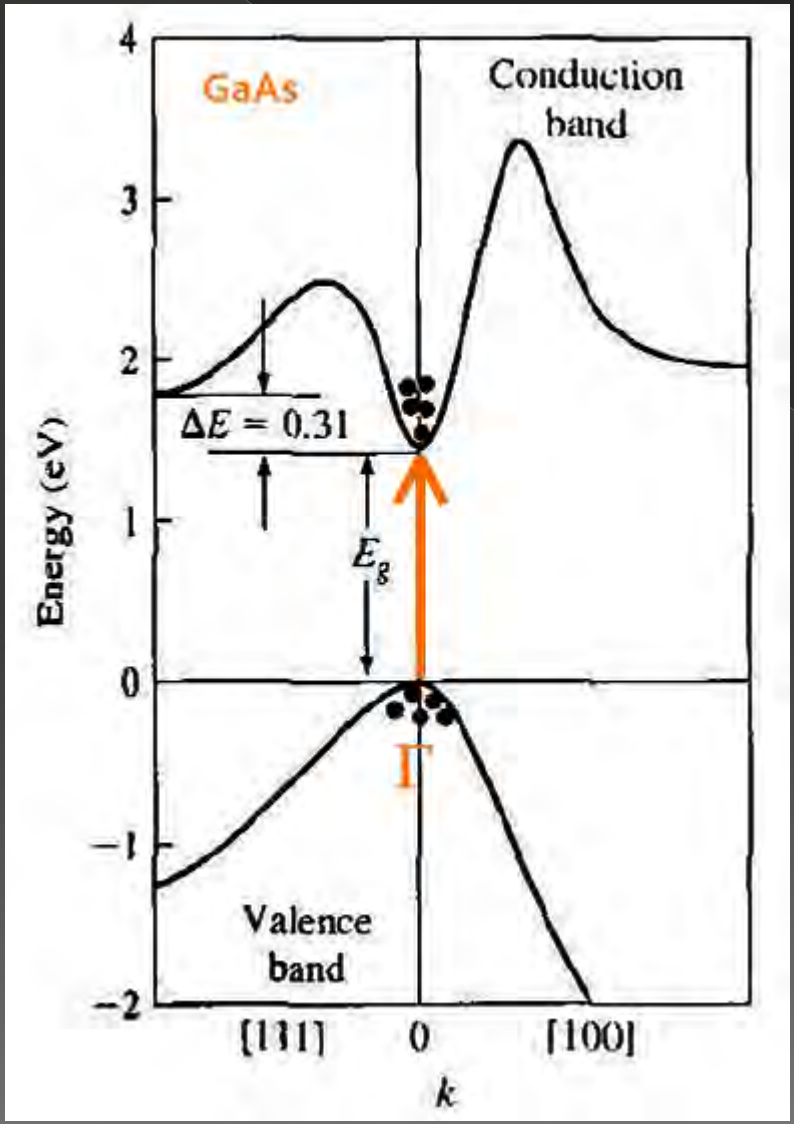

Indirect transition

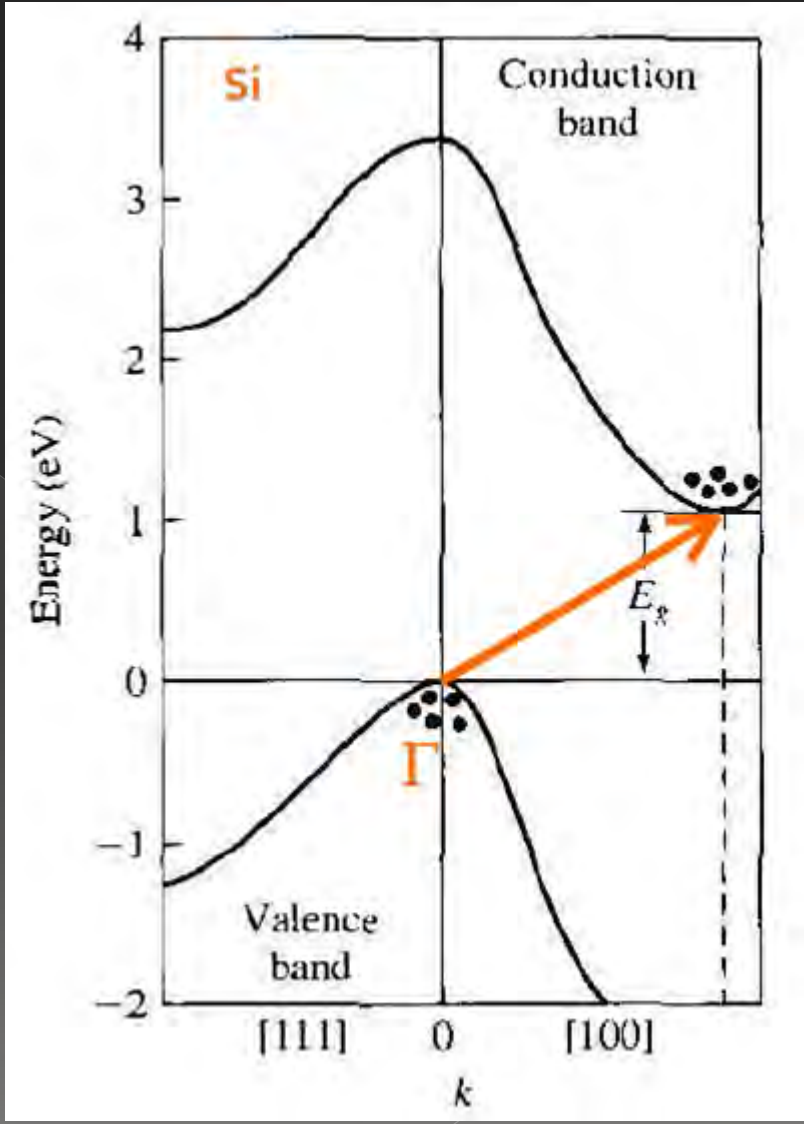

- Why did we evaluate ΔH (instead of ΔG)?
- Usually $\Delta G°$ is due mostly to system's free energy, as:

$$\Delta G = \Delta H - \Delta(TS)$$

Usually ≅ 1-2% of ΔG in solid dissolutions (ppm)

$$\Delta H = \Delta U + \Delta(PV)$$

negligible in SOLIDS

$$\Rightarrow \Delta G \cong \Delta H \cong \Delta U$$

$$0 < \left[Ti_{Mg}^{\bullet\bullet} \right] < 1$$

qualitatively:

$$n_O = n_{Mg} = n_{MgO} = N_A \frac{\rho_{MgO}}{MW_{MgO}} =$$

$$= \frac{6.023 \cdot 10^{23} \frac{molecules}{\cancel{mol}} \cdot 3.58 \frac{\cancel{g}}{cm^3}}{40.03 \frac{\cancel{g}}{\cancel{mol}}} \cong 4 \cdot 10^{22} \, {}^{\#}/_{cm^3}$$

If it is:

$$n_{Ti_{Mg}^{\bullet\bullet}} \cong 4 \cdot 10^{16} \, {}^{\#}/_{cm^3}$$

$$\Rightarrow \left[Ti_{Mg}^{\bullet\bullet} \right] \cong 10^{-6}$$

$$U_U^{\times} \xrightarrow{UO_2} U_i^{\bullet\bullet\bullet\bullet} + V_U^{''''}$$

$[U_U]$ is <u>SUBSTANTIALLY 1</u>:

- Given a generic compound $M_A X_B$,
- With, e.g. 10^9 atoms of M:

$$[V_M] = 10^{-9} = \frac{1\,\#V}{10^9\,\#M}$$

$$[M_M] = \frac{\#M_{left}/CC}{\#M_{in}/CC} = \frac{\#M_{left}}{\#M_{in}} = \frac{\#M_{in} - \#V}{\#M_{in}} = \frac{10^9 - 1}{10^9} \longrightarrow 1$$

Non-stoichiometry in Kroger Vink Notation

- $Cd_{1-x}O$ is non-stoichiometric (and this is due to the fact that more than one oxidation state is available for Cd)

- $\emptyset \rightarrow e^{/} + h^{\cdot}$ $\qquad [e^{/}][h^{\cdot}] = K_e \qquad K_e = e^{-E_g/RT}$

- $\emptyset \longrightarrow V_O^{\cdot\cdot} + V_{Cd}^{//}$ $\qquad [V_O^{\cdot\cdot}]\left[V_{Cd}^{//}\right] = K_S \qquad K_e = e^{-E_S/RT}$

- $O_O^x \longrightarrow \frac{1}{2}O_{2(g)} + V_O^{\cdot\cdot} + 2e^{/}$ $\qquad [V_O^{\cdot\cdot}]\left[e^{/}\right]P_{O_2}^{1/2} = K_P \qquad K_e = e^{-E_P/RT}$

- $\left[e^{/}\right]N_C + 2\left[V_{Cd}^{//}\right]N_A\frac{\rho}{PM} = [h^{\cdot}]\,N_V + 2\,[V_O^{\cdot\cdot}]N_A\frac{\rho}{PM}$

- N_c density of states in the conduction band
- N_v density of states in the valency band
- N_A Avogadro's number
- ρ Density of CdO
- PM molecular weight of CdO

Kroeger-Vink diagram for metal oxide semiconductor MO

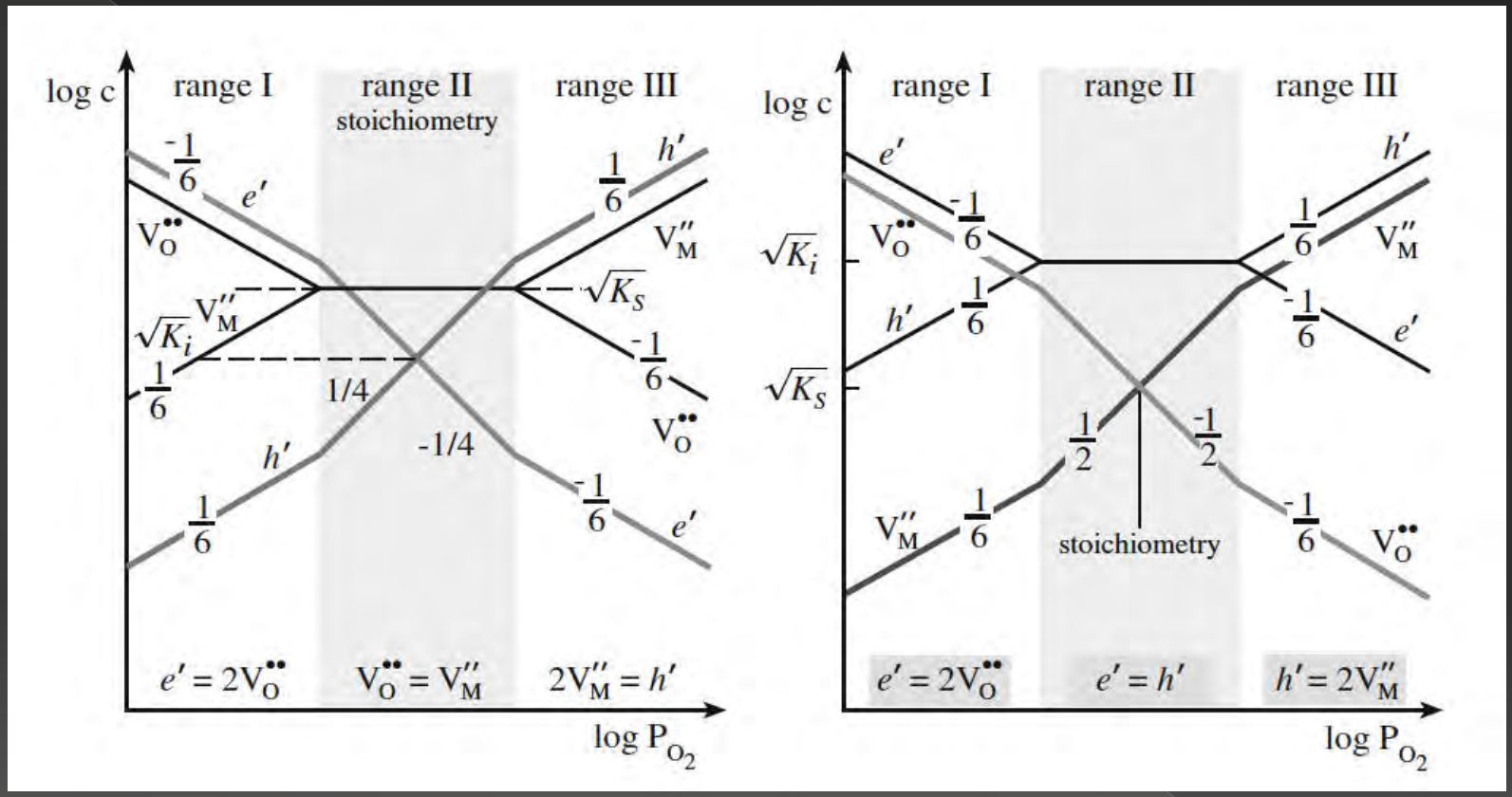

Schottki defects dominate

Electronic defects dominate

Famous case of non-stoichiometric compounds: ceramic superconductors

- $YBa_2Cu_3O_{7-x}$

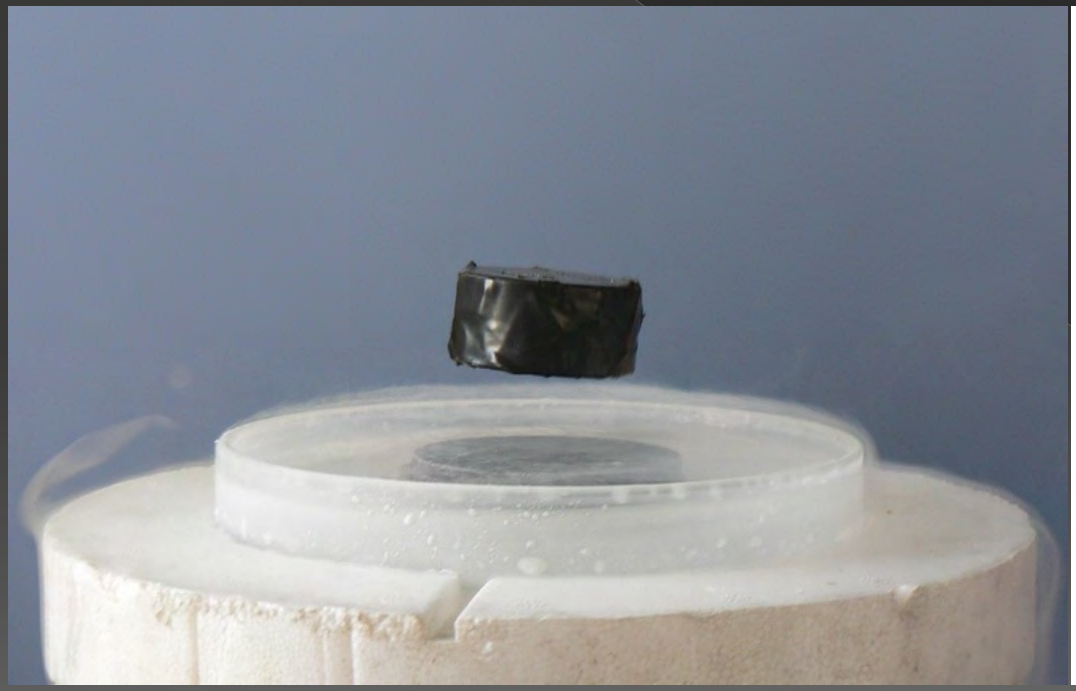

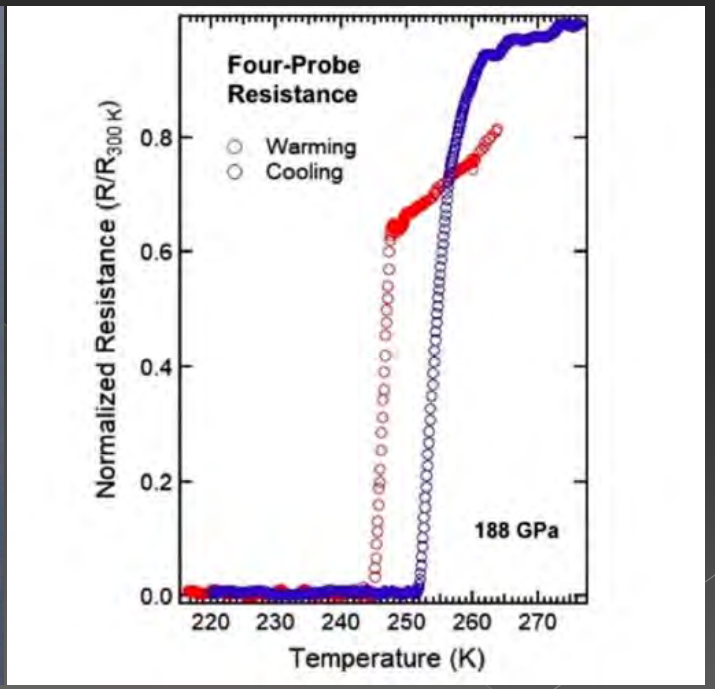

Properties of Ceramics

TABLE 7.1
Density of Ceramic, Metallic, and Organic Materials

Material	Composition	Reported Density,[a] g/cm³ (lb/in.³)	X-Ray Density,[b] g/cm³ (lb/in.³)
Ceramic Materials			
α-Aluminum oxide	α-Al_2O_3	3.95 (0.14)	3.987 (0.14)
Aluminum nitride	AlN	3.26 (0.12)	–
Mullite	$Al_6Si_2O_{13}$	–	3.166 (0.11)
Boron carbide	B_4C	2.51 (0.09)	–
Boron nitride	BN	2.20 (0.08)	–
Beryllium oxide	BeO		3.010 (0.10)
Barium titanate	$BaTiO_3$	5.80 (0.21)	–
Diamond	C	–	3.516 (0.13)
Graphite	C	–	2.267 (0.08)
Fluorite	CaF_2	–	3.179 (0.11)
Cerium oxide	CeO_2	–	7.216 (0.33)
Chromium oxide	Cr_2O_3	–	5.225 (0.19)
Spinel	$MgAl_2O_4$	–	3.583 (0.13)
Iron aluminum spinel	$FeAl_2O_4$	–	4.265 (0.15)
Magnetite	$FeFe_2O_4$	–	5.202 (0.13)
Hafnium oxide	HfO_2	9.68 (0.35)	10.108 (0.36)
β-Spondumene	$LiAlSi_2O_6$	–	2.379 (0.08)
Cordierite	$Mg_2Al_4Si_5O_{18}$	–	2.513 (0.09)
Magnesium oxide	MgO	–	3.584 (0.13)
Forsterite	Mg_2SiO_4	–	3.214 (0.12)
Quartz	SiO_2	–	2.648 (0.09)
Tridymite	SiO_2	–	2.192 (0.08)
Cristobalite	SiO_2	–	2.334 (0.08)
Silicon carbide	SiC	3.17 (0.11)	3.22 (0.12)
Silicon nitride	Si_3N_4	3.19 (0.12)	–
Titanium dioxide (rutile)	TiO_2		4.245 (0.15)
Tungsten carbide	WC	15.70 (0.57)	–
Zirconium oxide (monoclinic)	ZrO_2	5.56 (0.20)	5.827 (0.21)
Zircon	$ZrSiO_4$	–	4.669 (0.17)
Metals			
Aluminum	Al	2.7 (0.09)	–
α-Iron	Fe	–	7.875 (0.28)
Magnesium	Mg	1.74 (0.06)	–
1040 Steel	Fe-base alloy	7.85 (0.28)	–
Hastelloy X	Ni-base alloy	8.23 (0.29)	–
HS-25 (L605)	Co-base alloy	9.13 (0.33)	–
Brass	70 Cu-30 Zn	8.5 (0.30)	–
Bronze	95 Cu-5 Sn	8.8 (0.31)	–
Silver	Ag	10.4 (0.37)	10.501 (0.38)
Tungsten	W	19.4 (0.70)	–
Platinum	Pt	–	21.460 (0.77)
Organic Materials			
Polystyrene	Styrene polymer	1.05 (0.03)	–
Teflon	Polytetrafluoroethylene	2.2 (0.08)	–
Plexiglass	Polymethyl methacrylate	1.2 (0.04)	–

[a] Values reported from a variety of literature sources, but not specified whether bulk, crystallographic, or otherwise.
[b] X-ray crystallographic values, mostly from R. Robie, P. Bethke, and K. Beardsley, U.S. Geological Survey Bulletin 1248.

Melting temperatures

Al_2O_3	2054 ± 6
BaO	2013
BeO	2780 ± 100
Bi_2O_3	825
CaO	2927 ± 50
Cr_2O_3	2330 ± 15
Eu_2O_3	2175 ± 25
Fe_2O_3	Decomposes at 1735 K to Fe_3O_4 and oxygen
Fe_3O_4	1597 ± 2
Li_2O	1570
Li_2ZrO_3	1610
Ln_2O_3	2325 ± 25
MgO	2852
Mullite	1850
Na_2O (α)	1132
Nb_2O_5	1512 ± 30
Sc_2O_3	2375 ± 25
SrO	2665 ± 20
Ta_2O_5	1875 ± 25
ThO_2	3275 ± 25
TiO_2 (rutile)	1857 ± 20
UO_2	2825 ± 25
V_2O_5	2067 ± 20
Y_2O_3	2403
ZnO	1975 ± 25
ZrO_2	2677

B_4C	2470 ± 20
HfB_2	2900
HfC	3900
HfN	3390
HfSi	2100
$MoSi_2$	2030
NbC	3615
NbN	2204
SiC	2837
Si_3N_4	At 2151 K partial pressure of N_2 over Si_3N_4 reaches 1 atm
TaB_2	3150
TaC	3985
$TaSi_2$	2400
ThC	2625

TABLE 34.3 Predominantly Covalent Ceramics with Very High Melting Temperatures

Ceramic	T_m (°C)	*Covalent character of bond (%)*
HfC	3890	70
TiC	3100	78
WC	2775	85
B_4C	2425	94
SiC	2300	88
C (diamond)	3727	100

TABLE 34.4 Melting Temperatures of Alkaline Earth Metal Oxides

Oxide	T_m (°C)	*Covalent character (%)*	ϕ (nm^{-1}) = Z/r
BeO	2780	37	57
MgO	2852	27	28
CaO	2927	21	20
SrO	2665	21	17
BaO	2017	18	15

Heat capacity

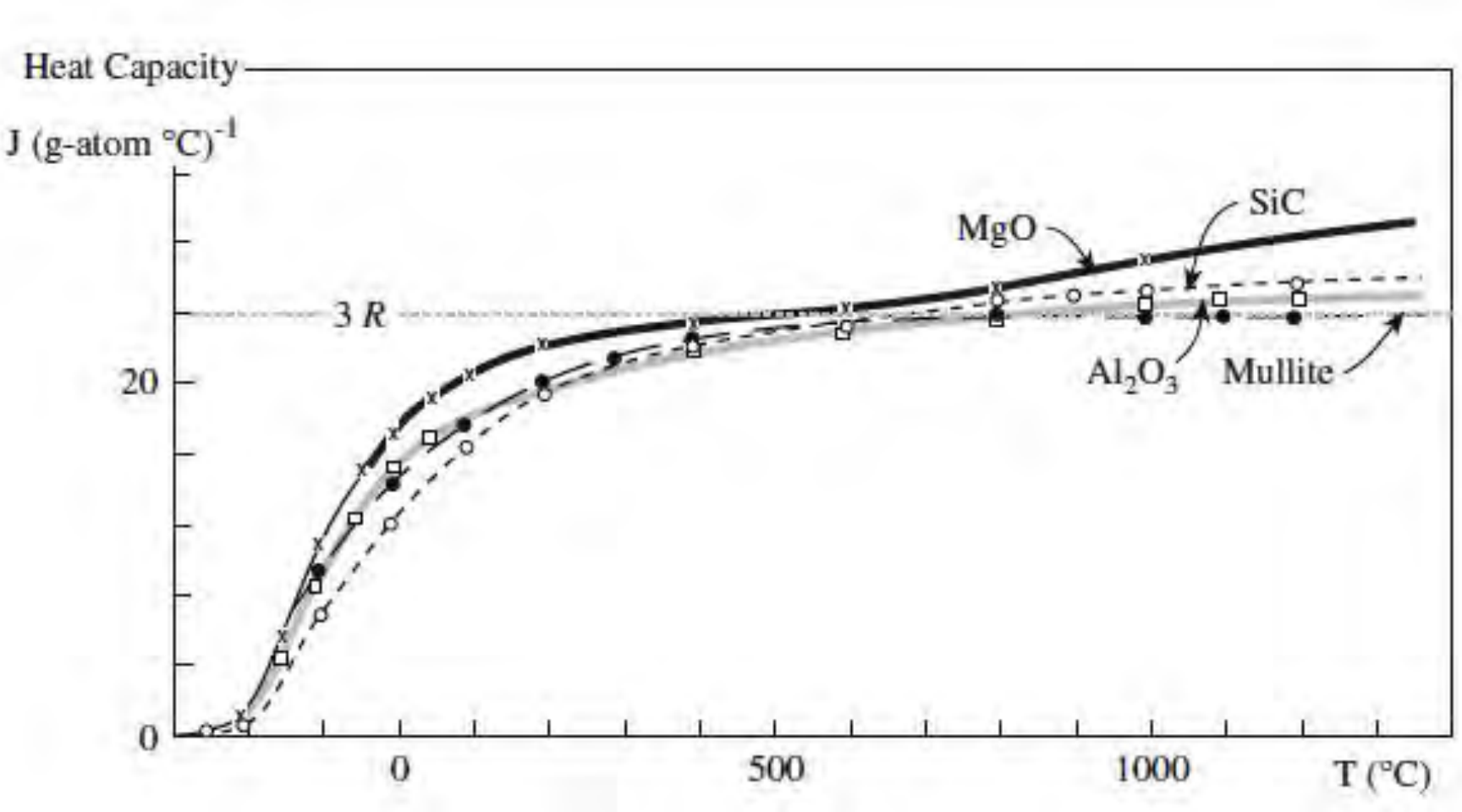

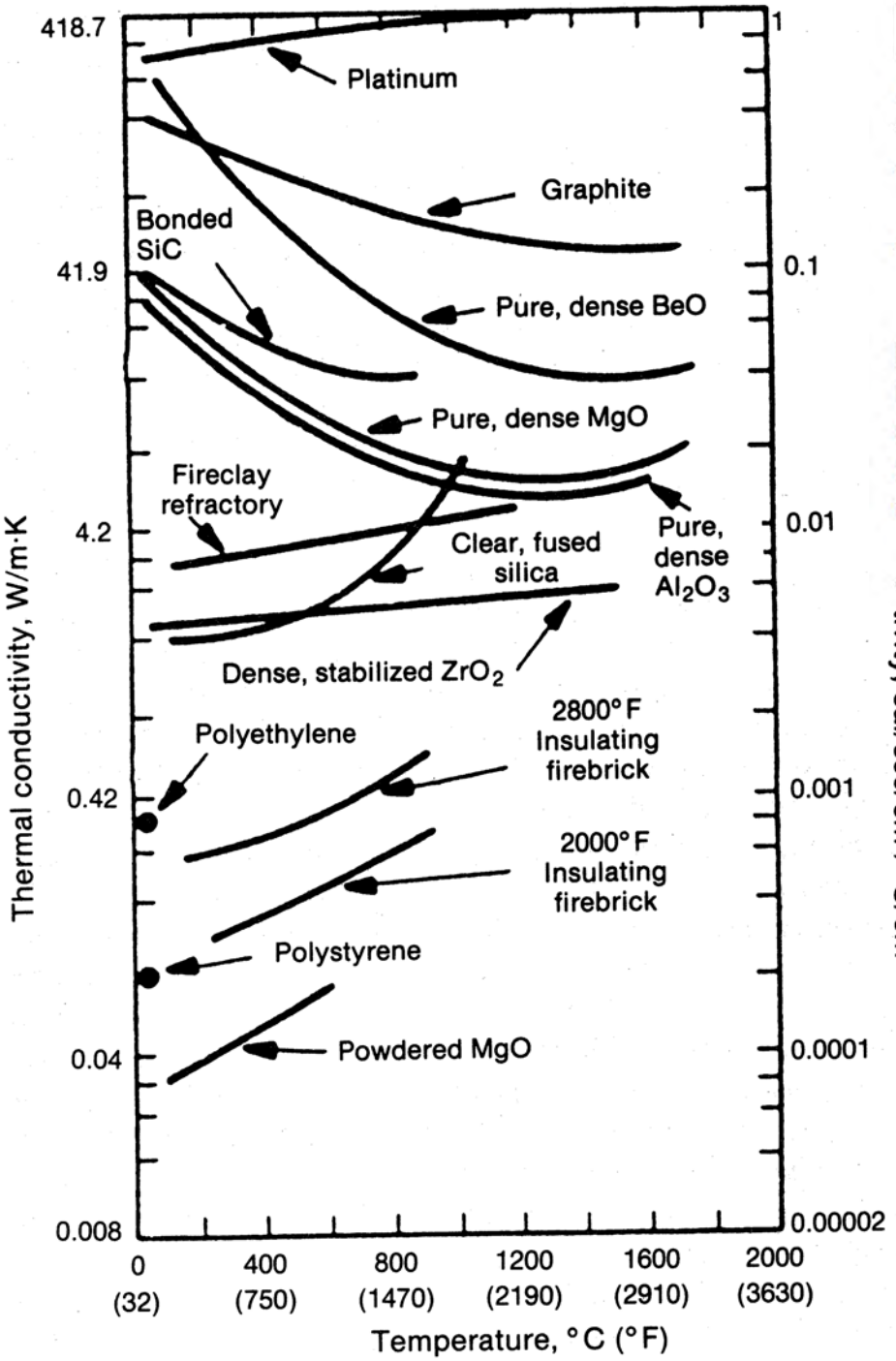

TABLE 34.7 The Thermal Conductivity of Some Ceramics

Material	*k* ($W m^{-1} K^{-1}$)	*Material*	*k* ($W m^{-1} K^{-1}$)
Al_2O_3	30.0–35.0	Spinel ($MgAl_2O_4$)	12.0
AlN	200.0–280.0	Soda–lime–silicate glass	1.7
BeO	63.0–216.0	TiB_2	40.0
MgO	37.0	PSZ	2.0
SiC	84.0–93.0	SiAlON	21.0
SiO_2	1.4	Si_3N_4	25.0
Cordierite (Mg-aluminosilicate)	4.0	Forsterite	3.0

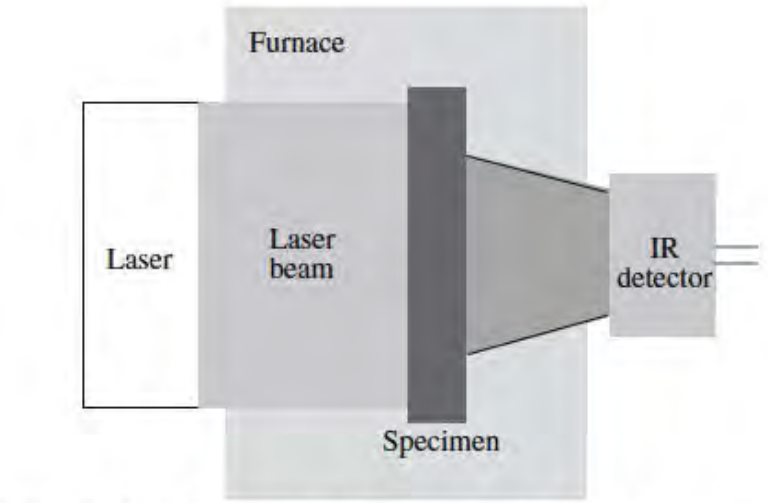

FIGURE 34.5 Schematic of the laser flash method used for measuring thermal conductivity of ceramics.

AlN contains always some Al_2O_3. Industrially some CaO or Y_2O_3 is added, which reacts with Al_2O_3 but then it remains isolated in triple junctions

$$Al_2O_3 \rightarrow 2Al_{Al}^{x} + 3O_N^{\cdot} + V_{Al}^{'''}$$

Thermal condutivity for binary systems

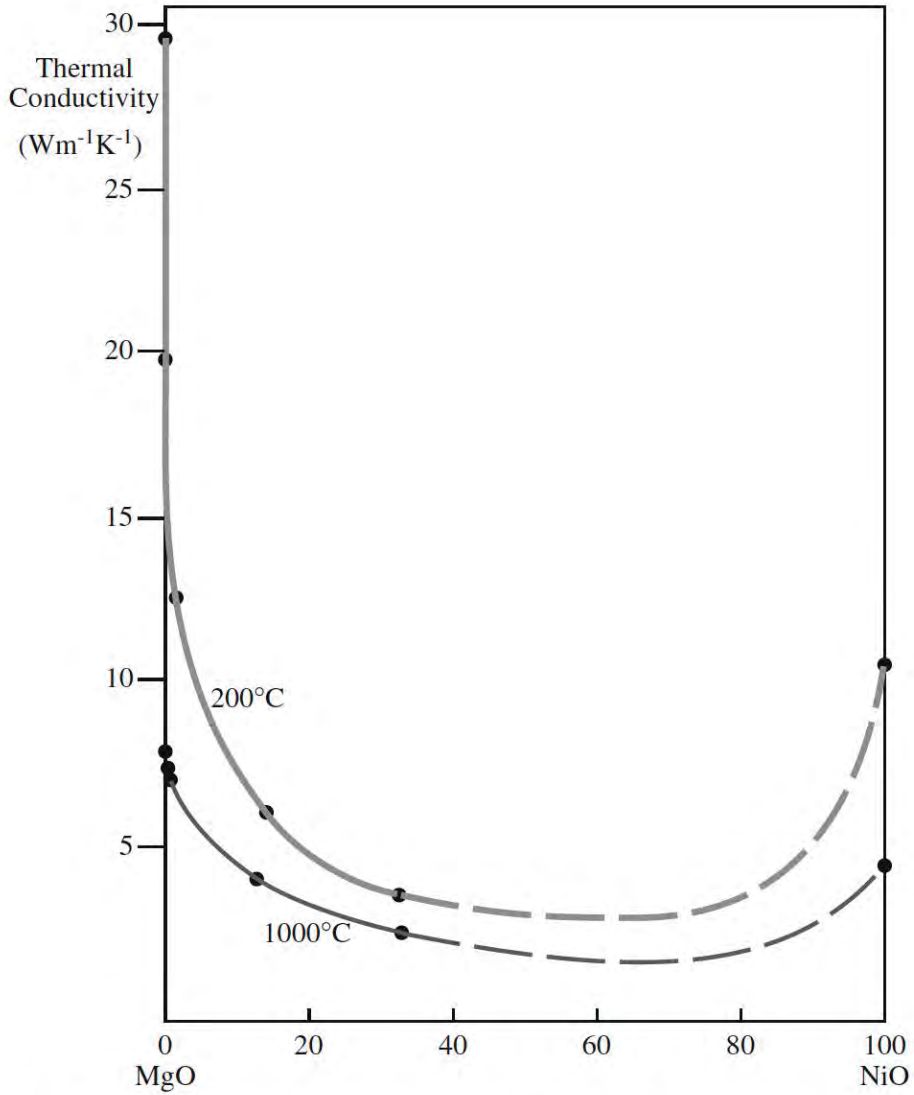

FIGURE 34.6 The thermal conductivities of solid solutions in the MgO–NiO system.

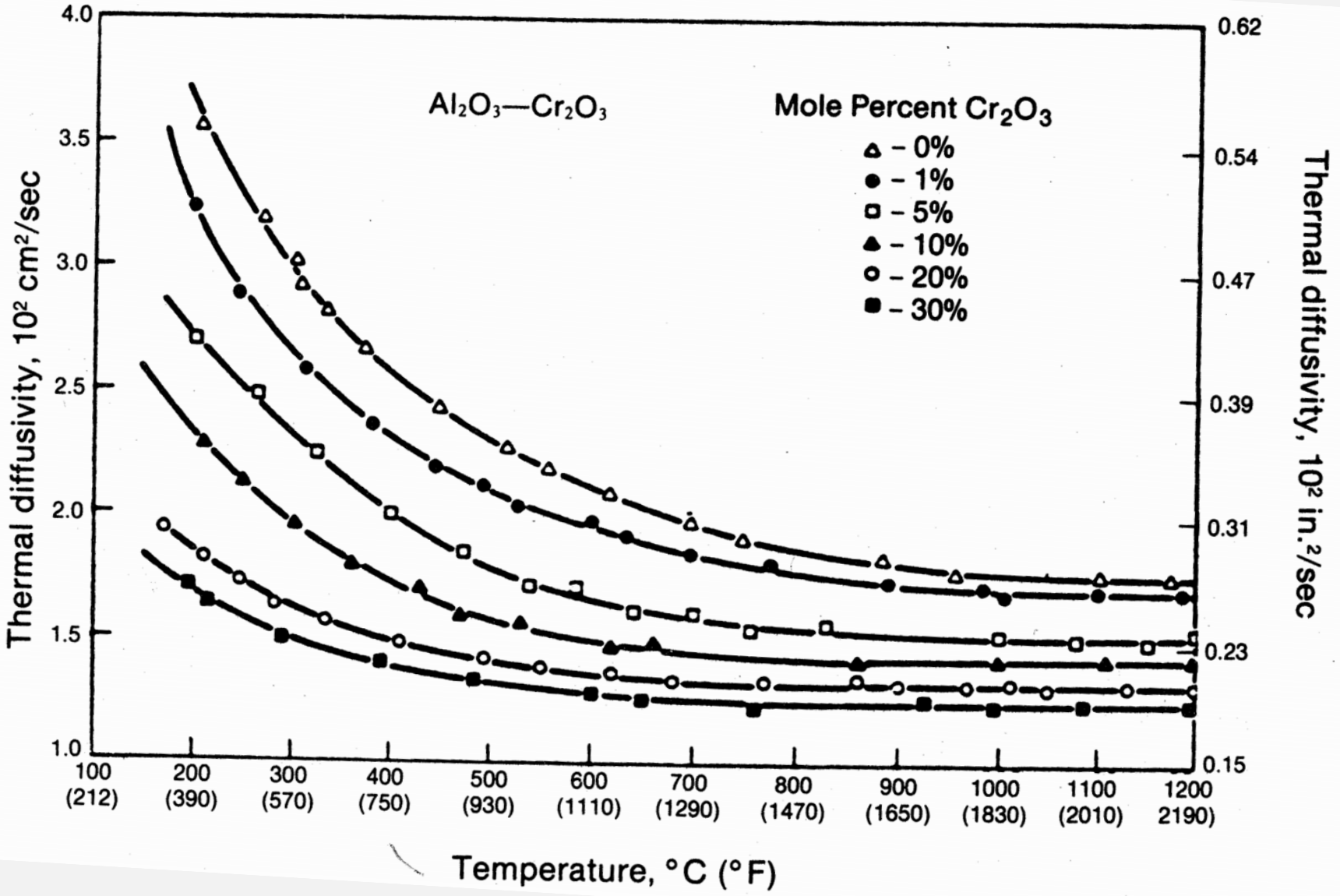
Al_2O_3—Cr_2O_3
Mole Percent Cr_2O_3
△ – 0%
● – 1%
□ – 5%
▲ – 10%
○ – 20%
■ – 30%
Thermal diffusivity, 10^2 cm^2/sec
Thermal diffusivity, 10^2 $in.^2$/sec
4.0
3.5
3.0
2.5
2.0
1.5
1.0
0.62
0.54
0.47
0.39
0.31
0.23
0.15
100 (212)
200 (390)
300 (570)
400 (750)
500 (930)
600 (1110)
700 (1290)
800 (1470)
900 (1650)
1000 (1830)
1100 (2010)
1200 2190)
Temperature, °C (°F)

Thermal expansion

Definition of
Thermal Expansion Coefficient

$$\alpha = \frac{\Delta l}{l_0 \Delta T}$$

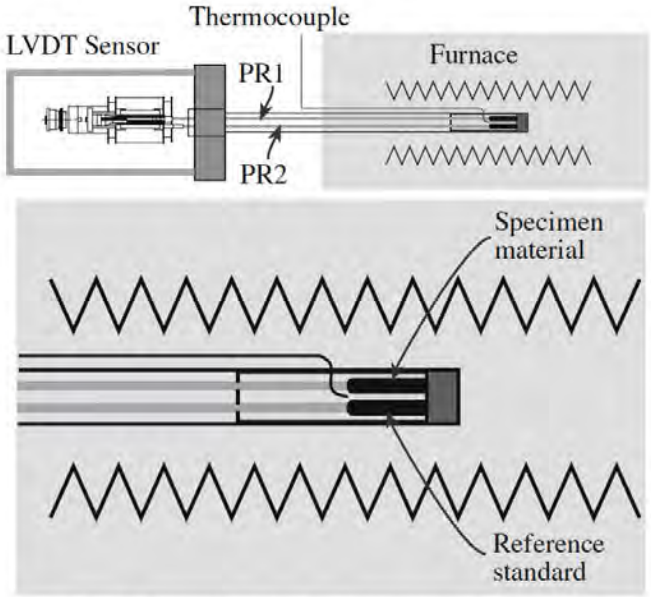

FIGURE 34.14 Schematic of a double pushrod differential dilatometer.

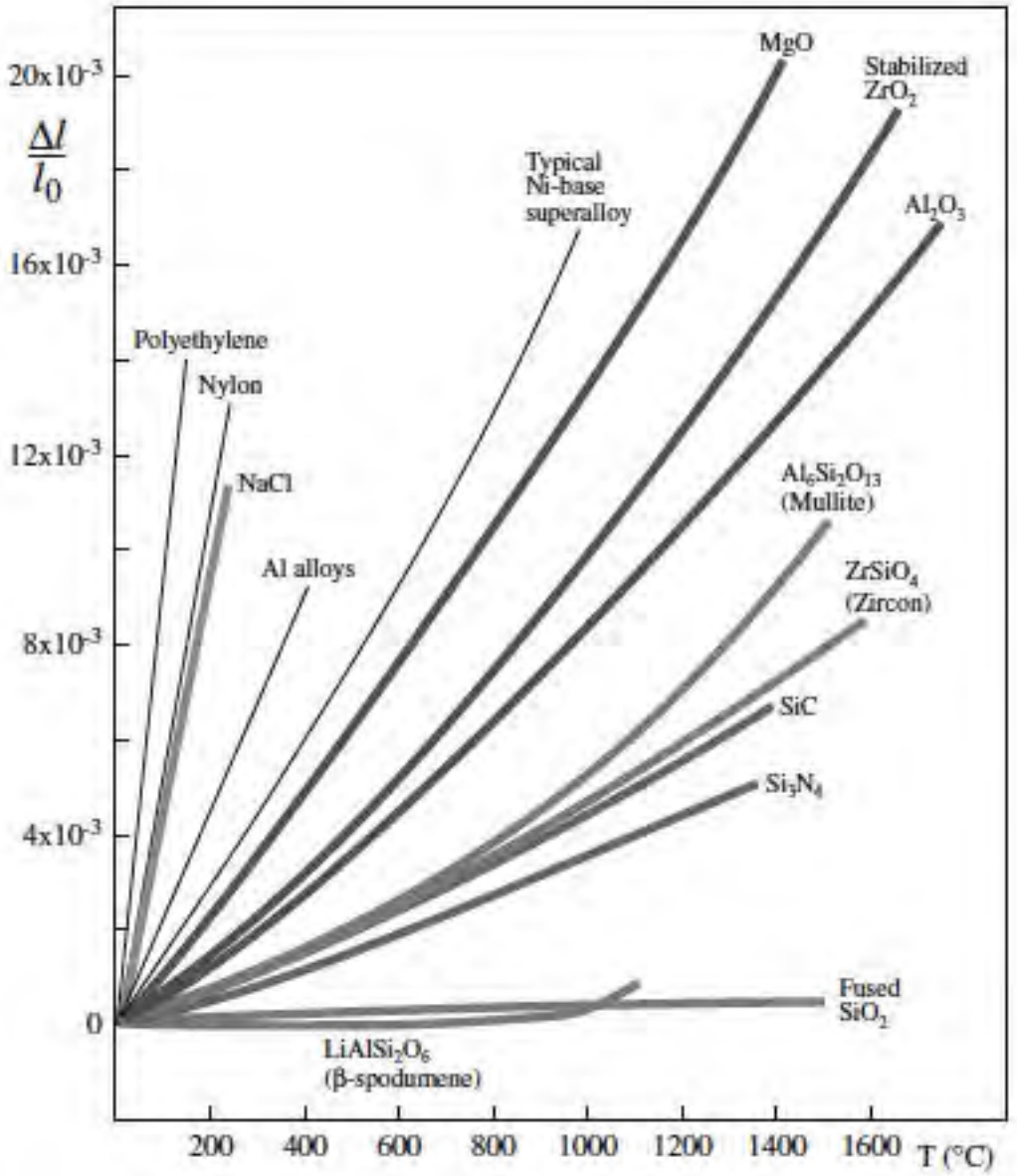

Thermal expansion

TABLE 34.9 Mean Thermal Expansion Coefficients of Various Ceramics

Ceramic	*α (ppm/°C)*	*Ceramic*	*α (ppm/°C)*
	Binary oxides		
α-Al_2O_3	7.2–8.8	ThO_2	9.2
BaO	17.8	TiO_2	8.5
BeO	8.5–9.0 (25–1000)	UO_2	10.0
Bi_2O_3 (α)	14.0 (RT–730°C)	WO_2	9.3 (25–1000)
Bi_2O_3 (δ)	24.0 (650–825°C)	Y_2O_3	8.0 (*c* axis)
Dy_2O_3	8.5	ZnO	4.0 (*a* axis)
Gd_2O_3	10.5	ZrO_2 (monoclinic)	7.0
HfO_2	9.4–12.5	ZrO_2 (tetragonal)	12.0
MgO	13.5		

Ceramic	*α (ppm/°C)*	*Ceramic*	*α (ppm/°C)*
	Borides, nitrides, carbides, and silicides		
AlN	5.6 (25–1000)	SiC	4.3–4.8
B_4C	5.5	TaC	6.3
BN	4.4	TiB_2	7.8
Cr_3C_2	10.3	TiC	7.7–9.5
HfB_2	5.0	TiN	9.4
HfC	6.6	$TiSi_2$	10.5
$MoSi_2$	8.5	ZrB_2	5.7–7.0
β-Mo_2C	7.8	ZrC	6.9 (25–1000)
NbC	6.6	$ZrSi_2$	7.6 (25–2700)
Si_3N_4	3.1–3.7	ZrN	7.2

If grains are too large, fractures due to thermal expansion mismatch can occur also in pure compunds if they have thermal expansion anysostropy.

TABLE 34.10 Thermal Expansion Coefficients for Some Anisotropic Crystals (ppm/°C)

Crystal	*Normal to c axis*	*Parallel to c axis*
Al_2O_3	8.3	9.0
Al_2TiO_5	–2.6	+11.5
$3Al_2O_3 \cdot 2SiO_2$	4.5	5.7
TiO_2	6.8	8.3
$ZrSiO_4$	3.7	6.2
$CaCO_3$	–6	25
SiO_2 (quartz)	14	9
$NaAlSi_3O_8$ (albite)	4	13
C (graphite)	1	27

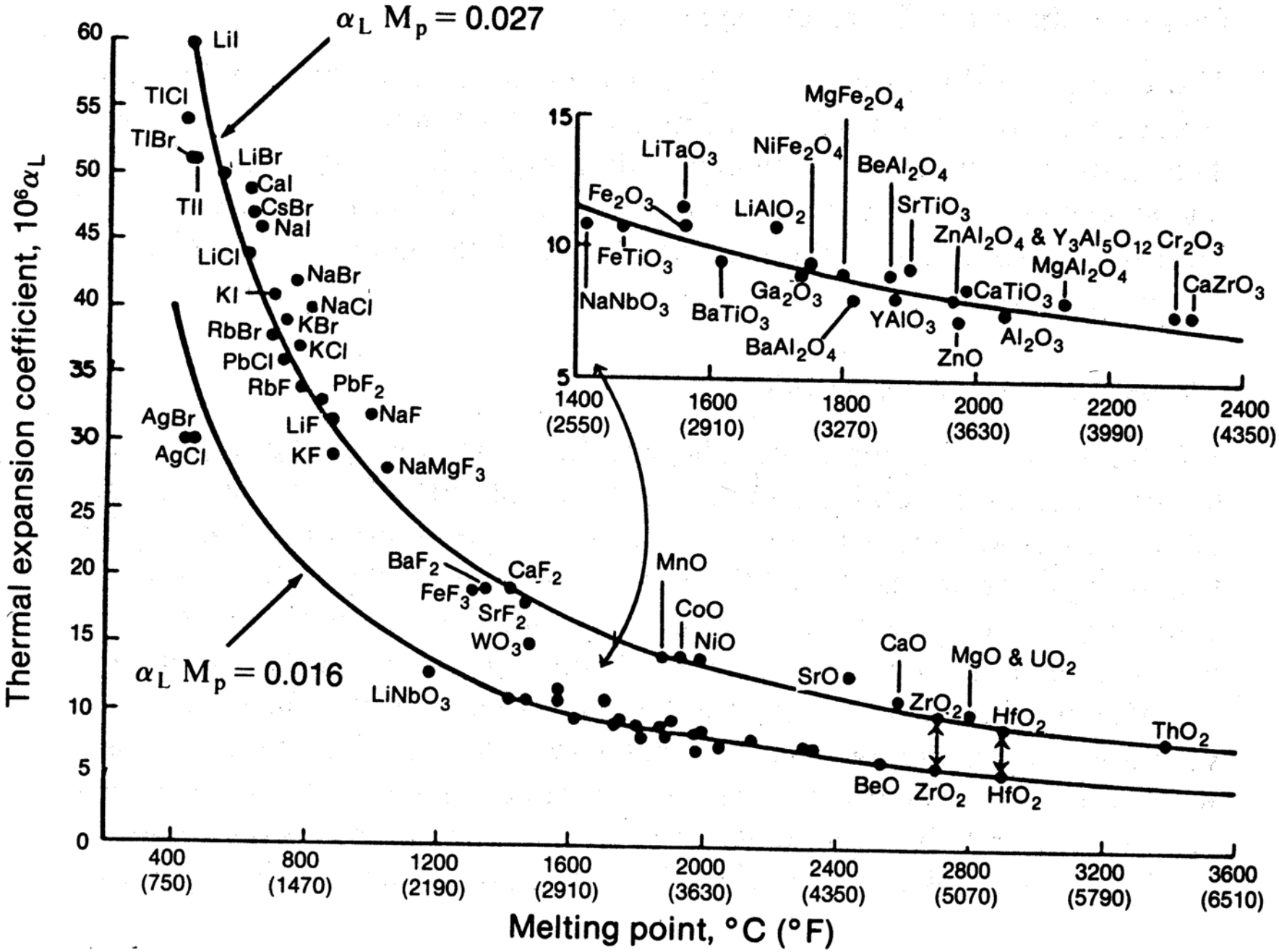
α_L $M_p = 0.027$
α_L $M_p = 0.016$
Thermal expansion coefficient, $10^6\alpha_L$
Melting point, °C (°F)
LiI
TlCl
TlBr
LiBr
CaI
CsBr
NaI
TlI
LiCl
NaBr
KI
NaCl
KBr
RbBr
KCl
PbCl
RbF
PbF_2
NaF
AgBr
AgCl
LiF
KF
$NaMgF_3$
BaF_2
CaF_2
FeF_3
SrF_2
WO_3
$LiNbO_3$
MnO
CoO
NiO
SrO
CaO
MgO & UO_2
ZrO_2
HfO_2
ThO_2
BeO
ZrO_2
HfO_2
$MgFe_2O_4$
$LiTaO_3$
$NiFe_2O_4$
$BeAl_2O_4$
Fe_2O_3
$LiAlO_2$
$SrTiO_3$
$ZnAl_2O_4$ & $Y_3Al_5O_{12}$
Cr_2O_3
$MgAl_2O_4$
$FeTiO_3$
$CaZrO_3$
$NaNbO_3$
$BaTiO_3$
Ga_2O_3
$CaTiO_3$
$YAlO_3$
$BaAl_2O_4$
Al_2O_3
ZnO
60
55
50
45
40
35
30
25
20
15
10
5
0
15
10
5
400 (750)
800 (1470)
1200 (2190)
1600 (2910)
2000 (3630)
2400 (4350)
2800 (5070)
3200 (5790)
3600 (6510)
1400 (2550)
1600 (2910)
1800 (3270)
2000 (3630)
2200 (3990)
2400 (4350)

Preparazione di uno specchio telescopico in vetroceramica ZERODUR della Schott: CTE 0,02x 10^{-7} k^{-1} (0° - 50° C)

Young's modulus

$$E = CMf^2$$

C constant on shape

M mass of the component

f flexural resonating frequency

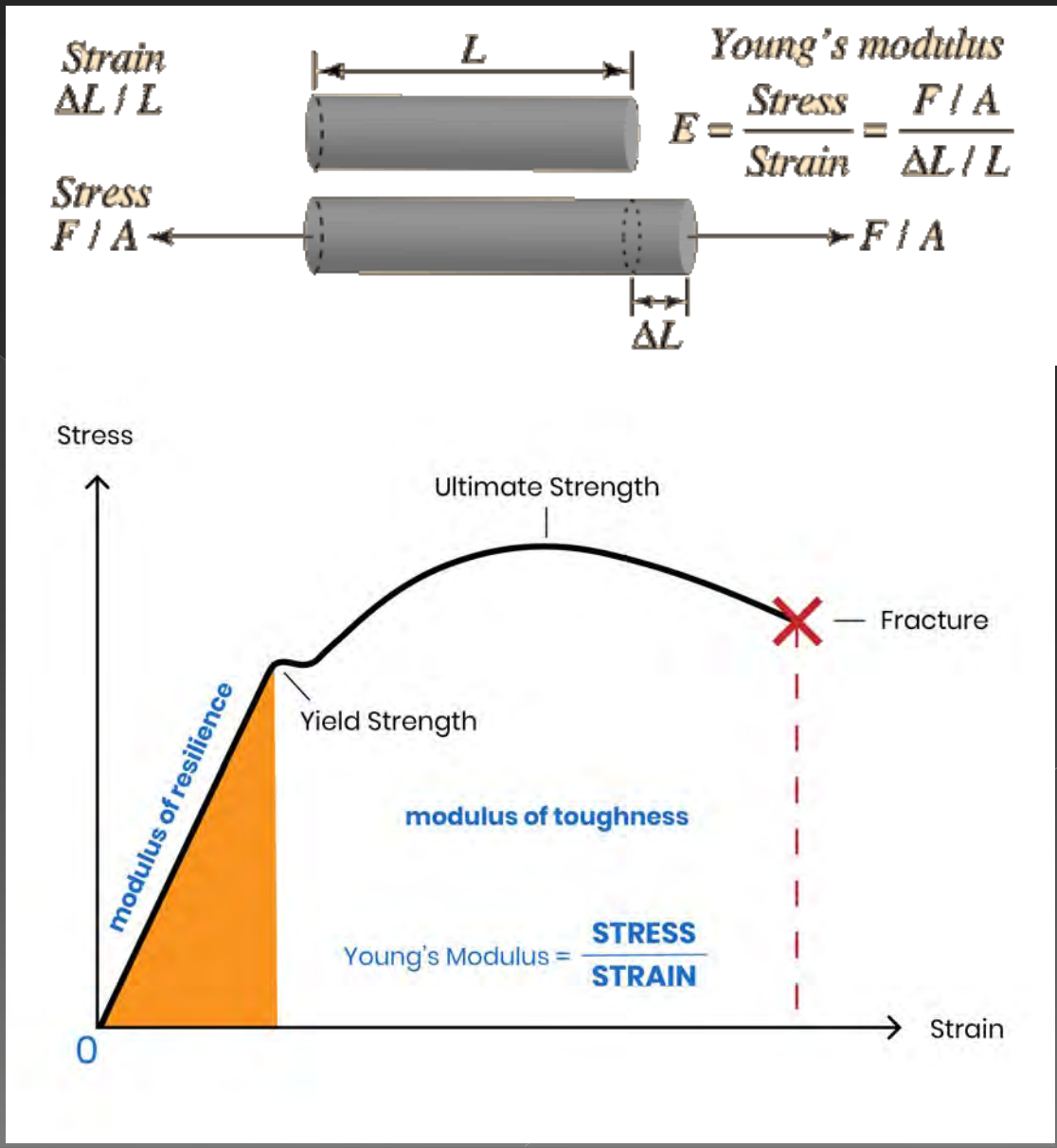

Poisson'modulus: it is the ration of the transverse strain (x) to the axial strain (y)

- $\upsilon = \frac{\Delta L_x / L_x^0}{\Delta L_y / L_y^0}$

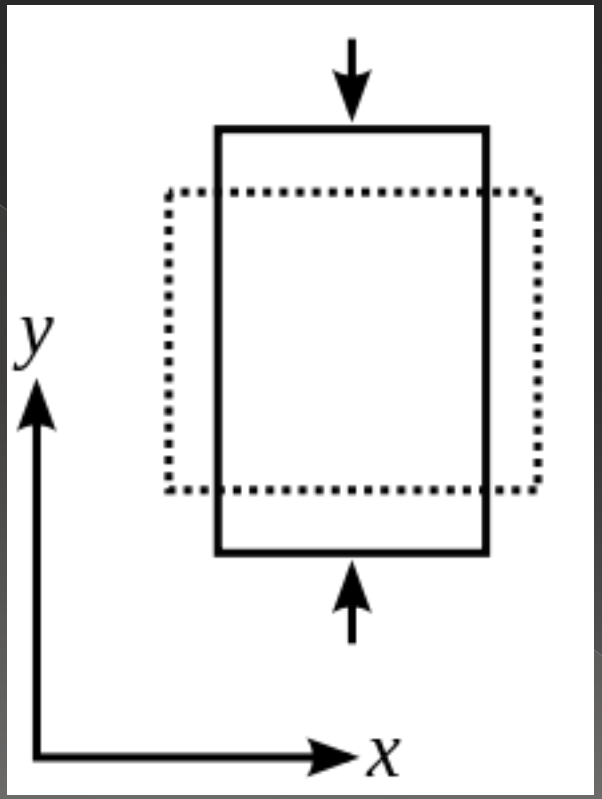

Rigidity modulus: it is the ratio of the shear stress to the shear strain

- $G = \frac{F}{A}\frac{L}{\Delta x}$

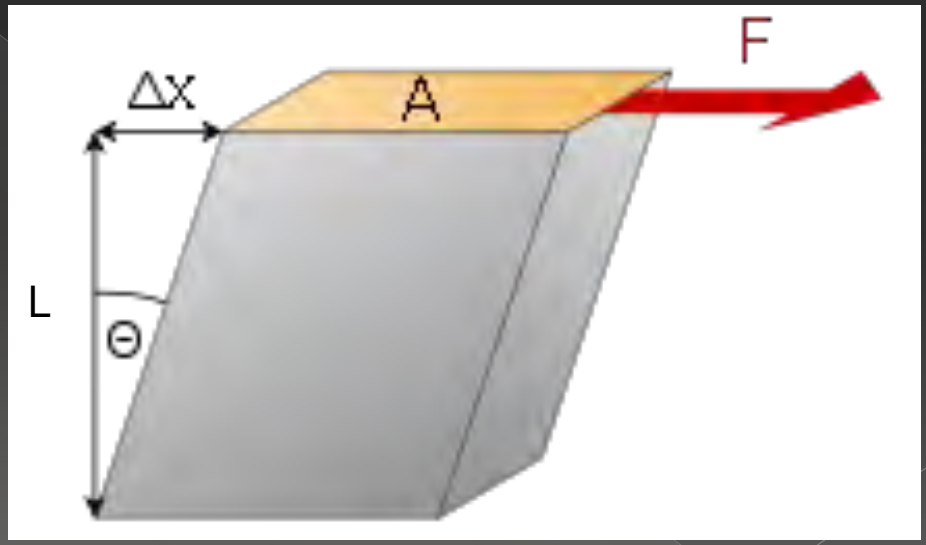

Bulk modulus: it is the ratio of the isostatic stress (pressure) to the volumetric strain

- $K = -P\frac{V^{\circ}}{\Delta V}$

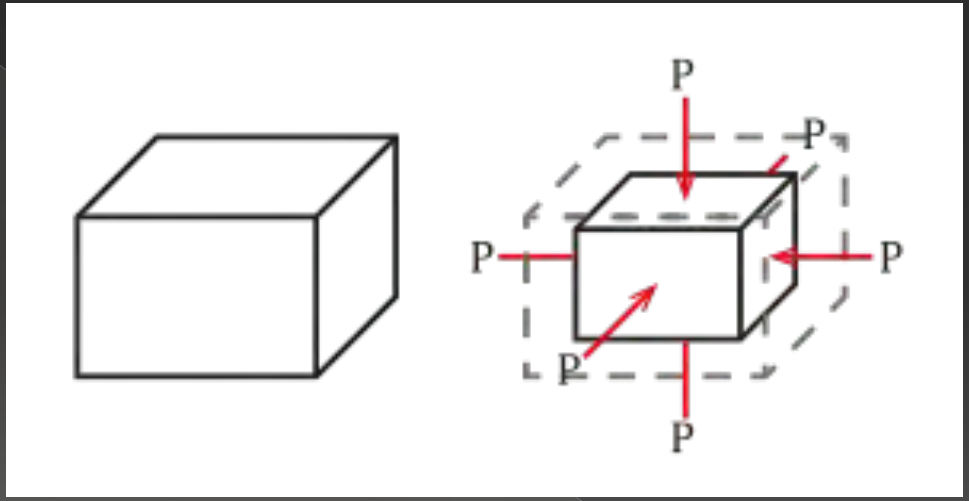

Relations among elastic constants

- E , Young modulus
- ν , Poisson modulus
- G, Rigidity (shear) modulus
- K, bulk modulus

- $E = 2G(1 + \nu)$ $\quad$ $E=3K(1-2\nu)$

- $E=9KG/(3K-G)$ $\quad$ $\nu=(3K-2G)/(6K+2G)$

Importance of TEC: Stress build-up

T_o , $\alpha_1 > \alpha_2$

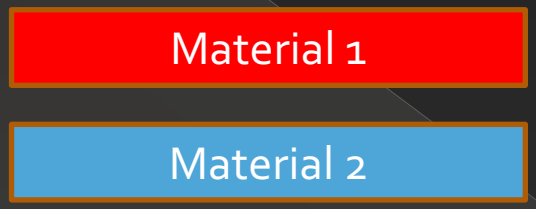

$T_1 > T_0$

If materials are joined together there must be displacement compatibility, which generates stresses

$$\sigma_1 = \frac{E_1}{(1-\upsilon_1)}(\alpha_2 - \alpha_1)\Delta T$$

Asby map Young modulus/density

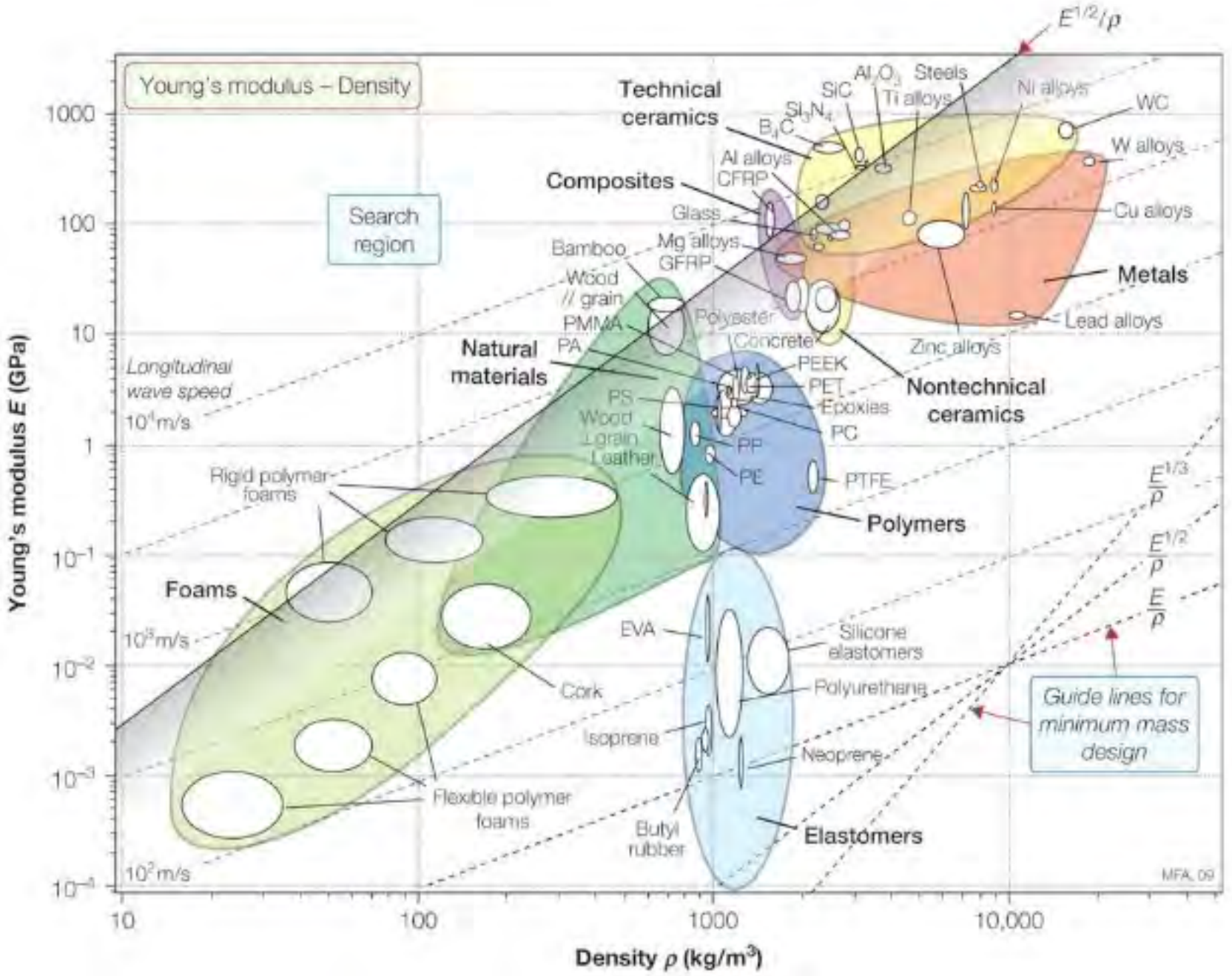

TABLE 16.2 Elastic Constants of Selected Polycrystalline Ceramics (20°C)

Material	*Crystal type*	*μ (GPa)*	B *(GPa)*	*ν*	*E (GPa)*
Carbides					
C	Cubic	468	416	0.092	1022
SiC	Cubic	170	210	0.181	402
TaC	Cubic	118	217	0.270	300
TiC	Cubic	182	242	0.199	437
ZrC	Cubic	170	223	0.196	407
Oxides					
Al_2O_3	Trigonal	163	251	0.233	402
$Al_2O_3 \cdot MgO$	Cubic	107	195	0.268	271
$BaO \cdot TiO_2$	Tetragonal	67	177	0.332	178
BeO	Tetragonal	165	224	0.204	397
CoO	Cubic	70	185	0.332	186
$FeO \cdot Fe_2O_3$	Cubic	91	162	0.263	230
Fe_2O_3	Trigonal	93	98	0.140	212
MgO	Cubic	128	154	0.175	300
$2MgO \cdot SiO_2$	Orthorhombic	81	128	0.239	201
MnO	Cubic	66	154	0.313	173
SrO	Cubic	59	82	0.210	143
$SrO \cdot TiO_2$	Cubic	266	183	0.010	538
TiO_2	Tetragonal	113	206	0.268	287
UO_2	Cubic	87	212	0.319	230
ZnO	Hexagonal	45	143	0.358	122
ZrO_2–$12Y_2O_3$	Cubic	89	204	0.310	233
SiO_2	Trigonal	44	38	0.082	95

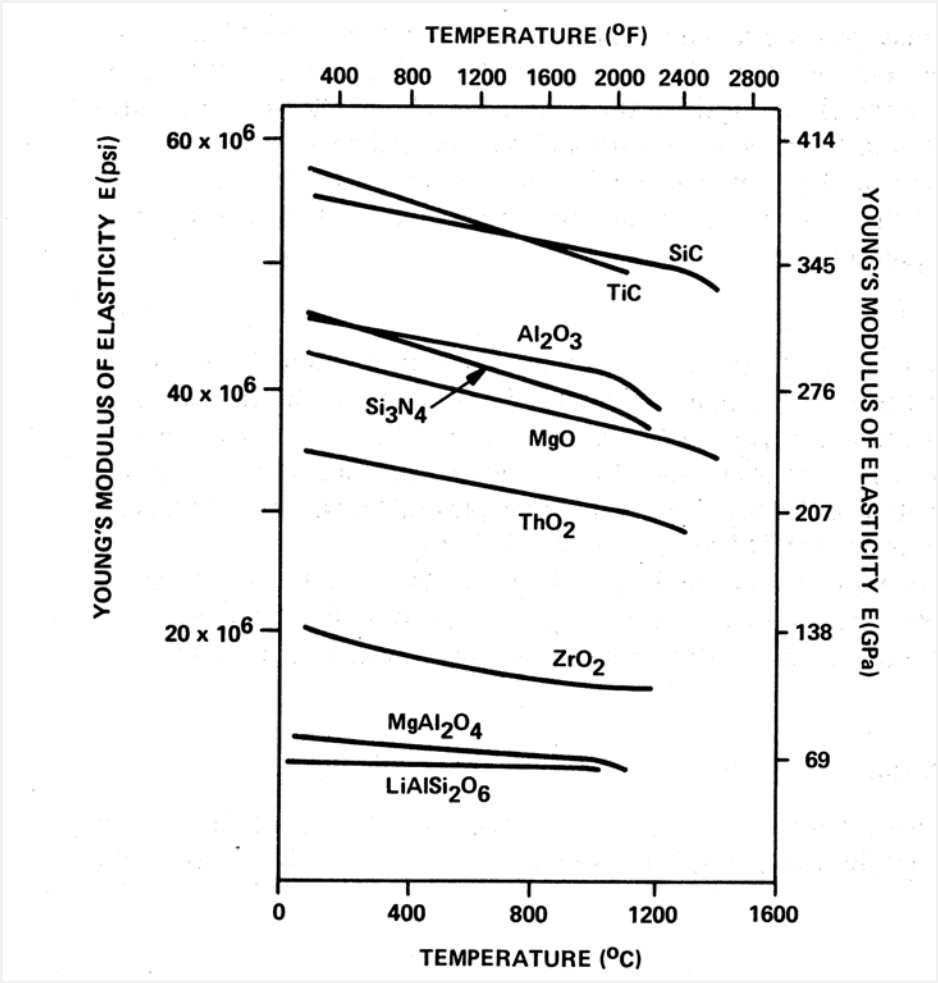
TEMPERATURE (°F)
400
800
1200
1600
2000
2400
2800
YOUNG'S MODULUS OF ELASTICITY E(psi)
60 x 10^6
40 x 10^6
20 x 10^6
YOUNG'S MODULUS OF ELASTICITY E(GPa)
414
345
276
207
138
69
SiC
TiC
Al2O3
Si3N4
MgO
ThO2
ZrO2
MgAl2O4
LiAlSi2O6
0
400
800
1200
1600
TEMPERATURE (°C)

Commonly Used Mechanical Testing Techniques

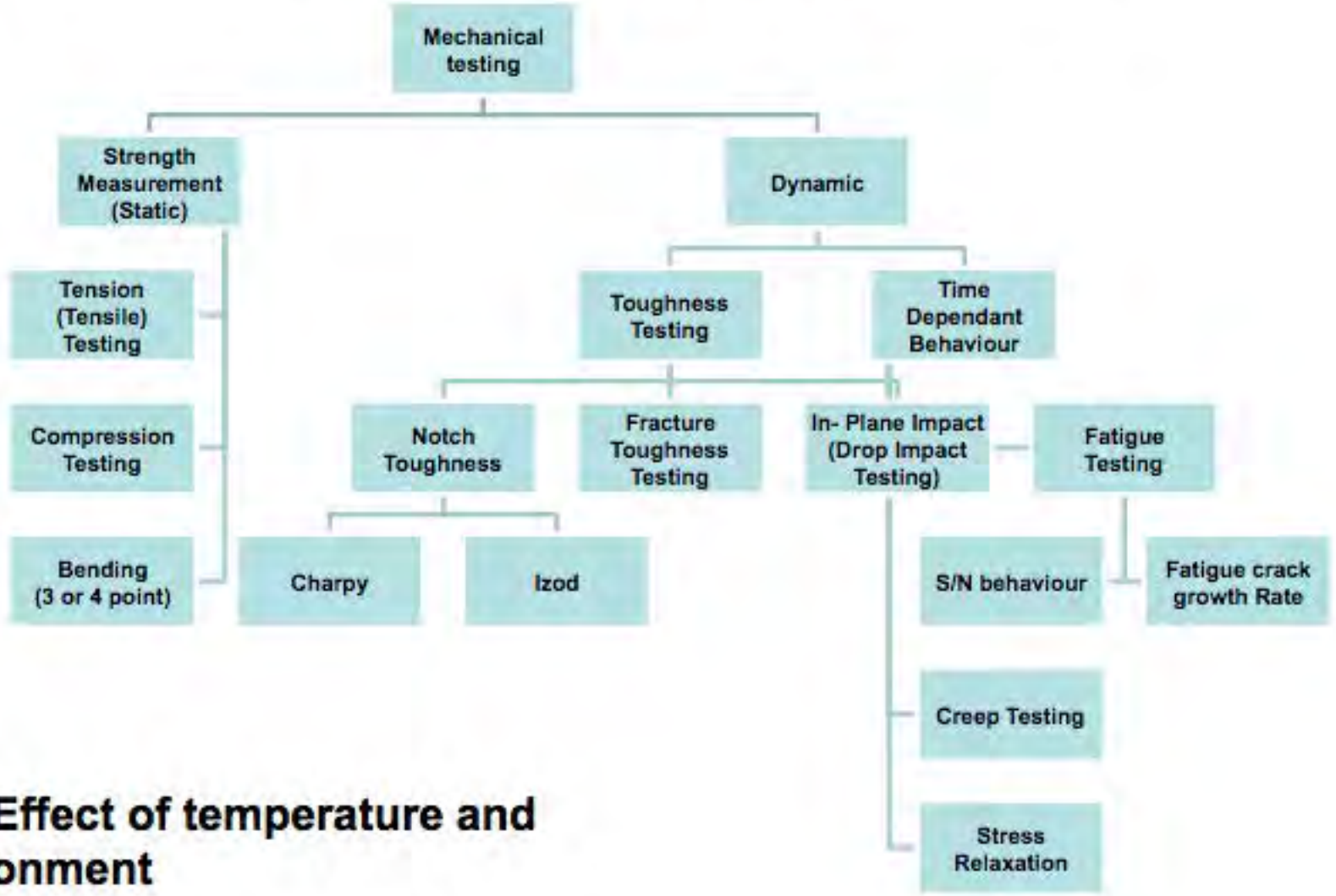

Plus Effect of temperature and environment

Strength

MODULUS OR RUPTURE EQUATIONS

Three-point bend: $\sigma_r = \frac{3PL}{2BW^2}$

Four-point bend: $\sigma_r = \frac{3PD}{BW^2}$

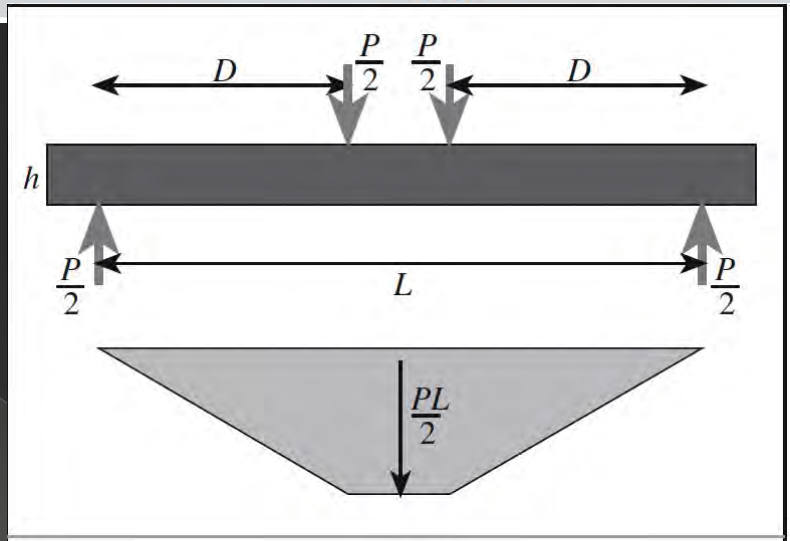

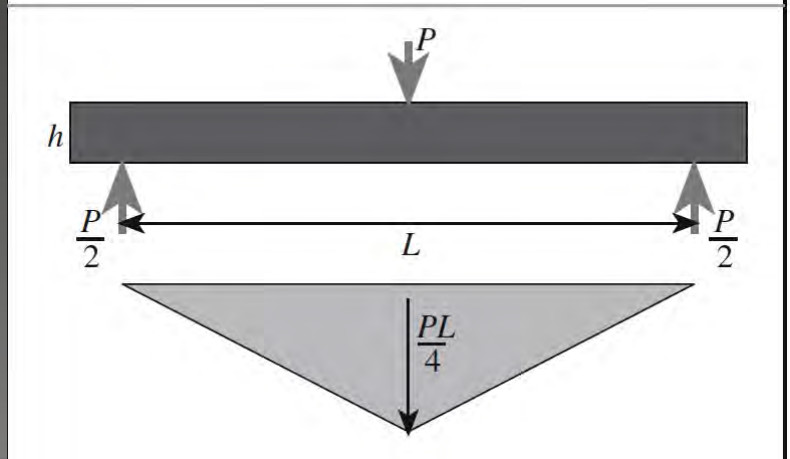

Tensile tests with and without luders behaviour
https://www.youtube.com/watch?v=D8U4G5kcpcM

Bending strength in 3-points

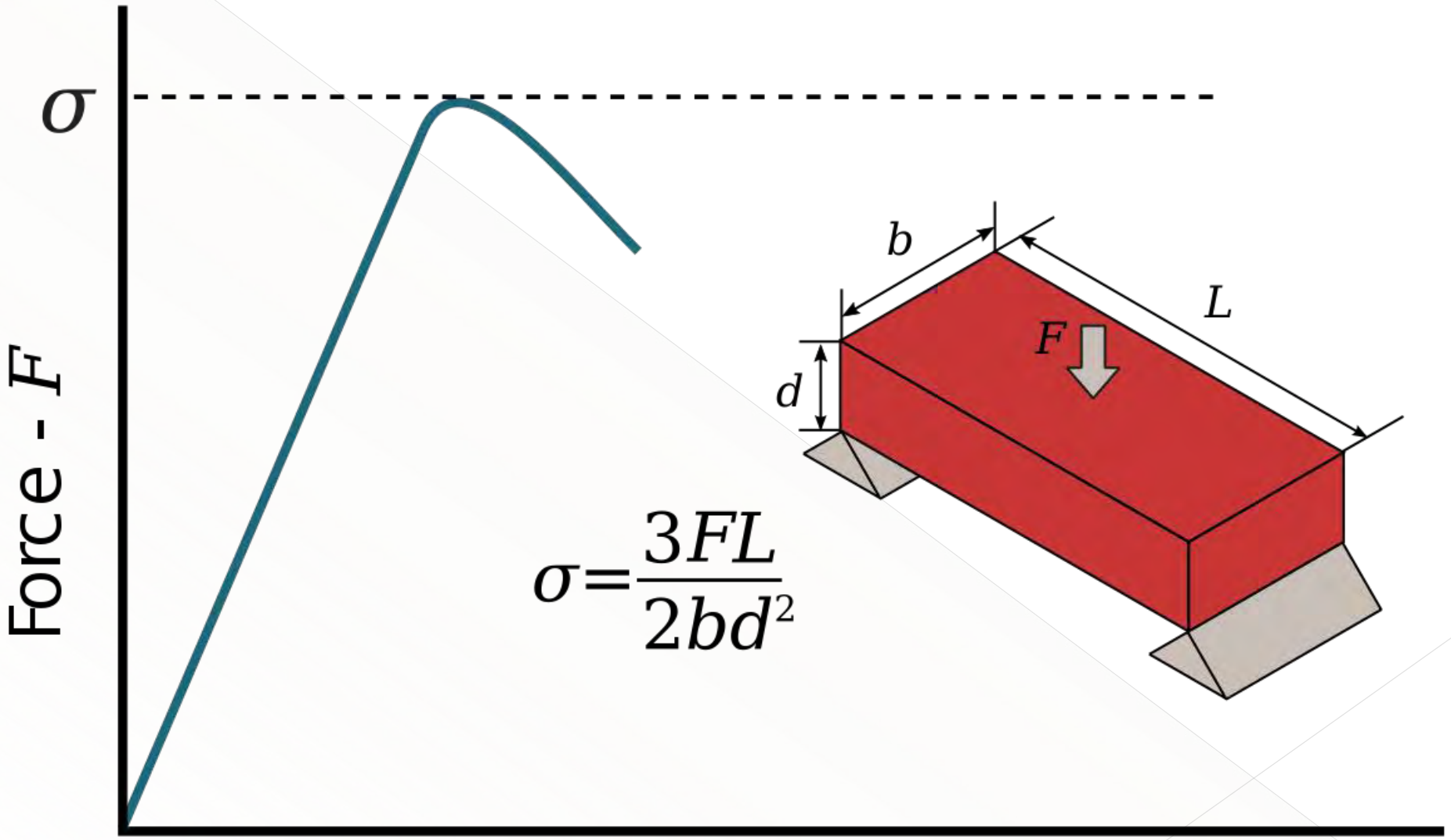

$$\sigma = \frac{3FL}{2bd^2}$$

Ashby map strength/density

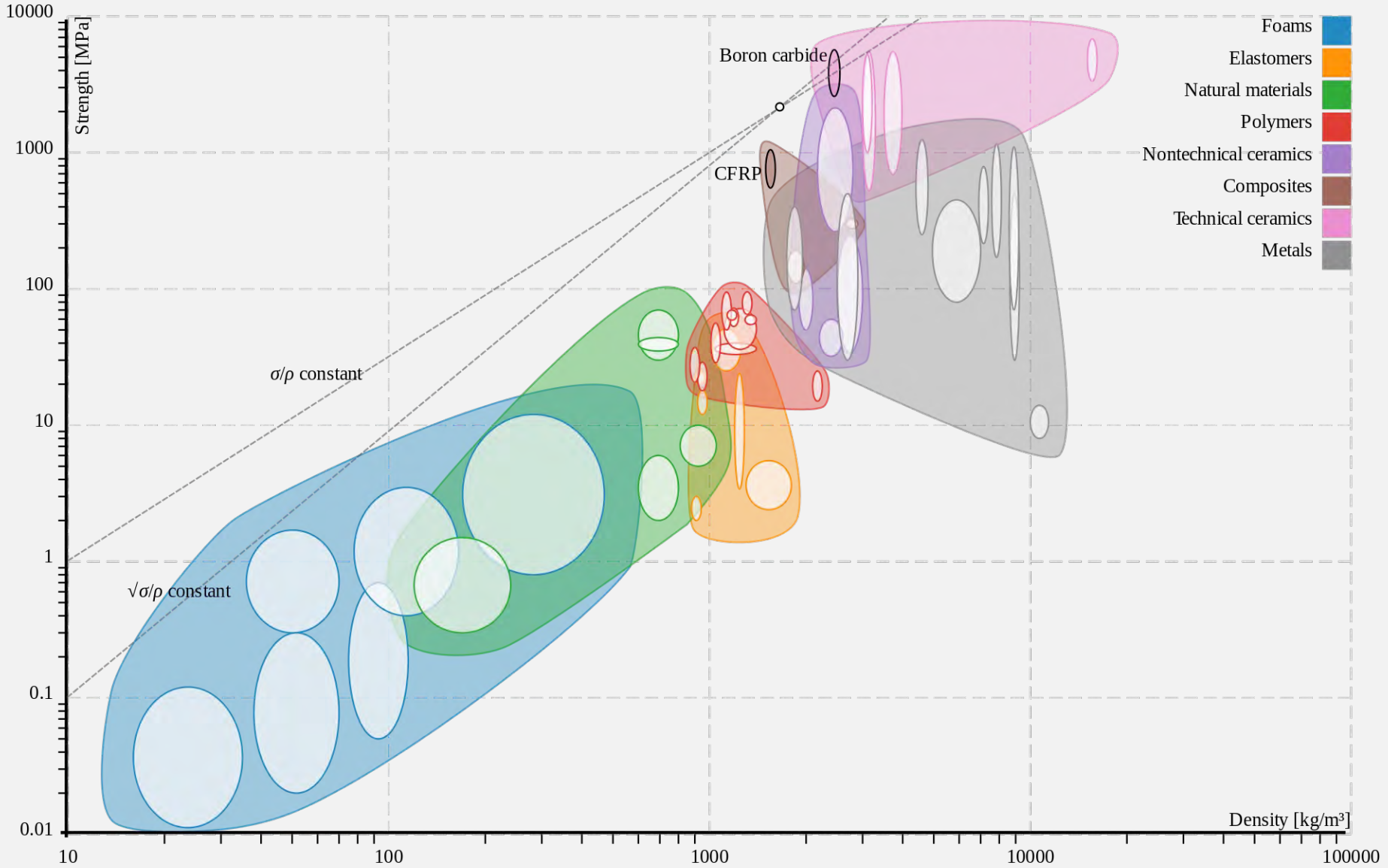

Ashby map strength/density

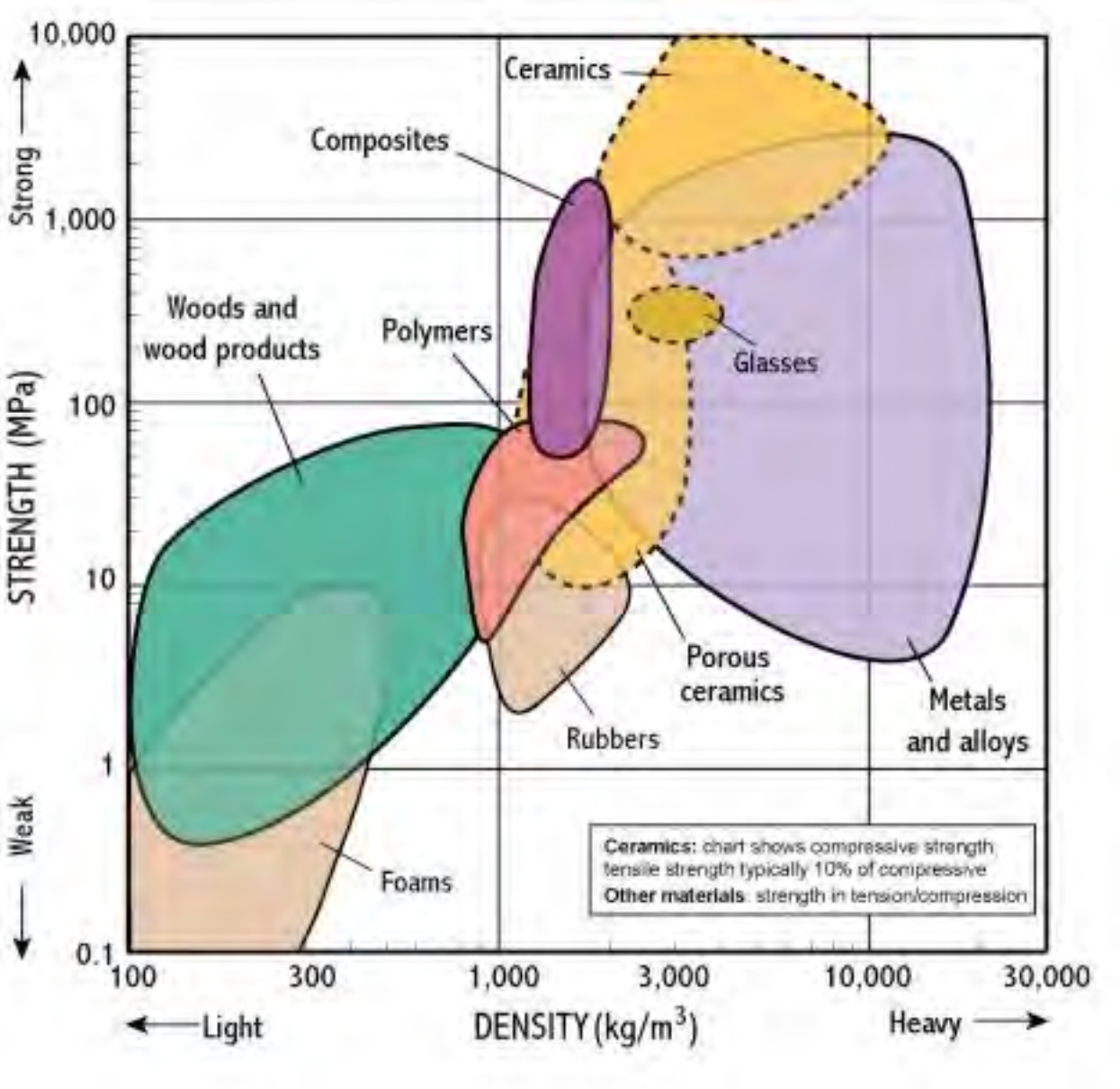

Orowan approach

$$\sigma th = \sqrt{\left(\frac{E\gamma}{a_0}\right)}$$

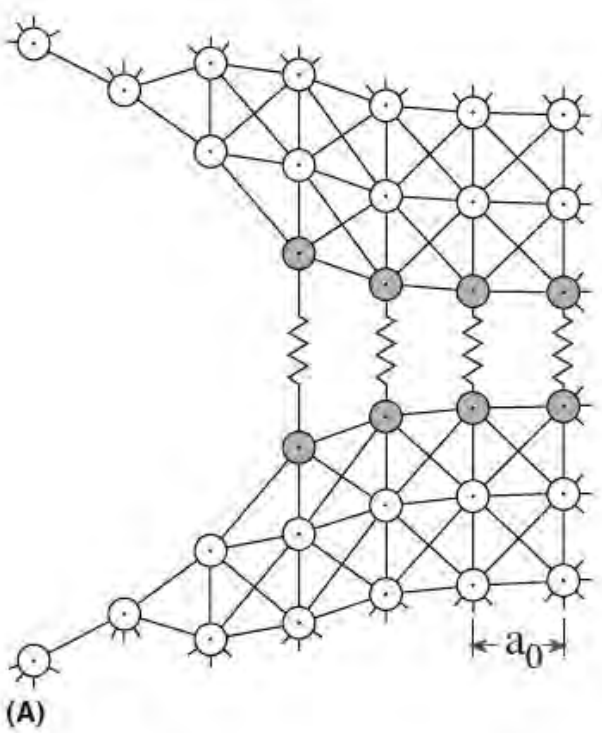

Table 5.3 Comparison of Theoretical Strength and Actual Strength

Material	*E* [GPa (psi)]	Estimated theoretical strength [GPa (psi)]	Measured strength of fibers [GPa (psi)]	Measured strength of polycrystalline specimen [GPa (psi)]
Al_2O_3[a]	380 (55×10^6)	38 (5.5×10^6)	16 (2.3×10^6)	0.4 (60×10^3)
SiC	440 (64×10^6)	44 (6.4×10^6)	21 (3.0×10^6)	0.7 (100×10^3)

[a]From R. J. Stokes, *The Science of Ceramic Machining and Surface Finishing*, NBS Special Publication 348, U.S. Government Printing Office, Washington, D.C., 1972, p. 347.

Flaws are Stress Concentrators

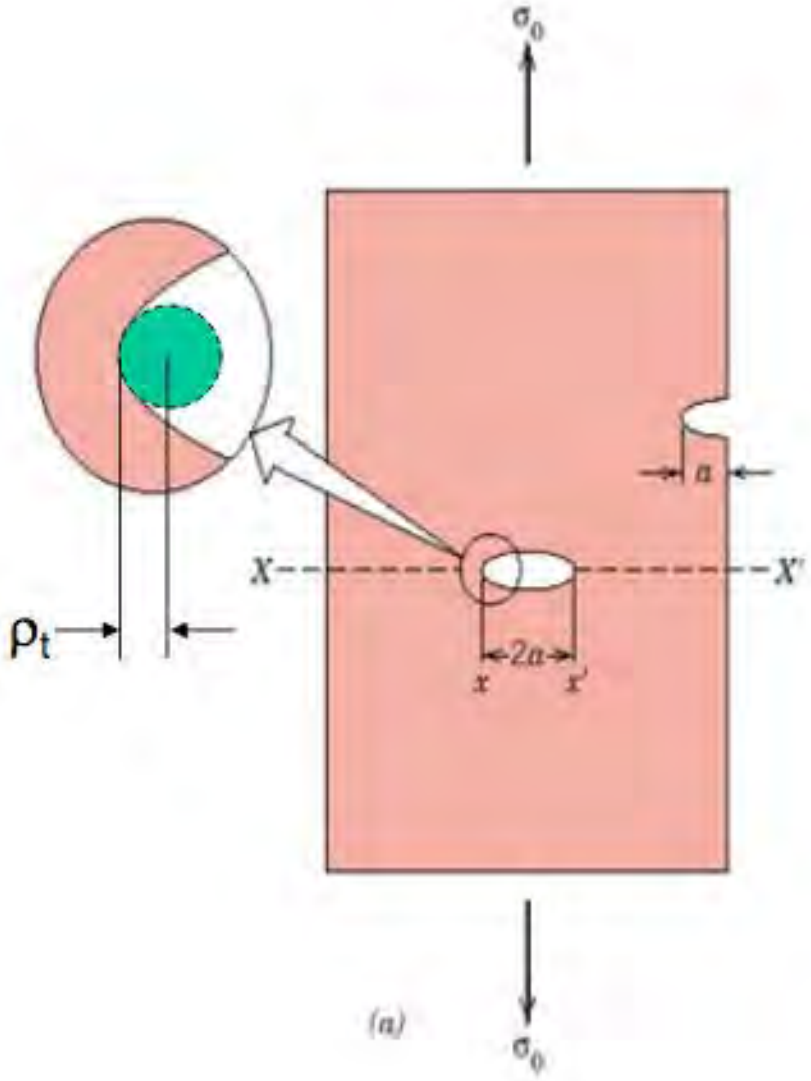

If the crack is similar to an elliptical hole through plate, and is oriented perpendicular to applied stress, the maximum stress σ_m=

$$\sigma_m = 2\sigma_o\left(\frac{a}{\rho_t}\right)^{1/2} = K_t\sigma_o$$

where

ρ_t = radius of curvature

σ_o = applied stress

σ_m = stress at crack tip

a = length of surface crack or ½ length of internal crack

$\sigma_m/\sigma_o = K_t$ the stress concentration factor

Concentration of Stress at Crack Tip

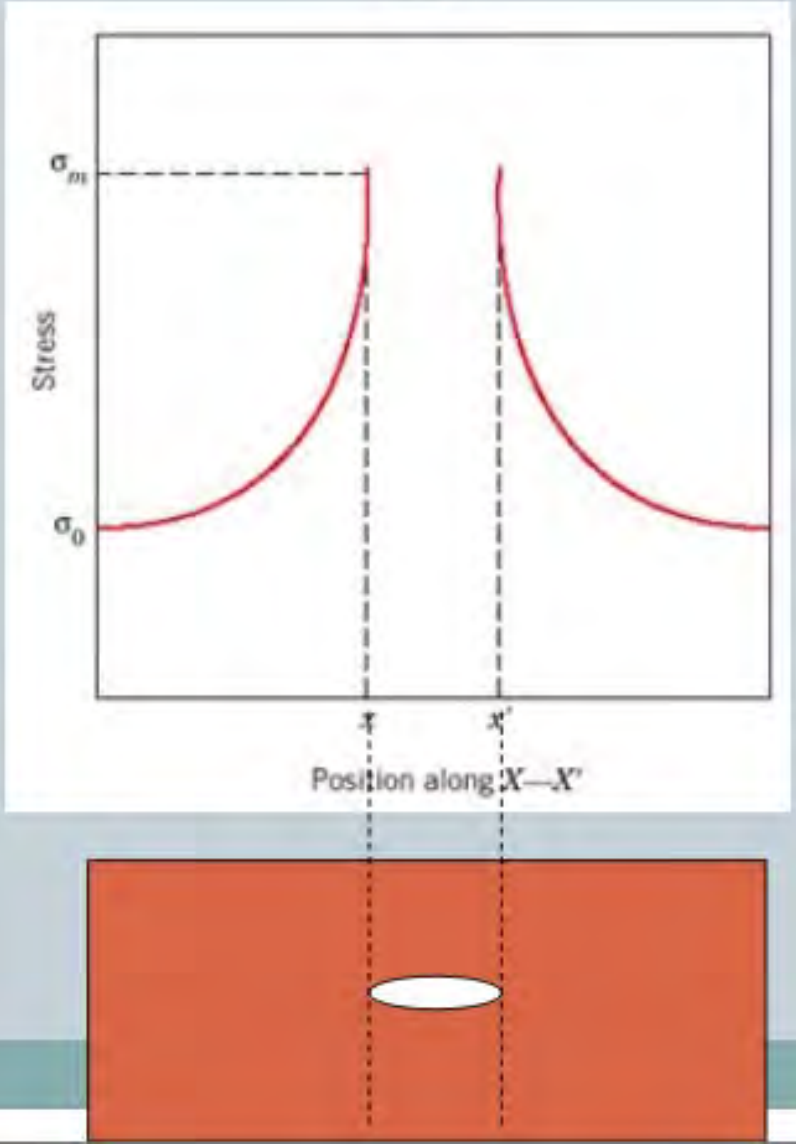

Griffith equation
(***a*** is crack length)

$$\sigma_c = \sqrt{\frac{2E\gamma}{\pi a}}$$

IRWIN approach: consider together stress AND crack length

$$K = Y\sigma\sqrt{\pi\, a}$$

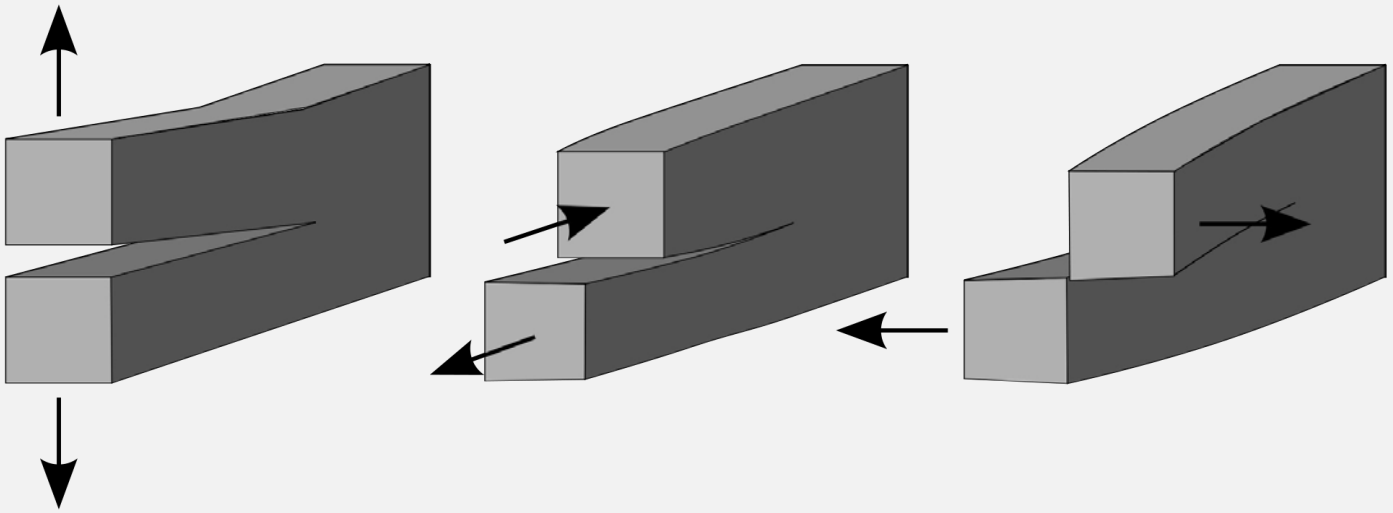

Mode I:
Opening

Mode II:
In-plane shear

Mode III:
Out-of-plane shea

$$K = Y\sigma\sqrt{\pi\, a}$$

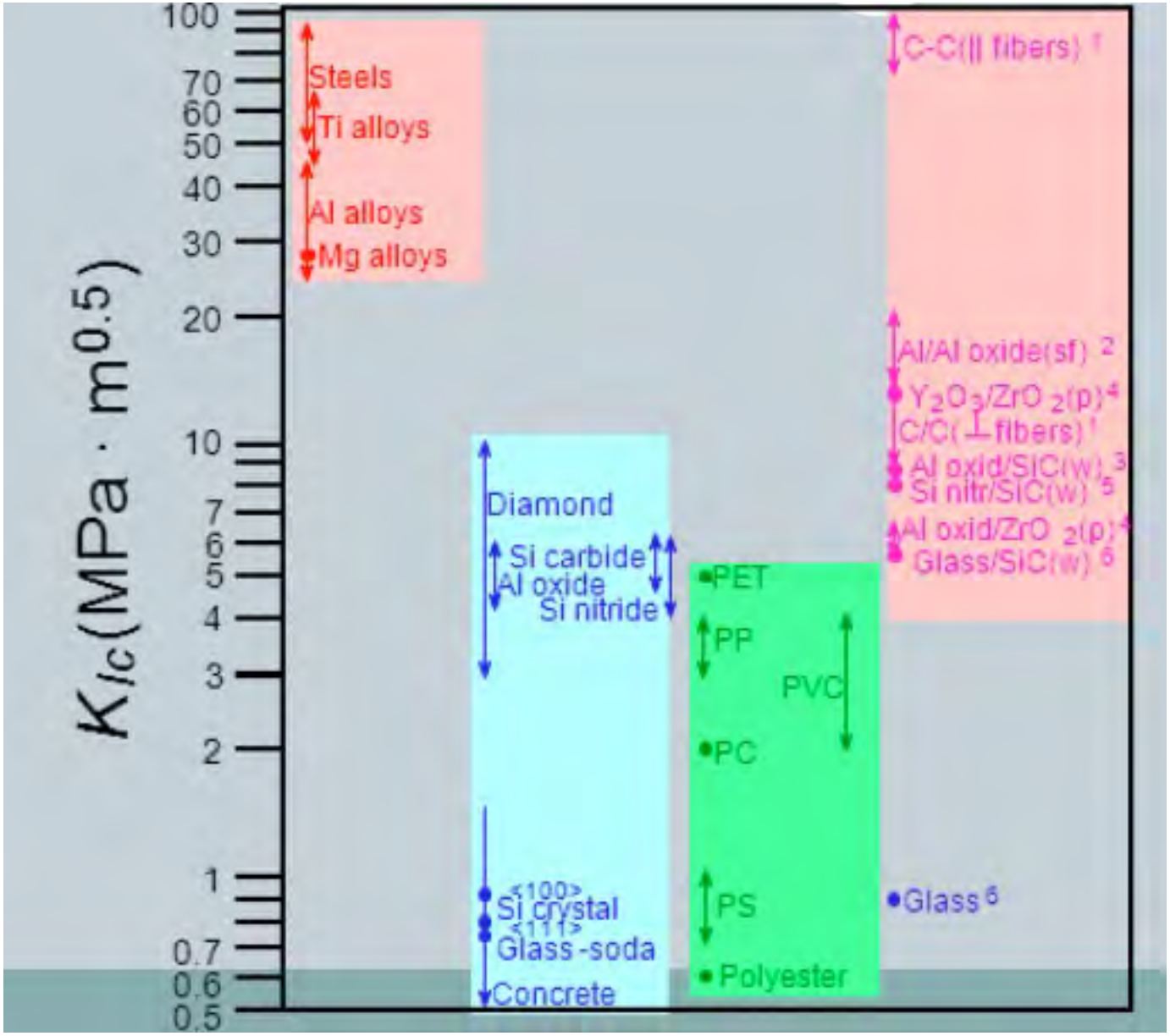

DESIGN AGAINST CRACK GROWTH

- **Crack growth condition:** $K \geq K_c$

$$K = Y\sigma\sqrt{\pi a}$$

- **Largest, most stressed cracks grow first.**

--Result 1: Max flaw size dictates design stress.

$$\sigma_{design} < \frac{K_c}{Y\sqrt{\pi a_{max}}}$$

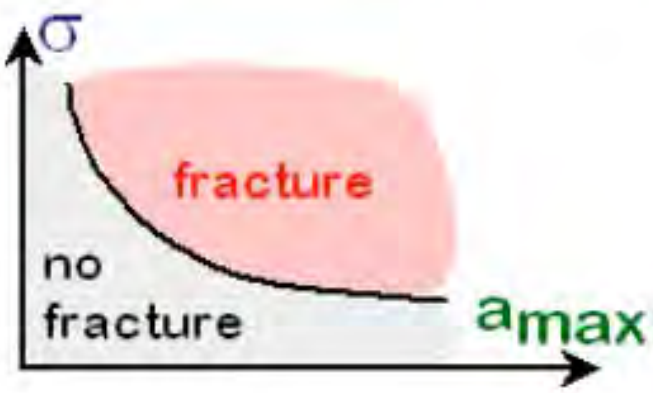

--Result 2: Design stress dictates max. flaw size.

$$a_{max} < \frac{1}{\pi}\left(\frac{K_c}{Y\sigma_{design}}\right)^2$$

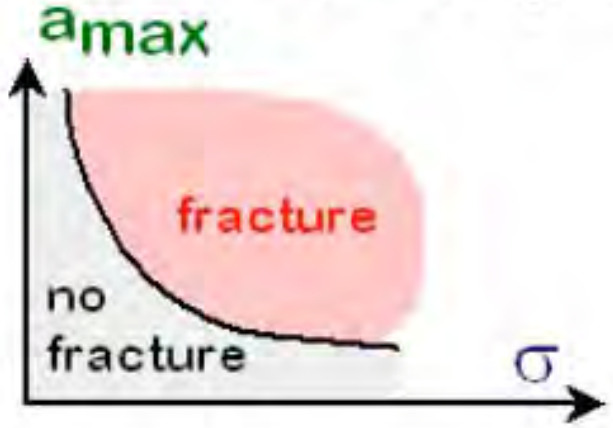

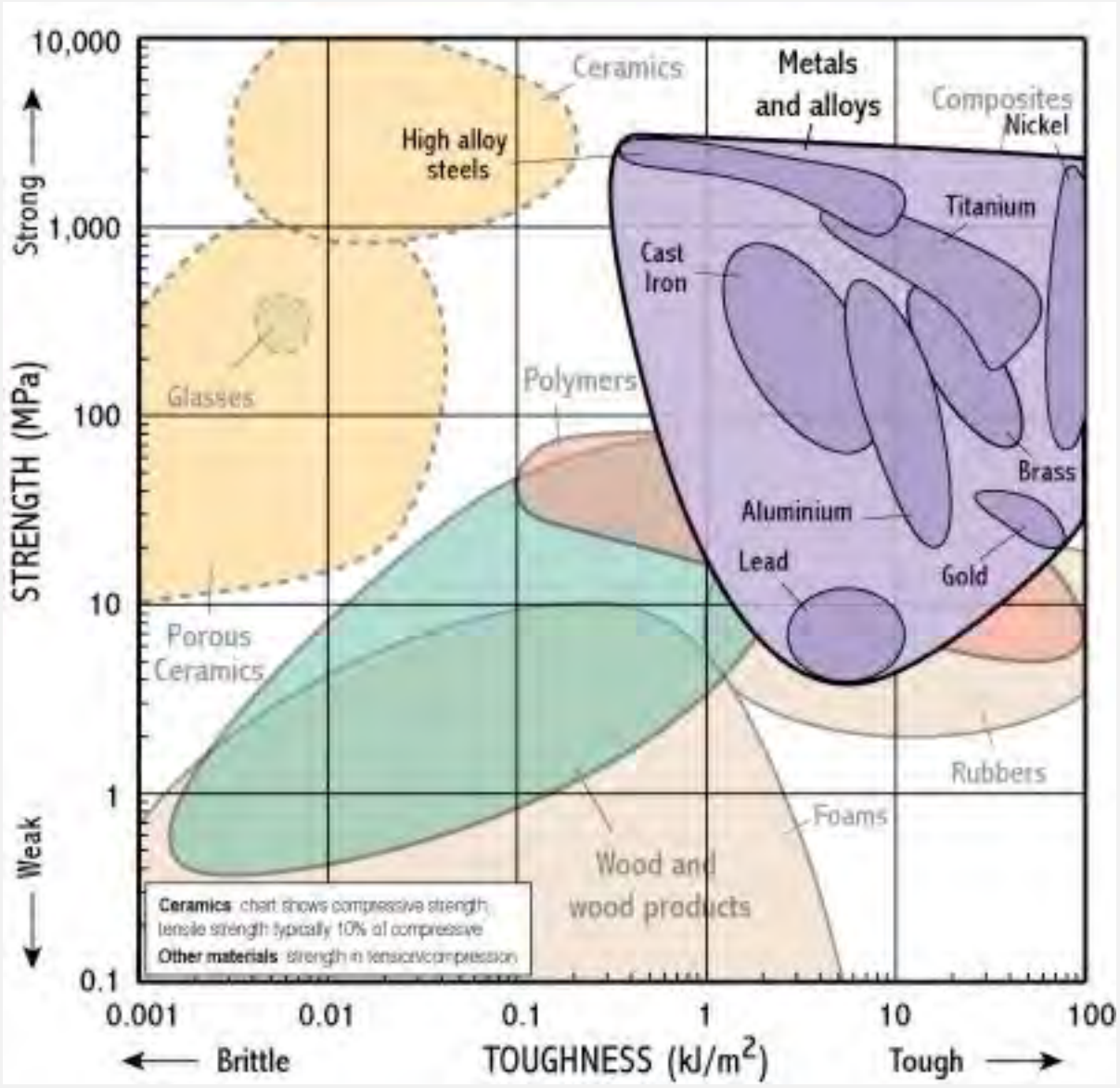
10,000
1,000
100
10
1
0.1
Strong
Weak
STRENGTH (MPa)
Ceramics
Metals
and alloys
Composites
Nickel
High alloy
steels
Titanium
Cast
Iron
Glasses
Polymers
Brass
Aluminium
Lead
Gold
Porous
Ceramics
Rubbers
Foams
Wood and
wood products
Ceramics chart shows compressive strength;
tensile strength typically 10% of compressive
Other materials strength in tension/compression
0.001
0.01
0.1
1
10
100
Brittle
TOUGHNESS (kJ/m2)
Tough

III.4 FRACTURE TOUGHNESS – STRENGTH

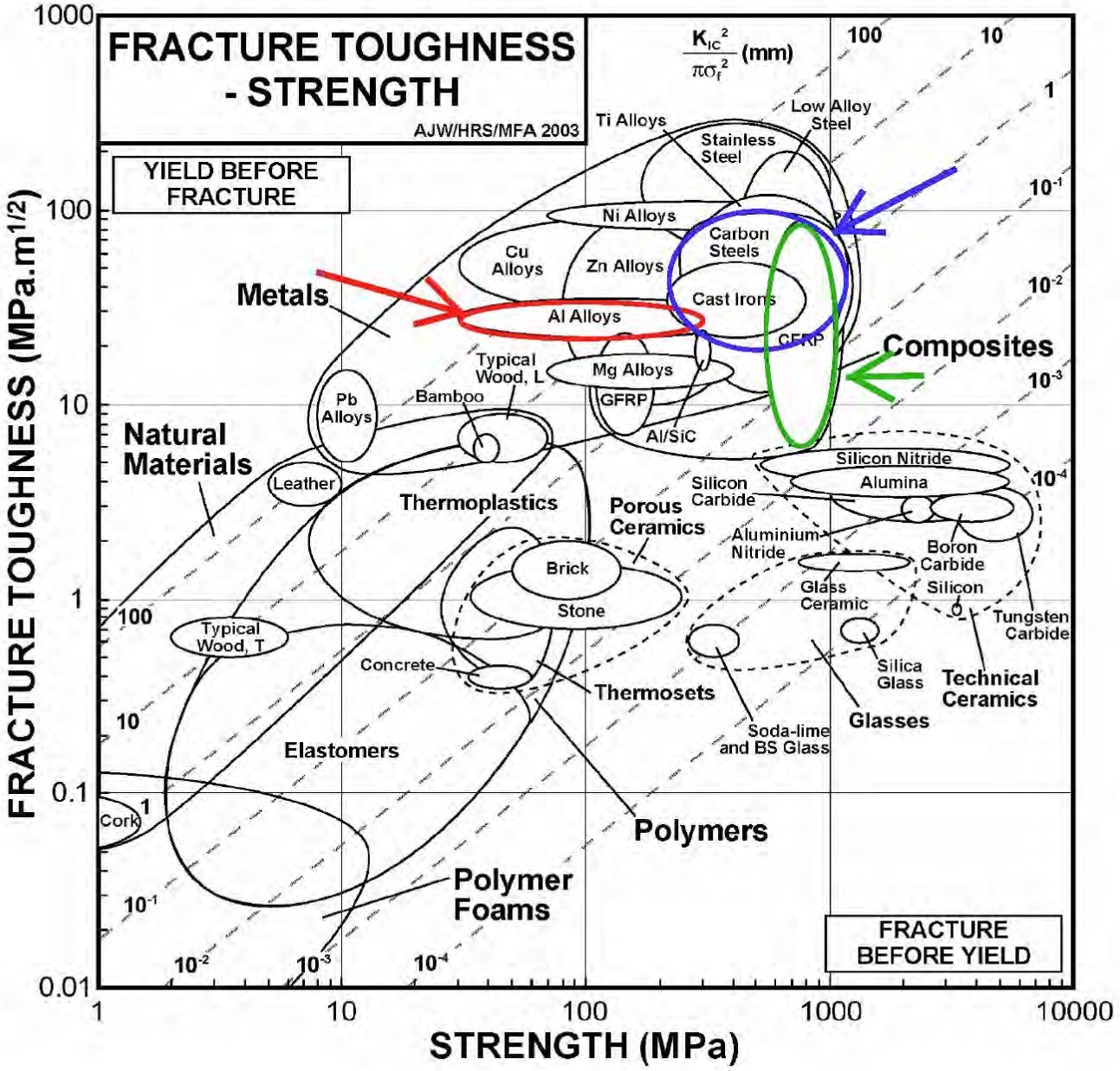

COMPARING CERAMICS AND METALS PART I					
Property	Density (g/cm2)	Elastic modulus (GPa)	Flexural strength (GPa)	Fracture toughness (MPa * m2)	Max. service temperature (°C)
Aluminum oxide (sintered)	3.9	395	300	3-4	1,700
Zirconium oxide (sintered)	6.1	210	1,050	7	1,500
Silicon carbide (hot press)	3.1	400	380	3	1,600
Silicon nitride (Reaction bonded and sintered)	3.2	310	600	6	1,000
Boron nitride (hot press)	2.3	675	51	2.6	1,000
Silicon carbide (including fiber composite0	2.5	270	360	39	1,600
Advanced high-strength steel (QuesTek C61)	7.9	200	1,650	140	430

Accurate determinations of K_{IC}

(a) SINGLE-EDGE NOTCHED BEAM (SENB) SPECIMEN

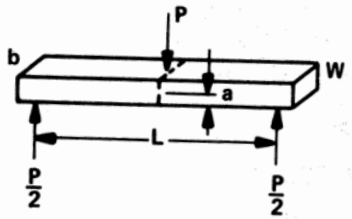

$$K_I = Y \frac{3PL}{2bW^2} \sqrt{a}$$

$$Y = 1{\cdot}96 - 2{\cdot}75\left(\frac{a}{W}\right) + 13{\cdot}66\left(\frac{a}{W}\right)^2$$
$$-23{\cdot}98\left(\frac{a}{W}\right)^3 + 25{\cdot}22\left(\frac{a}{W}\right)^4$$

(b) DOUBLE TORSION (DT) SPECIMEN

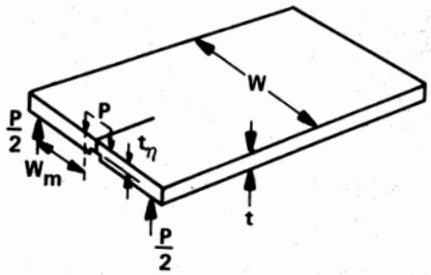

$$K_I = PW_m \left[\frac{3(1+\nu)}{Wt^3 t_\eta}\right]^{1/2}$$

(c) CONSTANT-MOMENT SPECIMEN

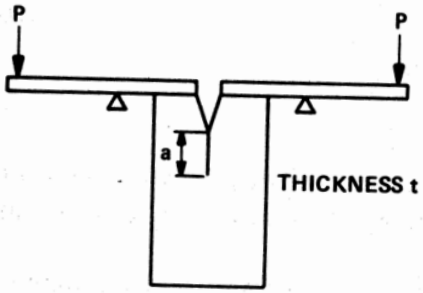

$$K_I = \frac{\text{MOMENT}}{\sqrt{It}}$$

I IS INERTIA OF ONE ARM.

(d) TAPERED DOUBLE CANTILEVER BEAM (TCB) SPECIMEN

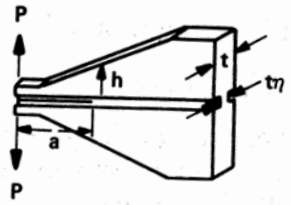

$$K_I = 2P\left(\frac{m}{tt_\eta}\right) \qquad M = \frac{1}{t}$$

SENB Specimen

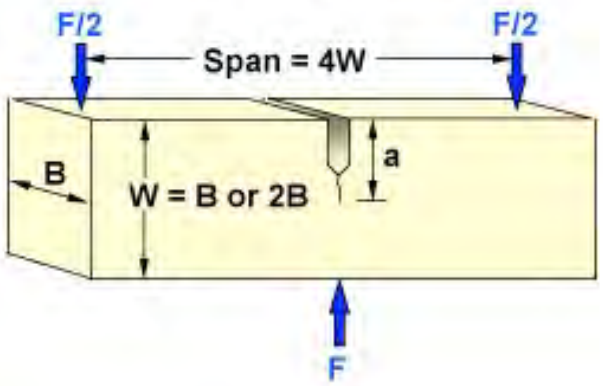

CT Specimen

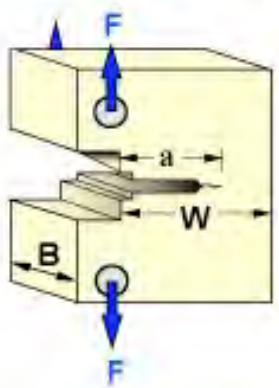

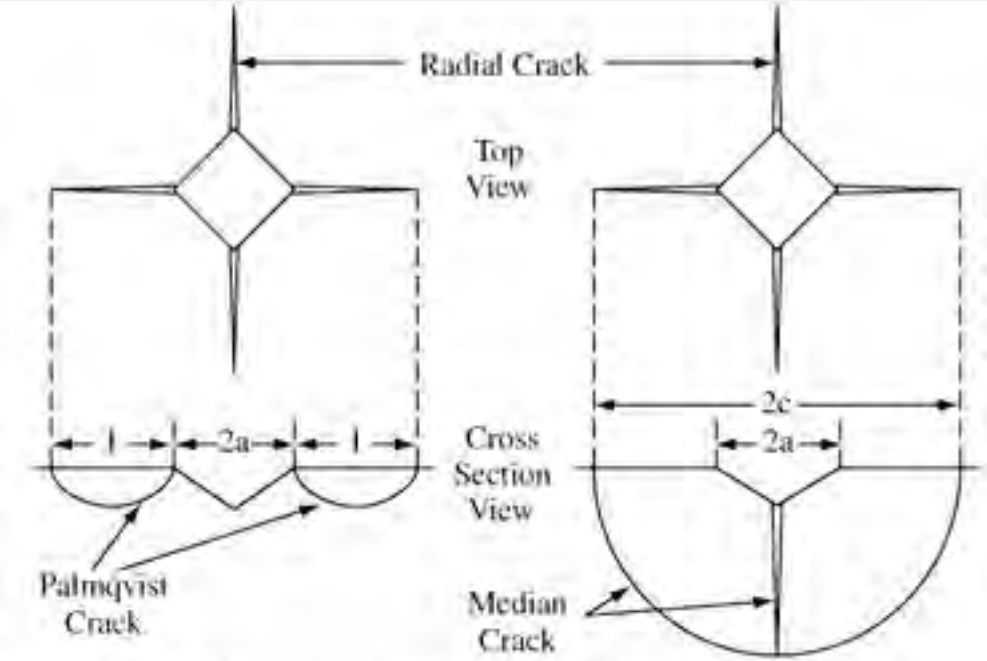

Figure 1. Crack formation by Vickers indentation.

$$K_c = 0{,}016\left(\frac{E}{H_V}\right)^{0,5}\frac{P}{c^{1,5}}$$

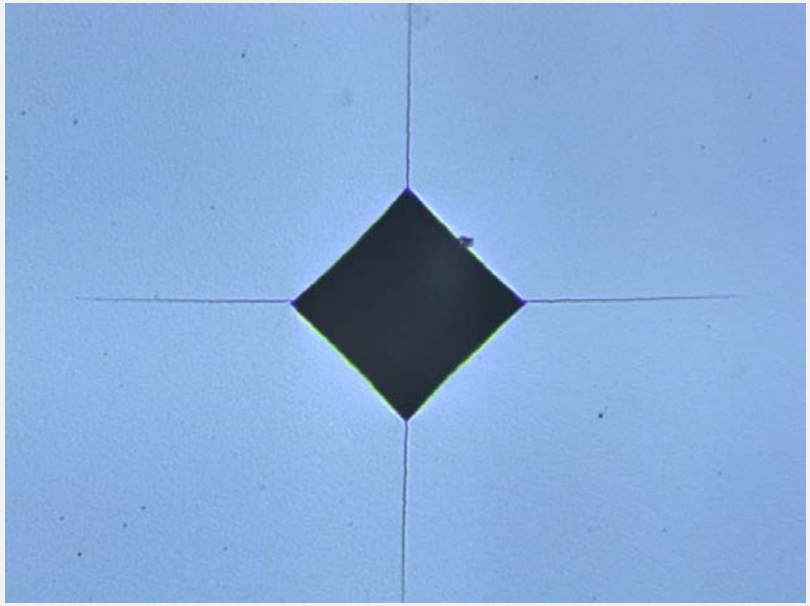

Table I. Materials Used in Indentation Toughness Studies

Material	Characterization	Grain size (μm)	E(GPa)	H(GPa)	K_c(MPa•m$^{1/2}$)	Toughness measurement[e]
Glass-ceramic (C9606)[a]	Glass-ceramic	1	108	8.4	2.5	DCB (standard)
Soda-lime glass I[b]	Amorphous		70	5.5	0.74	DCB (standard)
Soda-lime glass II[c]	Amorphous		73	5.6	0.75	DCB (standard) (Ref. 27)
Aluminosilicate glass[c]	Amorphous		89	6.6	0.91	DCB (standard) (Ref. 27)
Lead alkali glass[c]	Amorphous		65	4.9	0.68	DCB (standard) (Ref. 27)
Al_2O_3 (AD999)[d]	Polycrystal	3	406	20.1	3.9	DCB (standard)
Al_2O_3 (AD90)[d]	Polycrystal	4	390	13.1	2.9	DCB (standard)
Al_2O_3 (Vi)[e]	Polycrystal	20	305	19.1	4.6	DCB (D. B. Marshall)
Al_2O_3 (sapphire)[f]	Monocrystal[j]		425	21.8	2.1	DT (A. G. Evans[*] and E. A. Charles,[†] Ref. 20)
Si_3N_4 (NC132)[g]	Polycrystal	2	300	18.5	4.0	DCB (standard)
Si_3N_4 (NC350)[g]	Polycrystal	10	170	9.6	2.0	DT (S. M. Wiederhorn[‡] and N. J. Tighe[‡])
SiC(NC203)[g]	Polycrystal	4	436	24.0	4.0	DT (S. M. Wiederhorn[‡] and N. J. Tighe[‡])
ZrO (Ca-stabilized)[h]	Polycrystal	50	210	10.0	7.6	DCB (D. B. Marshall)
Si[i]	Monocrystal[k]		168	10.6	0.7	DT (S. M. Wiederhorn[‡] and E. R. Fuller[‡])
WC (Co-bonded)[c]	Polycrystal	3	575	13.2	12	DT (S. W. Freiman[‡])

[a]Pyroceram, Corning Glass Works, Corning, N. Y. [b]Commercial sheet glass. [c]National Bureau of Standards, Washington, D. C. [d]Coors Porcelain Co., Golden, Colo. [e]Vistal, Coors Porcelain Co. [f]Linde, Union Carbide Co., New York, N. Y. [g]Norton Co., Worcester, Mass. [h]CSIRO, Australia. [i]Texas Instruments, Inc., Dallas. [j]Rods, [0001] 30° to axis. [k]Disks, [111] parallel to axis. [l]DT = double torsion, DCB = double cantilever beam. [*]University of California, Berkeley. [†]Rockwell International Science Center, Thousand Oaks, Calif. [‡]National Bureau of Standards.

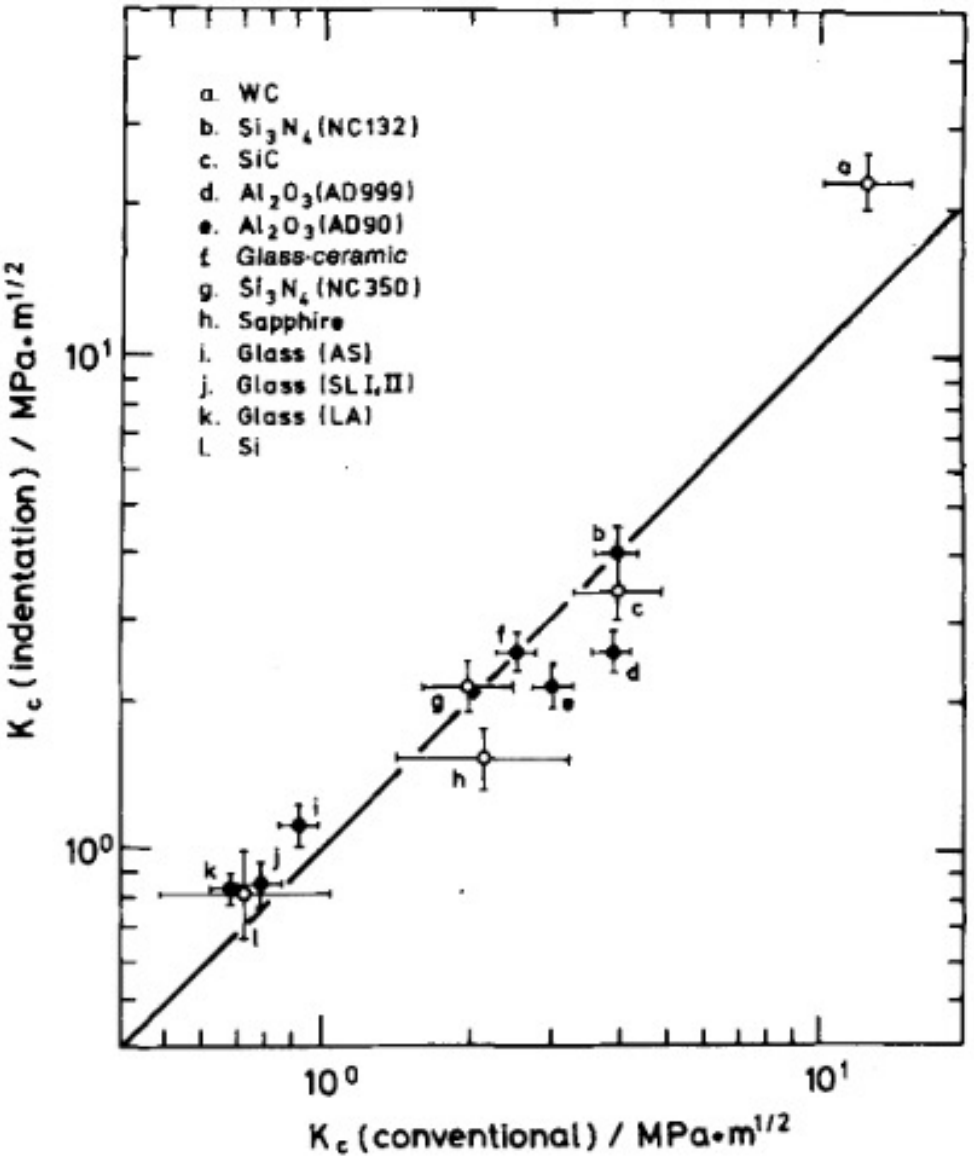

Fig. 5. Plot demonstrating correlation between toughness values determined by indentation and by conventional means. Filled symbols denote reference materials used to evaluate constant $\S_V^R$ in Eq. (4). Vertical error bars represent uncertainty (standard deviation) in parameter $P/c_0^{3/2}$ obtained from Fig. 4, horizontal error bars nominal accuracy of K_c values taken from Table I.

Indentation Strength in Bending, determination of K_{Ic}

Sample is indented and then tested in bending with indentation on the tensile side

$$K_{IC} = 0{,}59 \left(\frac{E}{H_V} \right)^{\frac{1}{8}} \left(\sigma_f \cdot p^{\frac{1}{3}} \right)^{\frac{3}{4}}$$

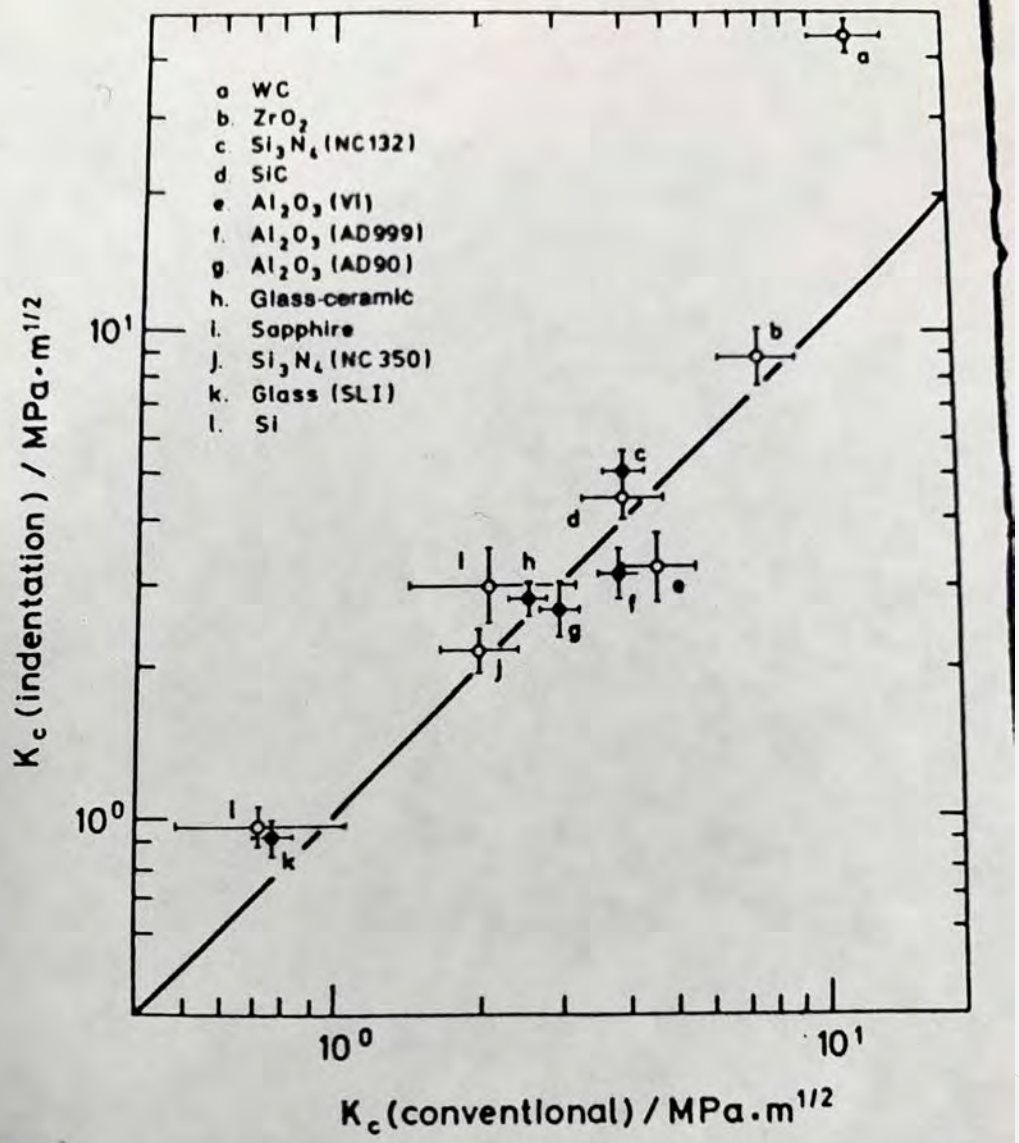

Fig. 6. Plot demonstrating correlation between toughness values determined by indentation and those determined by conventional means. Filled symbols denote reference materials used to evaluate η_V^R in Eq. (8). Vertical error bars represent uncertainty (standard deviation) in parameter $\sigma P^{1/3}$ obtained from Fig. 5, horizontal error bars represent nominal accuracy of K_c values taken from Table I in Part I.

Creep

Sample deformation at a constant stress (σ) vs. time

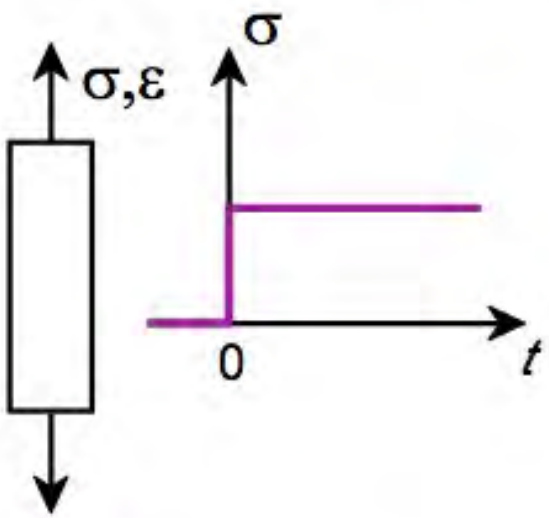

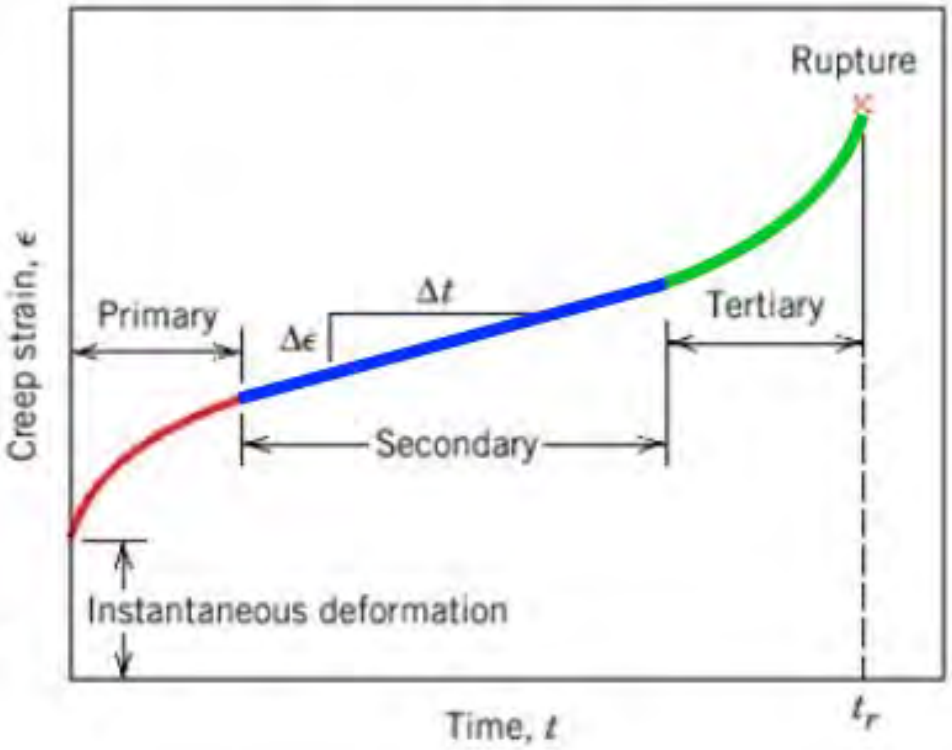

Primary Creep: slope (creep rate) decreases with time.

Secondary Creep: steady-state i.e., constant slope.

Tertiary Creep: slope (creep rate) increases with time, i.e. acceleration of rate.

Creep

- A typical creep test consists of subjecting a specimen to a constant load or stress while maintaining constant temperature.
- Upon loading, there is instant elastic deformation. The resulting creep curve consists of 3 regions: primary or transient creep adjusts to the creep level (creep rate may decrease); secondary creep- steady state-constant creep rate, fairly linear region (strain hardening and recovery stage); tertiary creep, there is accelerated rate of strain until rupture (grain boundary separation, internal crack formation, cavities and voids).

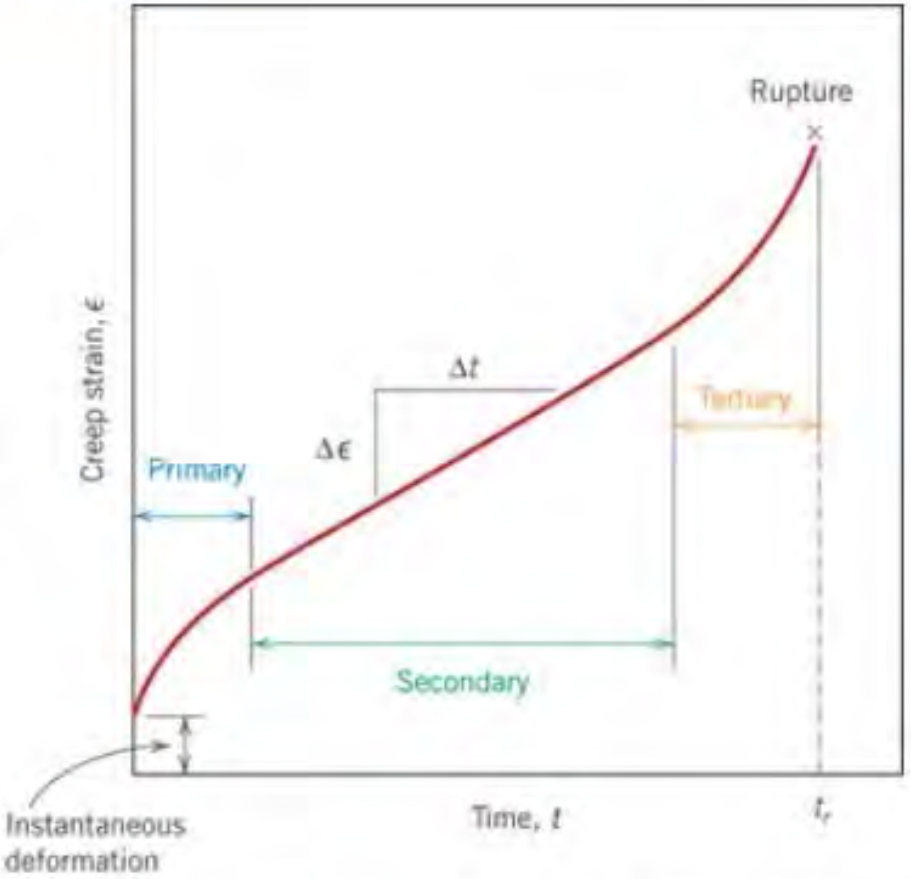

Creep strain vs time at constant load and constant elevated temperature. Minimum creep rate (steady-state creep rate), is the slope of the linear segment in the secondary region. Rupture lifetime t_r is the total time to rupture.

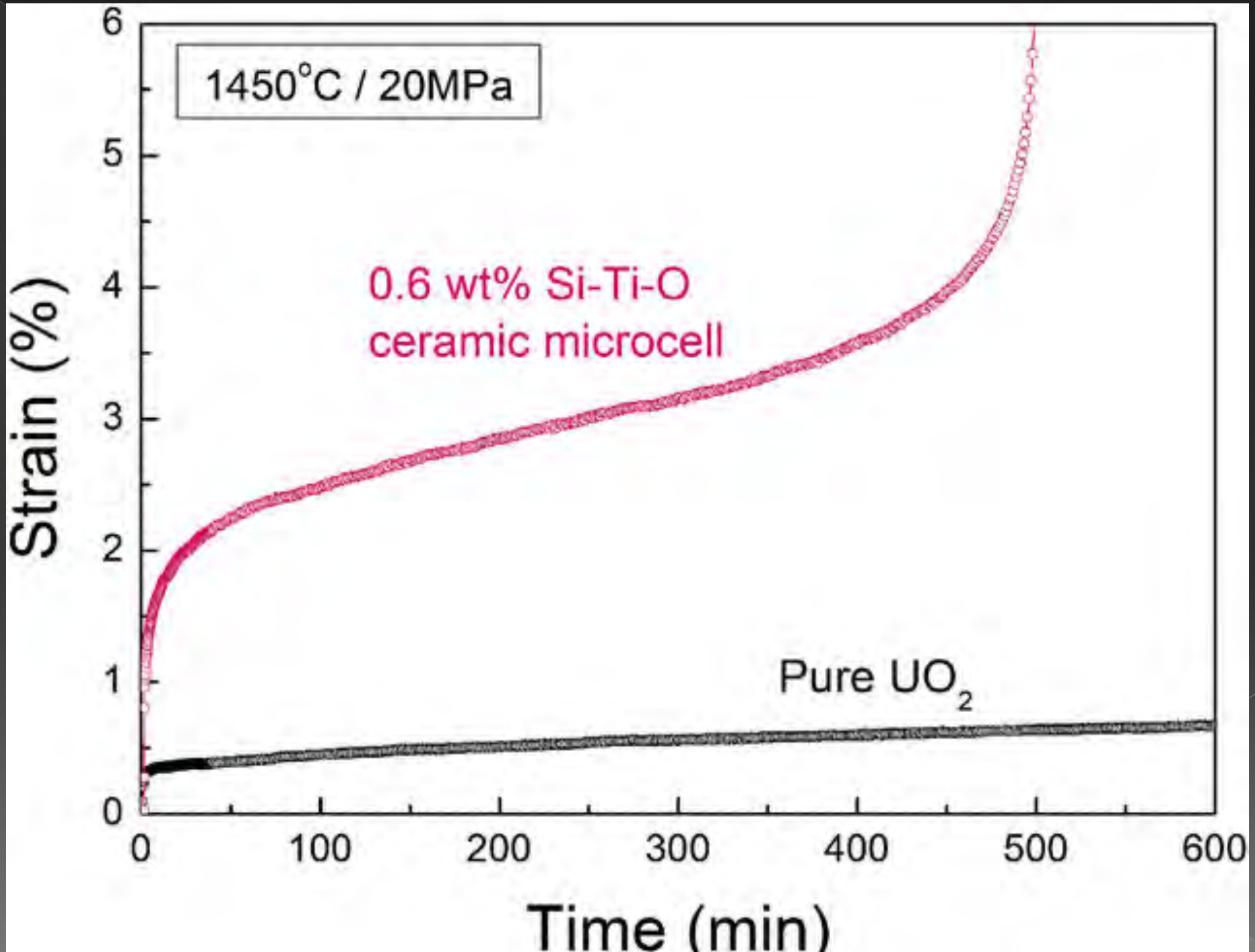
1450°C / 20MPa
0.6 wt% Si-Ti-O
ceramic microcell
Pure UO2
Strain (%)
Time (min)
0
1
2
3
4
5
6
0
100
200
300
400
500
600

Secondary Creep

- Strain rate is constant at a given T, σ
  -- strain hardening is balanced by recovery

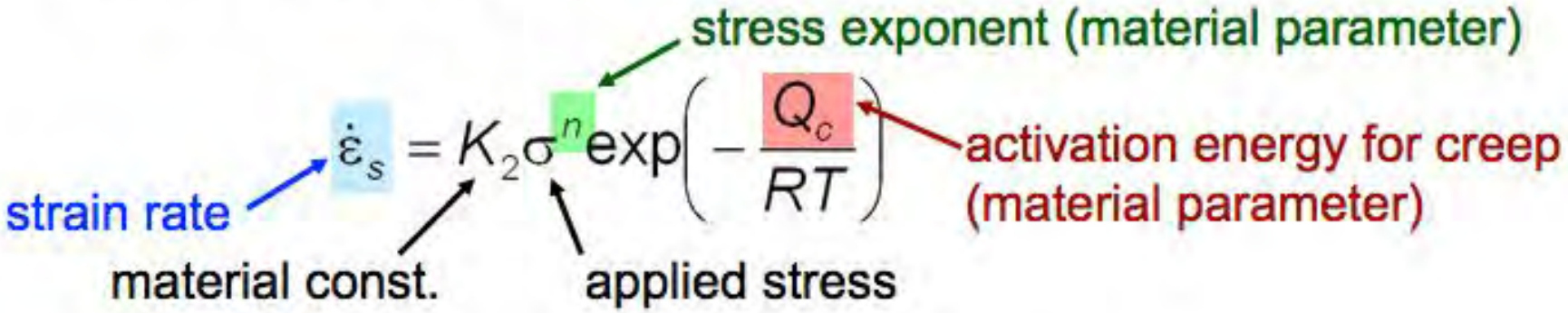

Creep tests

https://www.youtube.com/watch?v=k8Py4-SdjyU

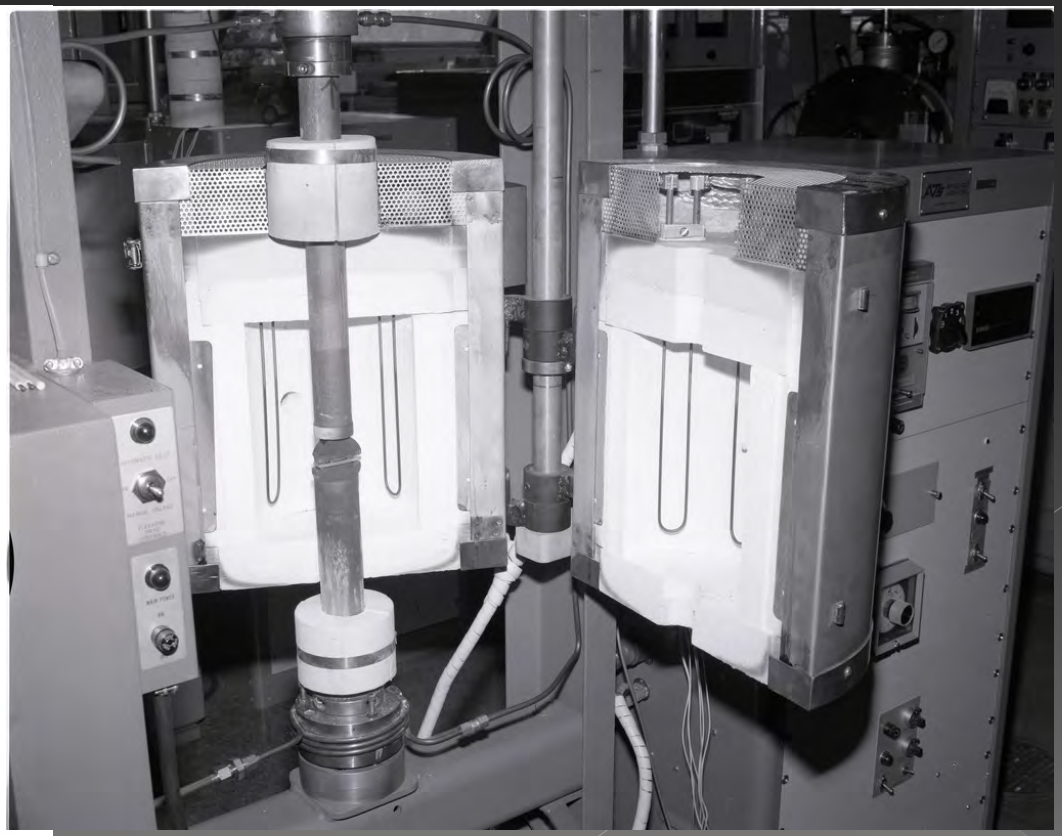

Microstructure: grains and grain boundaries

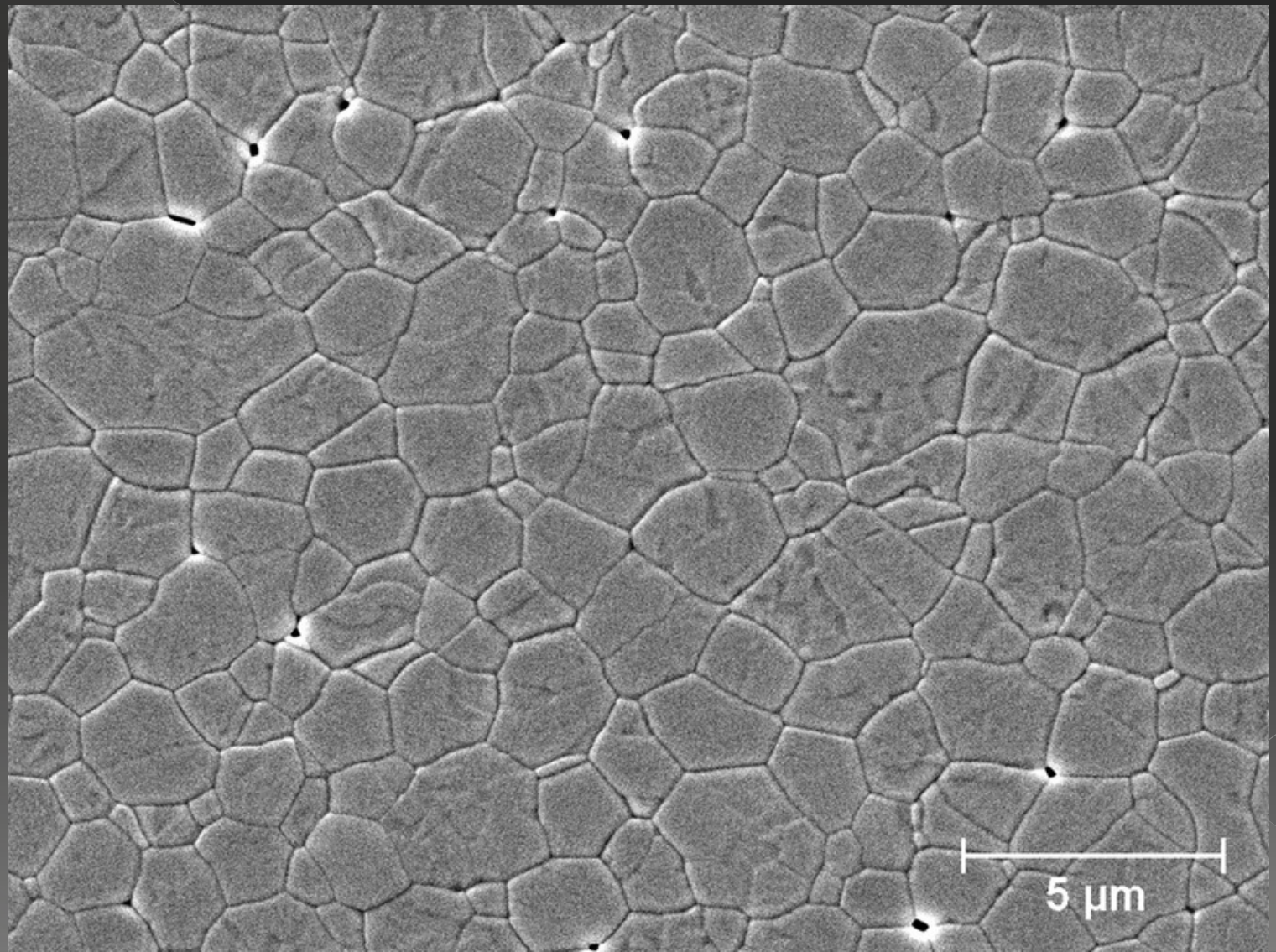

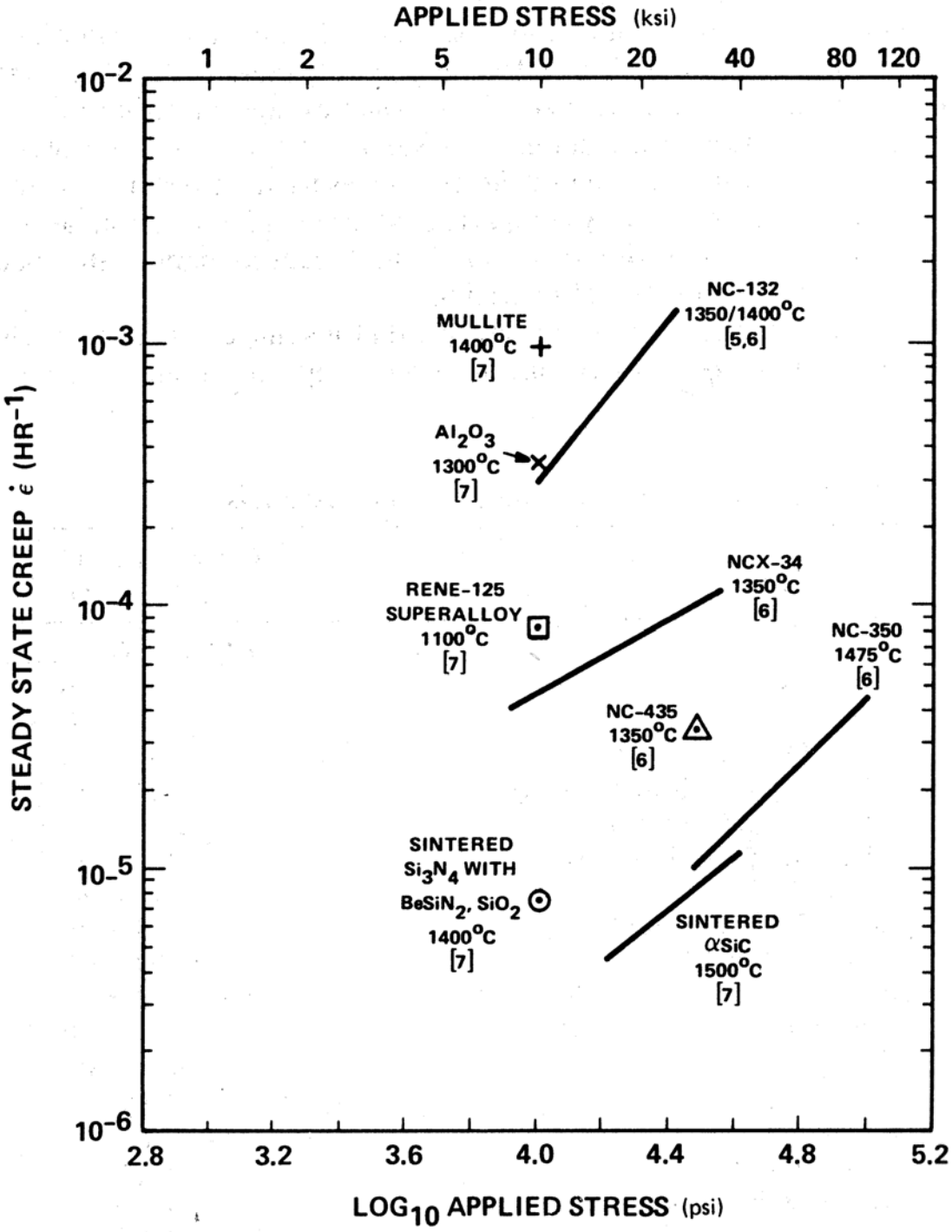
APPLIED STRESS (ksi)
1
2
5
10
20
40
80
120
10^{-2}
10^{-3}
10^{-4}
10^{-5}
10^{-6}
STEADY STATE CREEP $\dot{\epsilon}$ (HR^{-1})
MULLITE
1400°C
[7]
Al_2O_3
1300°C
[7]
NC-132
1350/1400°C
[5,6]
RENE-125
SUPERALLOY
1100°C
[7]
NCX-34
1350°C
[6]
NC-350
1475°C
[6]
NC-435
1350°C
[6]
SINTERED
Si_3N_4 WITH
$BeSiN_2$, SiO_2
1400°C
[7]
SINTERED
αSiC
1500°C
[7]
2.8
3.2
3.6
4.0
4.4
4.8
5.2
LOG_{10} APPLIED STRESS (psi)

Progress in the creep rate of Si_3N_4 from 1981 to 1998

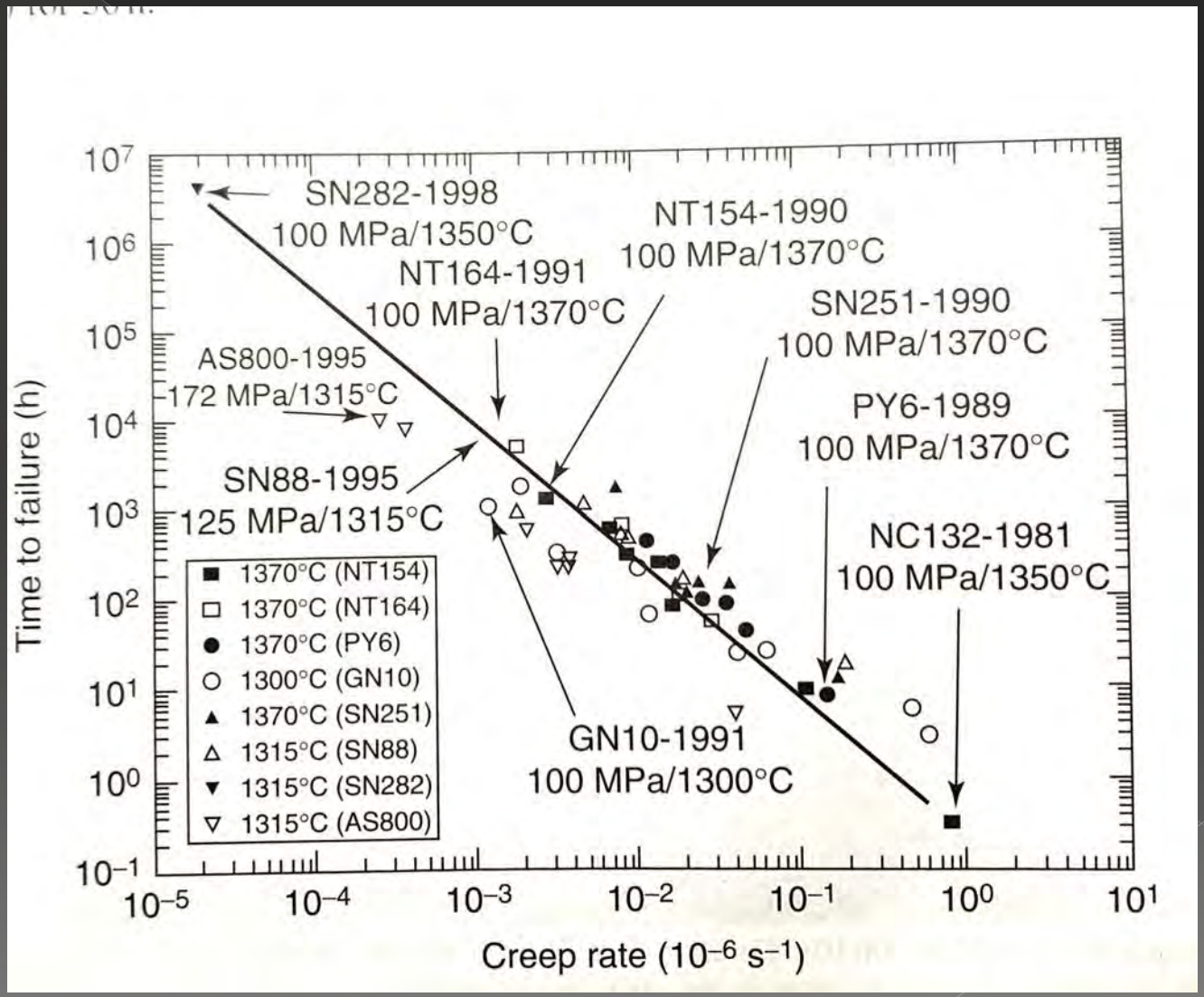

Flow mechanism in creep

$$\dot{\varepsilon} = \frac{\alpha D_L \sigma \Omega}{d^2 kT}$$

$$\dot{\varepsilon} = \frac{150 \Omega \delta D_{gb} \sigma}{\pi d^3 kT}$$

TERMS IN CREEP E

α	a constant
D_L	lattice diffusivity
k	Boltzmann's constant
b	Burgers vector
T	absolute temperature
σ	applied stress
μ	shear modulus
m	grain size exponent
n	stress exponent
φ	atomic volume
d	grain size
D_{gb}	grain boundary diffusivity
δ	grain boundary width
A	dimensionless constant
D	diffusion coefficient

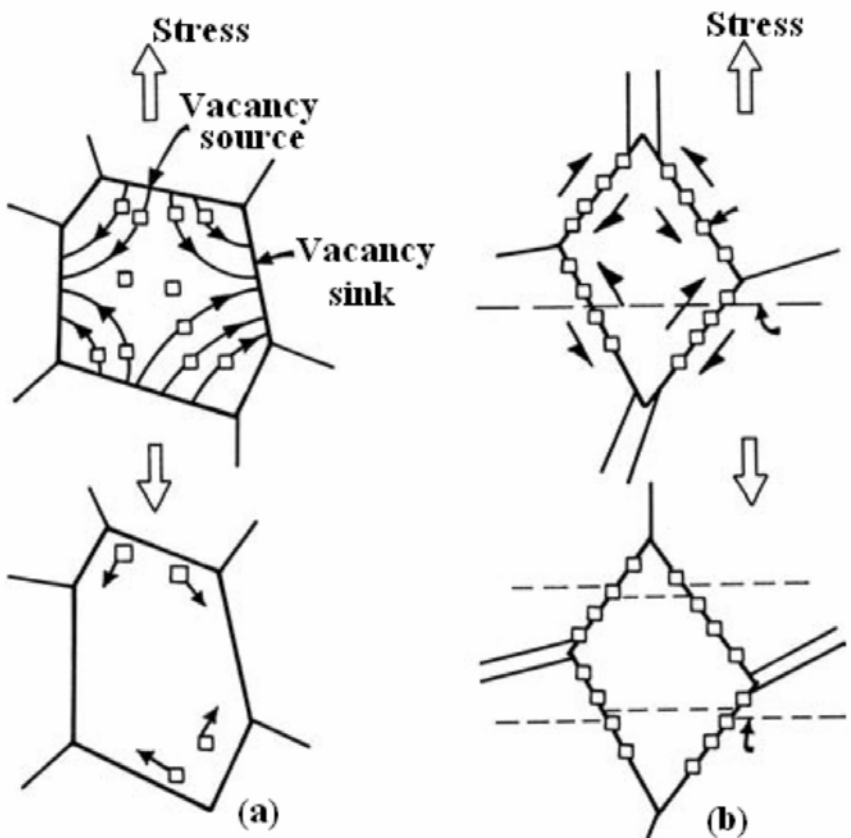

Flow of vacancies according to (a) Nabarro–Herring and (b) Coble mechanisms, resulting in an increase in the length of the specimen.

Typical exponents for GS and stress

TABLE 17.6 Creep Equation Exponents and Diffusion Paths for Various Creep Mechanisms

Creep mechanism	m	n	*Diffusion path*
Dislocation creep mechanism			
Dislocation glide climb, climb controlled	0	4–5	Lattice
Dislocation glide climb, glide controlled	0	3	Lattice
Dissolution of dislocation loops	0	4	Lattice
Dislocation climb without glide	0	3	Lattice
Dislocation climb by pipe diffusion	0	5	Dislocation core
Diffusional creep mechanisms			
Vacancy flow through grains	2	1	Lattice
Vacancy flow along grain boundaries	3	1	Grain boundary
Interface reaction control	1	2	Lattice/grain boundary
Grain boundary sliding mechanisms			
Sliding with liquid	3	1	Liquid
Sliding without liquid (diffusion control)	2–3	1	Lattice/grain boundary

Nabarro Herring Deformation maps

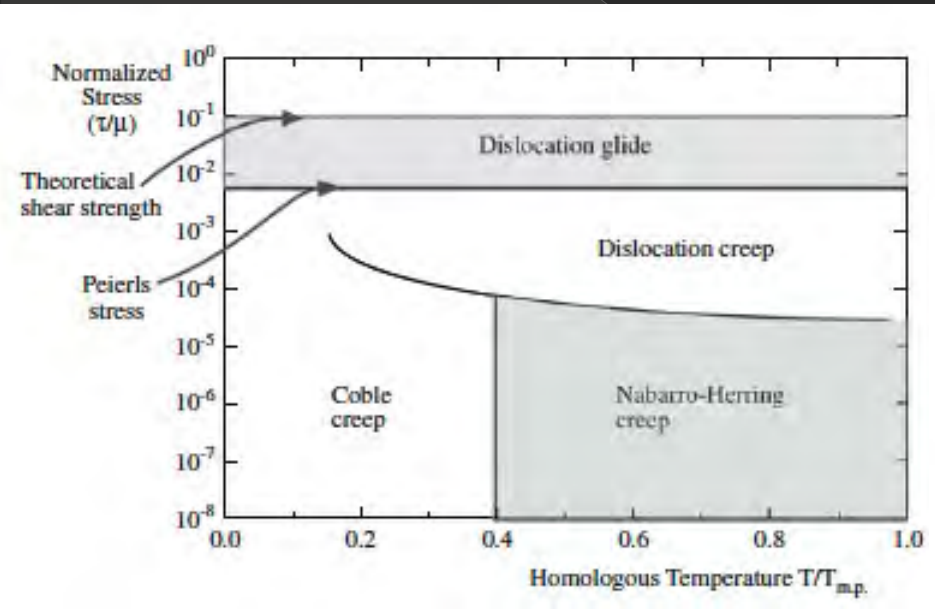

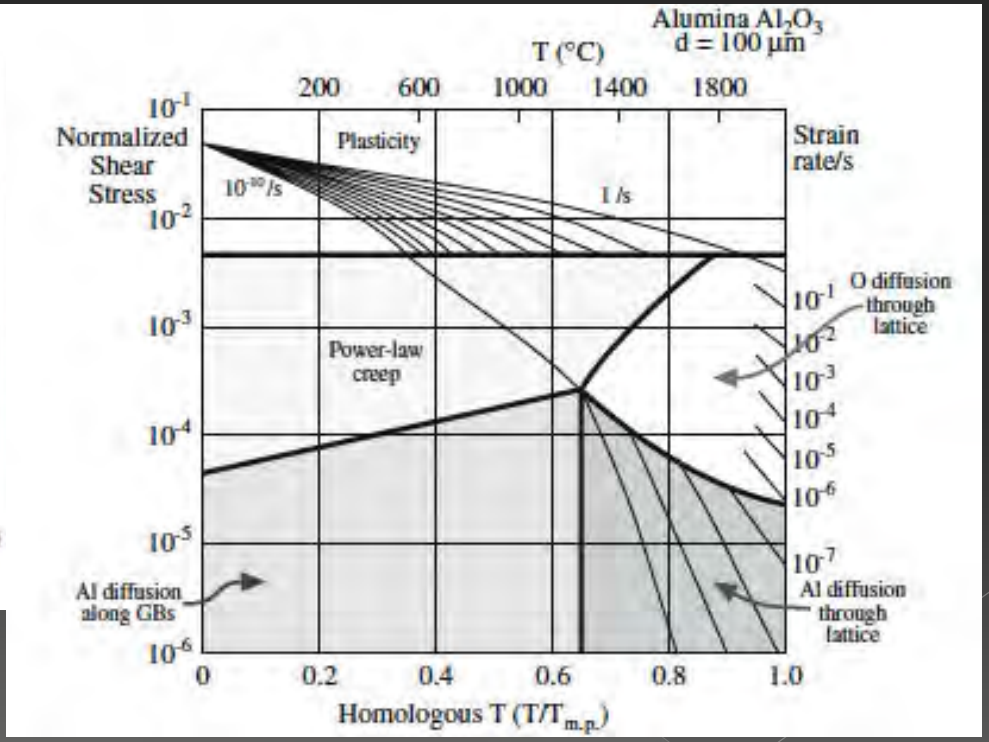

Ashby map Therm. Expan./therm Conduc

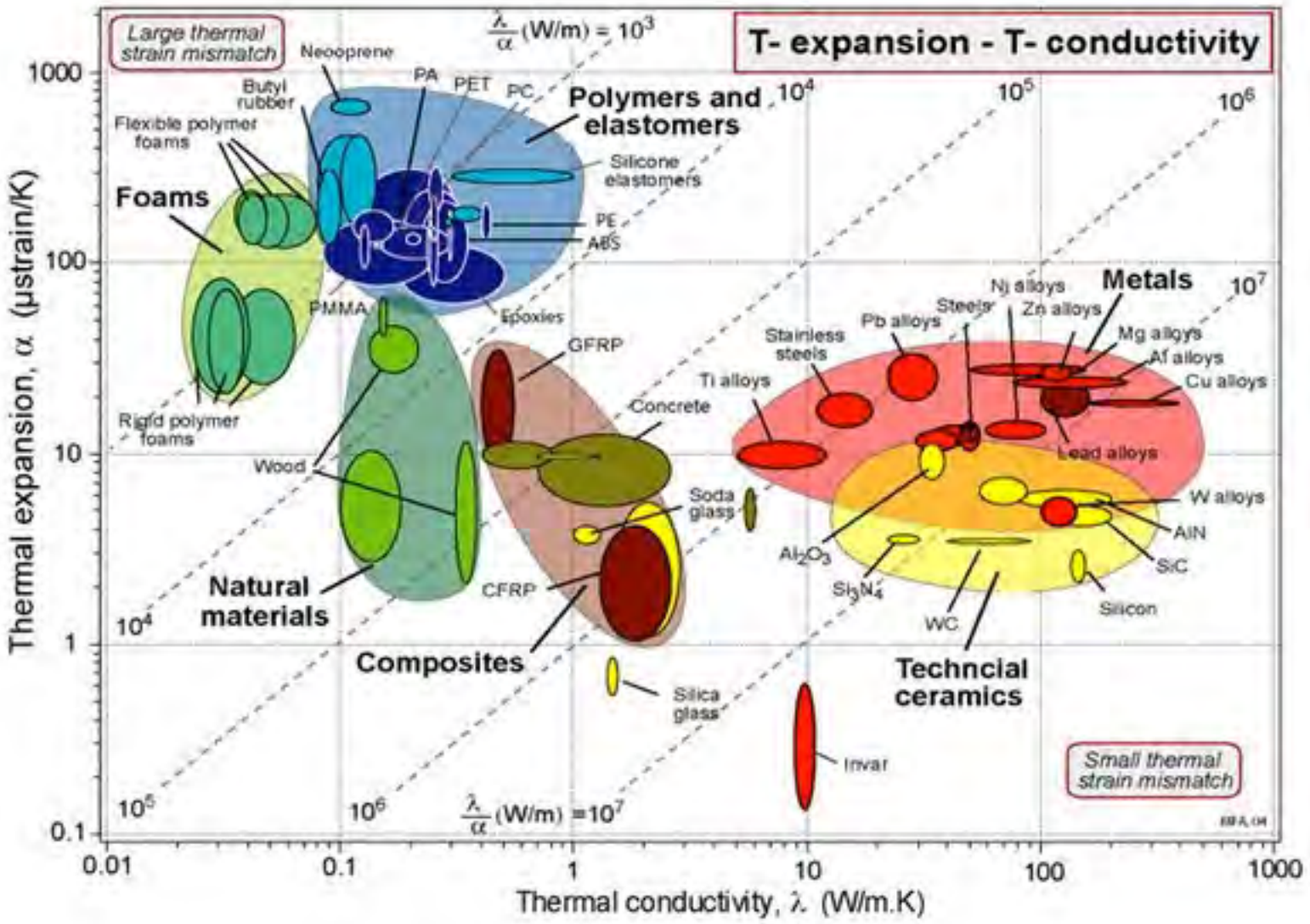

Thermal shock resistance

TABLE 9.7
Thermal Shock Resistance Parameters

Parameter Designation	Parameter Type	Parameter[a]	Physical Interpretation/ Heat Transfer Conditions	Typical Units
R	Resistance to fracture initiation	$\frac{\sigma(1-\nu)}{\alpha E}$	Maximum ΔT allowable for steady heat flow	°C
R'	Resistance to fracture initiation	$\frac{\sigma(1-\nu)k}{\alpha E}$	Maximum heat flux for steady flow	cal/cm · sec
R''	Resistance to fracture initiation	$\frac{\sigma(1-\nu)\alpha_{TH}}{\alpha E}$	Maximum allowable rate of surface heating	$cm^2 \cdot °C/sec$
R'''	Resistance to propagation damage	$\frac{E}{\sigma^2(1-\nu)}$	Minimum in elastic energy at fracture available for crack propagation	$(psi)^{-1}$
R''''	Resistance to propagation damage	$\frac{\gamma E}{\sigma^2(1-\nu)}$	Minimum in extent of crack propagation on initiation of thermal stress fracture	cm
R_{st}	Resistance to further crack propagation	$\left(\frac{\gamma}{\alpha^2 E}\right)^{1/2}$	Minimum ΔT allowed for propagating long cracks	$°C/m^{1/2}$

[a] σ, tensile strength; ν, Poisson's ratio; α, coefficient of thermal expansion; E, Young's modulus of elasticity; k, thermal conductivity; α_{TH}, thermal diffusivity; γ, fracture surface energy.

Thermal shock resistance

Table 8.8 Calculated Values of the Thermal Shock Parameter R for Various Ceramic Materials Using Typical Property Data

Material	Strength,[a] σ (psi)	Poisson's Ratio, ν	Thermal Expansion, α (in./in. · °C)	Elastic Modulus, E (psi)	$R = \frac{\sigma(1-\nu)}{\alpha E}$ (°C)
Al_2O_3	50,000	0.22	7.4×10^{-6}	55×10^6	96
SiC	60,000	0.17	3.8×10^{-6}	58×10^6	230
RSSN[b]	45,000	0.24	2.4×10^{-6}	25×10^6	570
HPSN[b]	100,000	0.27	2.5×10^{-6}	45×10^6	650
LAS[b]	20,000	0.27	-0.3×10^{-6}	10×10^6	4860

[a]Flexure strength used rather than tensile strength.
[b]RSSN, reaction-sintered silicon nitride; HPSN, hot-pressed silicon nitride; LAS, lithium aluminum silicate (β-spodumene).

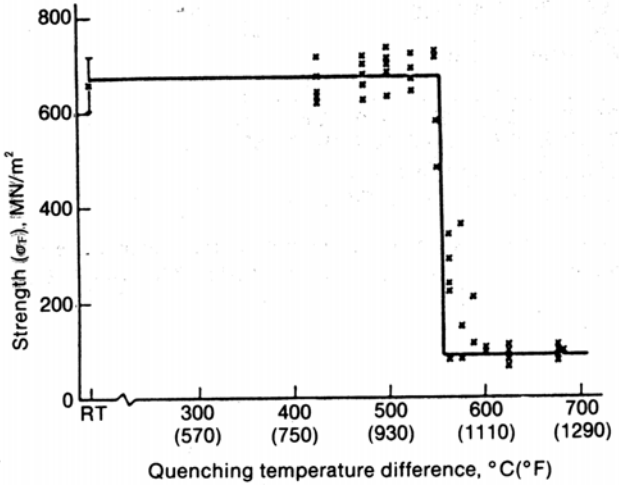

Figure 8.32 Typical results of retained strength versus thermal shock ΔT for quench test. Example is for hot-pressed Si_3N_4 material containing 3% MgO as a densification aid. (From G. Ziegler, in *Progress in Nitrogen Ceramics* [F. L. Riley, ed.] Martinas Nijhoff Publishers, The Hague, 1983.)

Thermal shock testing of Schott glasses

Stress data for Weibull plot

Ergebnisse:

Nr	P N	σ MPa	P_f	d mm	r3 mm
1	998,3	1190	0,00	1,185	6,735
2	993,3	1190	0,00	1,181	6,875
3	1034,9	1200	0,00	1,2	6,895
4	994,4	1190	0,00	1,181	6,88
5	1002,2	1180	0,00	1,192	6,935
6	1026,4	1210	0,00	1,192	6,9
7	1035,1	1210	0,00	1,194	6,915
8	940,4	1120	0,00	1,184	6,9
9	1026,8	1190	0,00	1,199	6,935
10	1000,4	1180	0,00	1,192	6,935
11	971,5	1170	0,00	1,176	6,945
12	993,2	1190	0,00	1,183	6,885

Nr	P N	σ MPa	P_f	d mm	r3 mm
13	1013,2	1200	0,00	1,19	6,885
14	1018,6	1210	0,00	1,185	6,945
15	994,4	1180	0,00	1,189	6,9
16	980,9	1170	-	1,186	6,9
17	1016,7	1210	-	1,186	6,92
18	992,1	1170	-	1,191	6,945
19	1033,9	1240	-	1,184	6,865
20	989,6	1170	-	1,188	6,88
21	998,7	1190	-	1,187	6,94
22	1025,5	1210	-	1,19	6,895
23	985,1	1170	-	1,188	6,915

Seriengrafik:

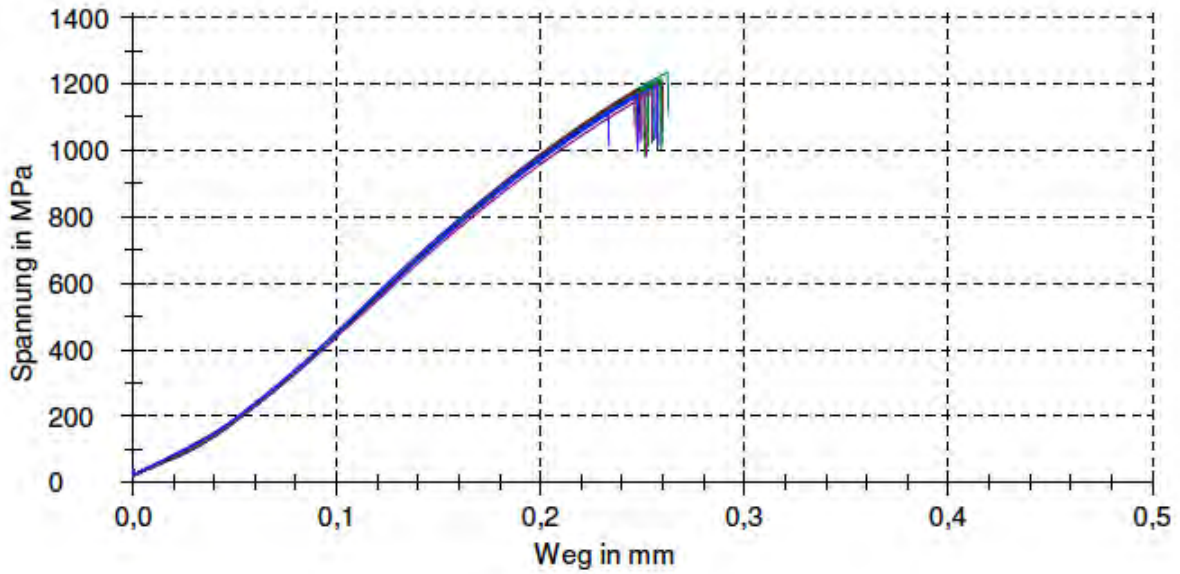

Data from SKF

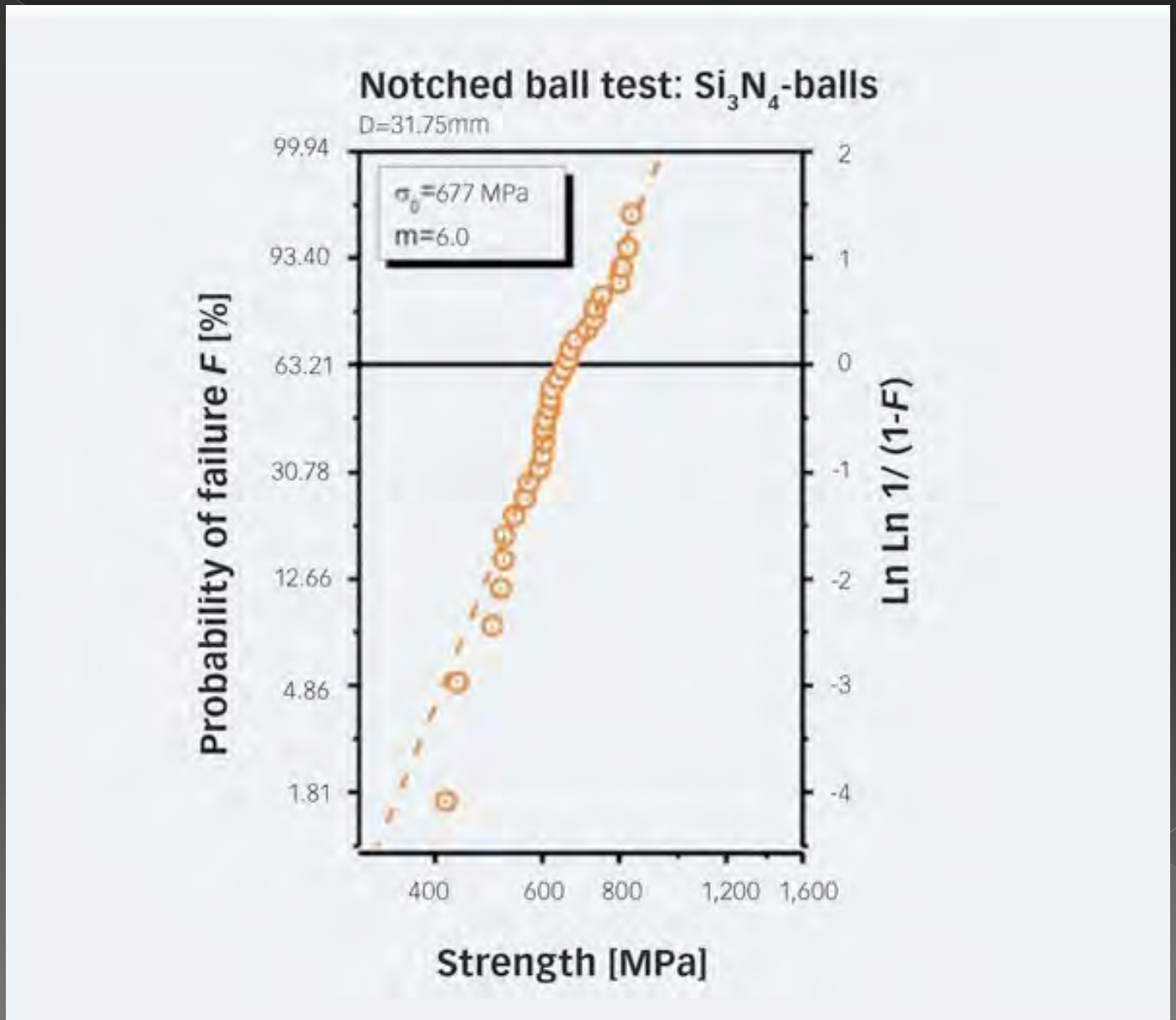

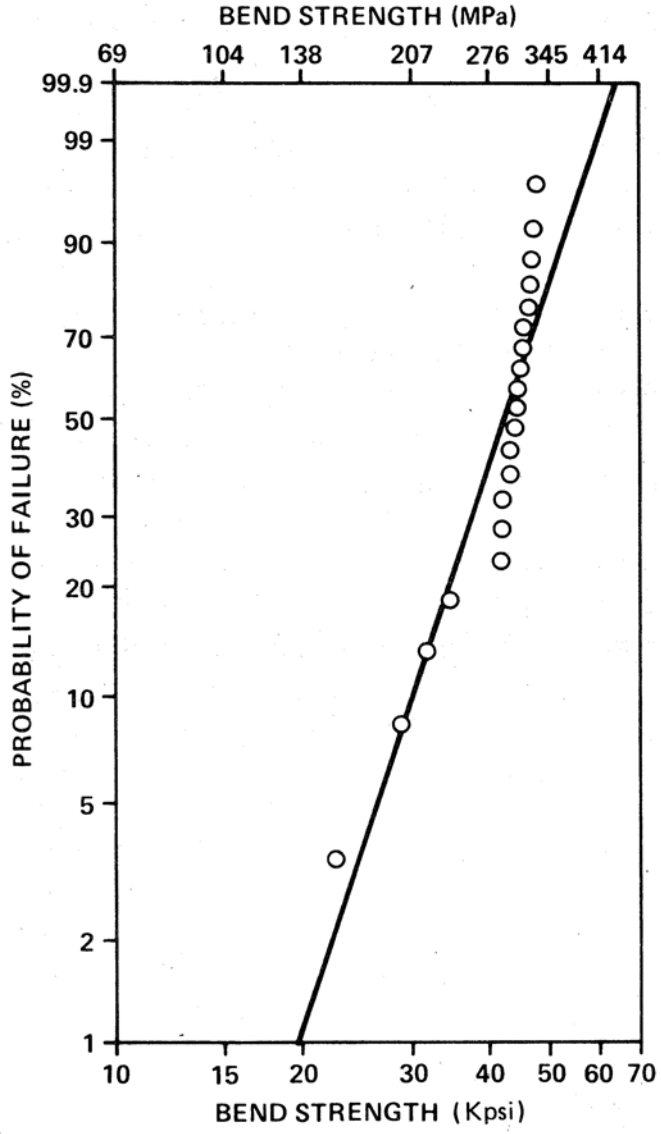

Figure 15.6 Example of Weibull curve generated from strength test data for reaction-bonded Si_3N_4. (Data from Ref. 6.)

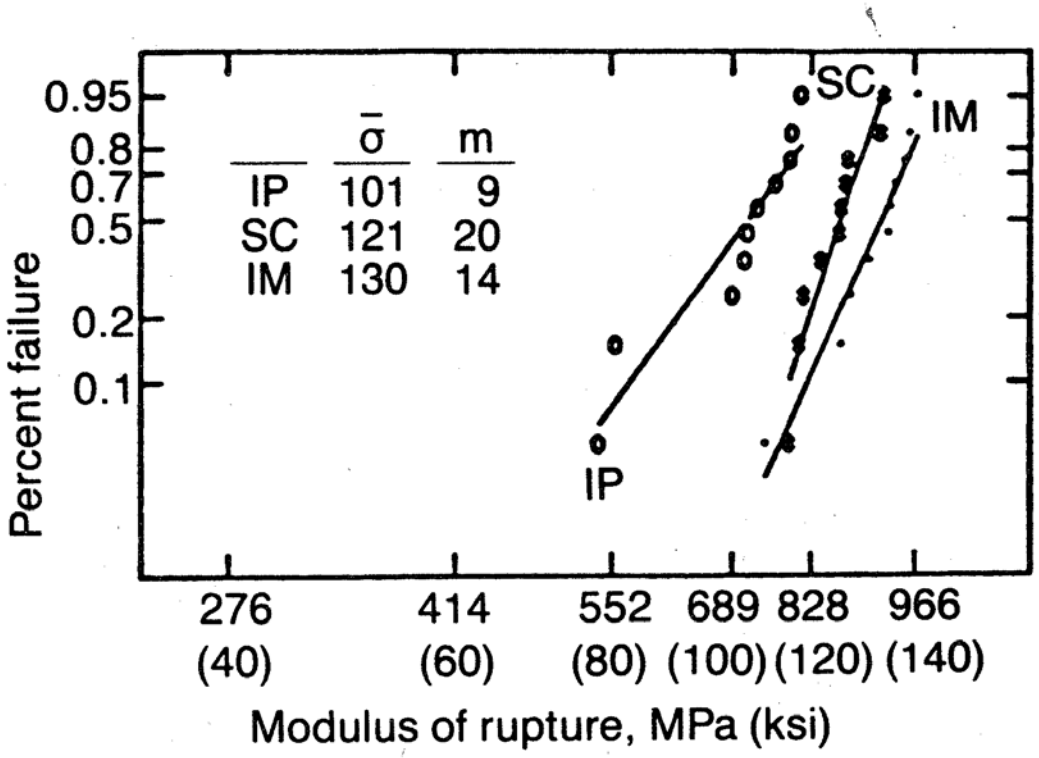

Figure 15.10 Weibull plots comparing the strength of a sintered Si_3N_4 fabricated by various techniques. IP is isostatically pressed, SC is slip-cast, and IM is injection-molded. (From A. Pasto, J. Neil, and C.L. Quackenbush, paper presented at International Conference on Ultrastructure Processing of Ceramics, Glasses and Composites, Gainesville, Florida, Feb. 13–17, 1983.)

Suggested failure probabilities with Weibull approach

TABLE 16.10 Suggested Failure Probabilities

P_F	*Possible consequences of failure*	*Example*
0.3	Slight inconvenience	Sticks of chalk
10^{-2}	Inconvenience and small expense	Ceramic cutting tool
10^{-6}	Injury	Window on a vacuum system
10^{-8}	Loss of life and significant expense	Ceramic protective tile on space shuttle

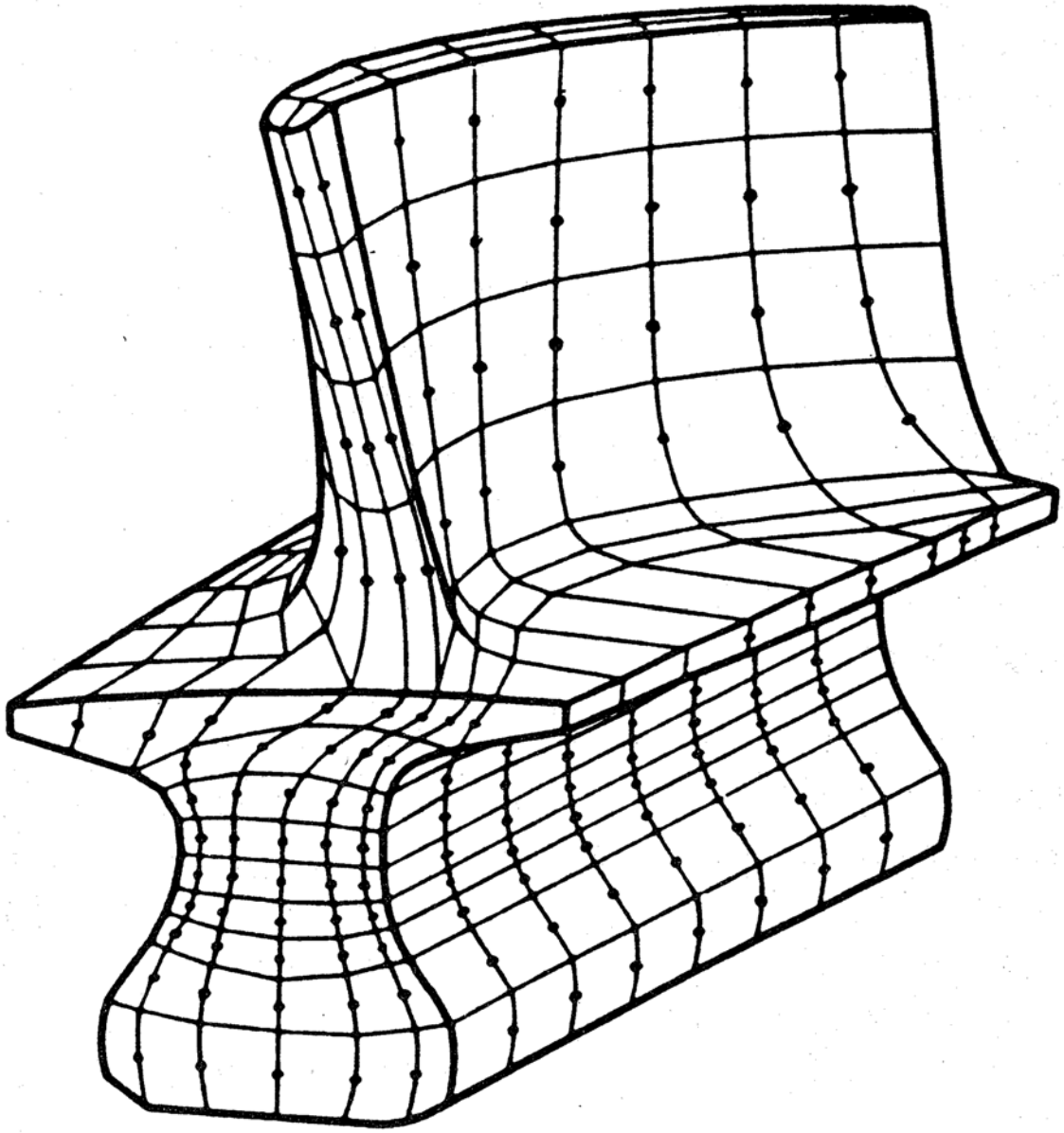

Figure 15.11 Finite-element analysis model for a ceramic rotor blade for a gas-turbine engine. (© ASM International.)

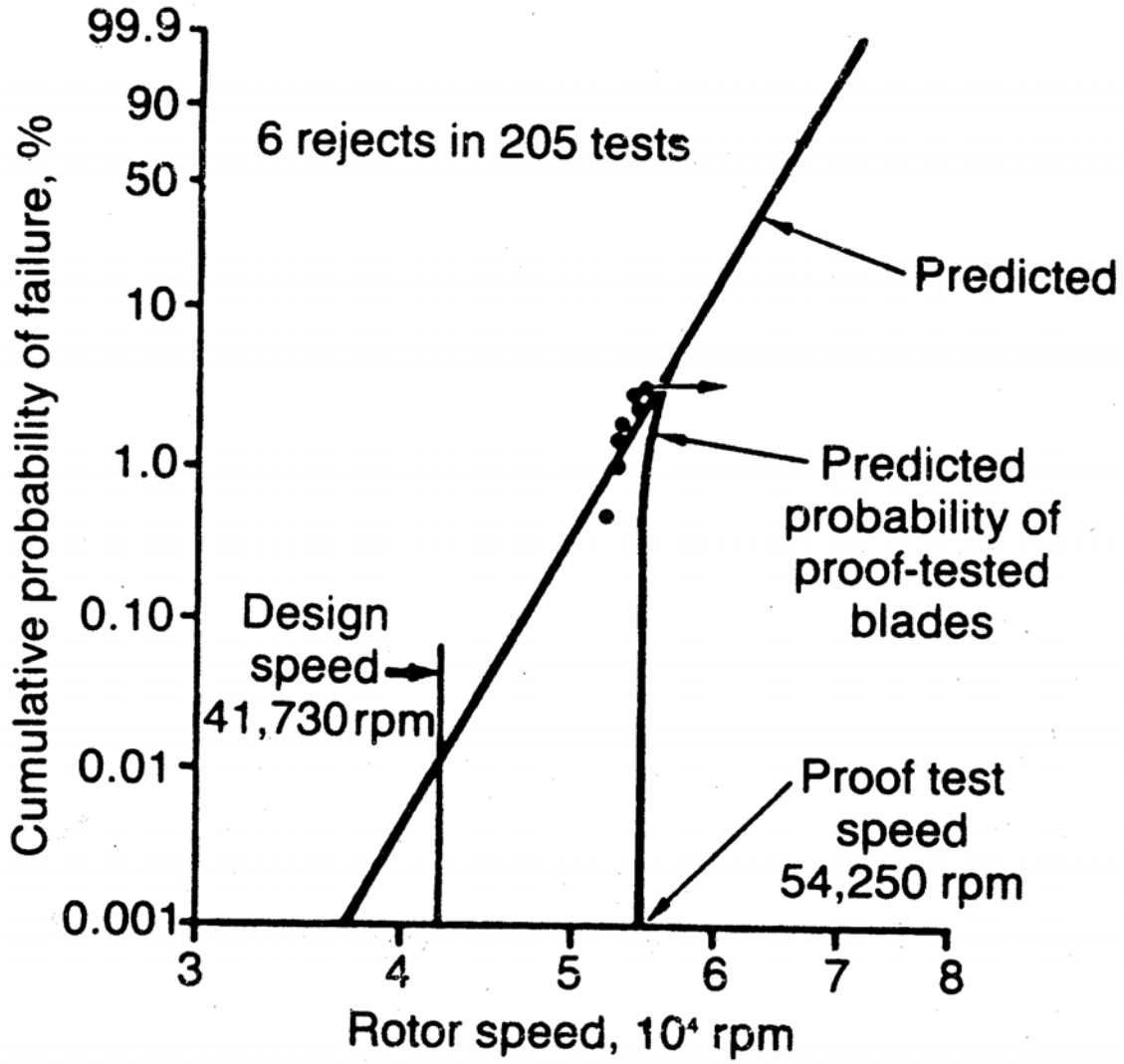

Figure 15.12 Rotor blade spin proof-test results that show good correlation between predicted and actual probability of failure for hot-pressed Si_3N_4 rotor blades. (From D. W. Richerson, Design with ceramics for heat engines, paper presented at U.S./Japan Seminar on Structural Ceramics, Seattle, Wash., Aug. 13–15, 1984.)

Ceramic cutting tools

Ceramic cutting tools

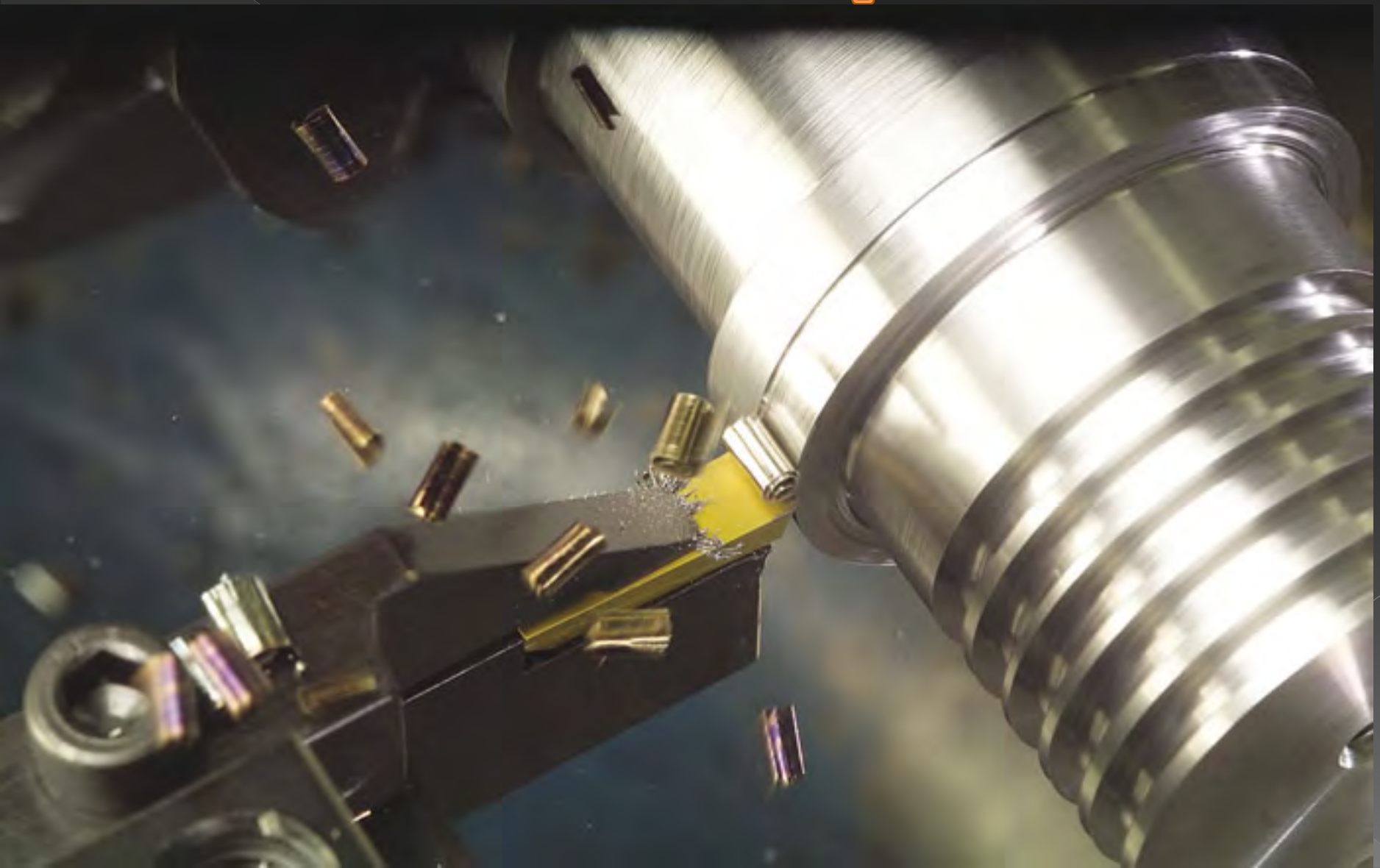

Toughening of ceramics: what can we do?

TABLE 18.6 Classification of Toughening Mechanisms in Ceramics

General mechanism	*Detailed mechanisms*
Crack deflection	Tilt and twist out of the crack plane around grains and second-phase additions
Crack bowing	Bowing in the crack plane between second-phase crack-pinning points
Crack branching	Crack may subdivide into two or more roughly parallel cracks
Crack tip shielding by process zone activity	Microcracking Transformation toughening Ductile yielding in process zone
Crack tip shielding by crack bridging	Second-phase brittle fibers with partial debonding Frictional and ligamentary grain bridges Second-phase ductile ligament bridging

Crack Deflection

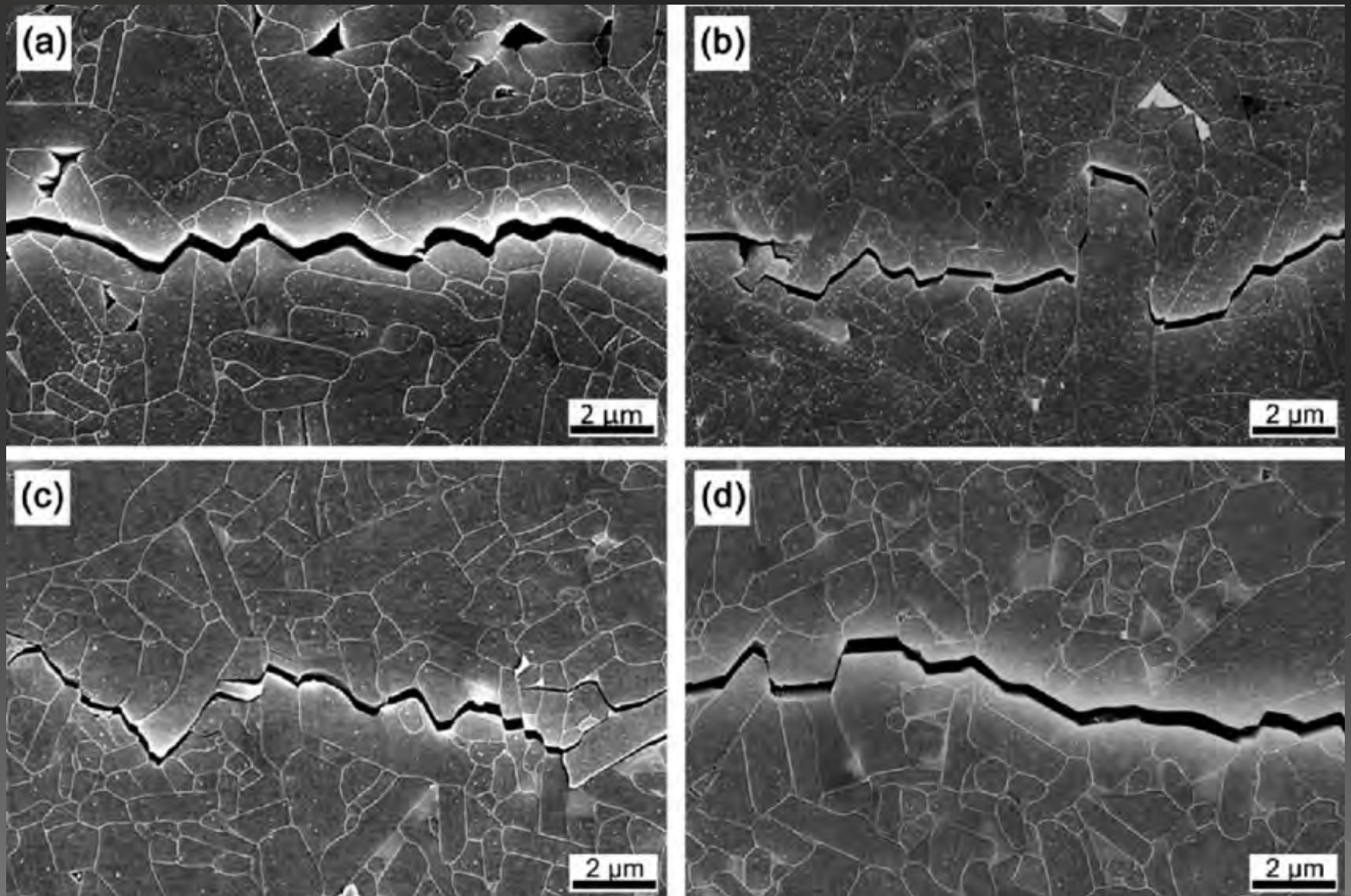

Second phase: fibers, whiskers, metal particles

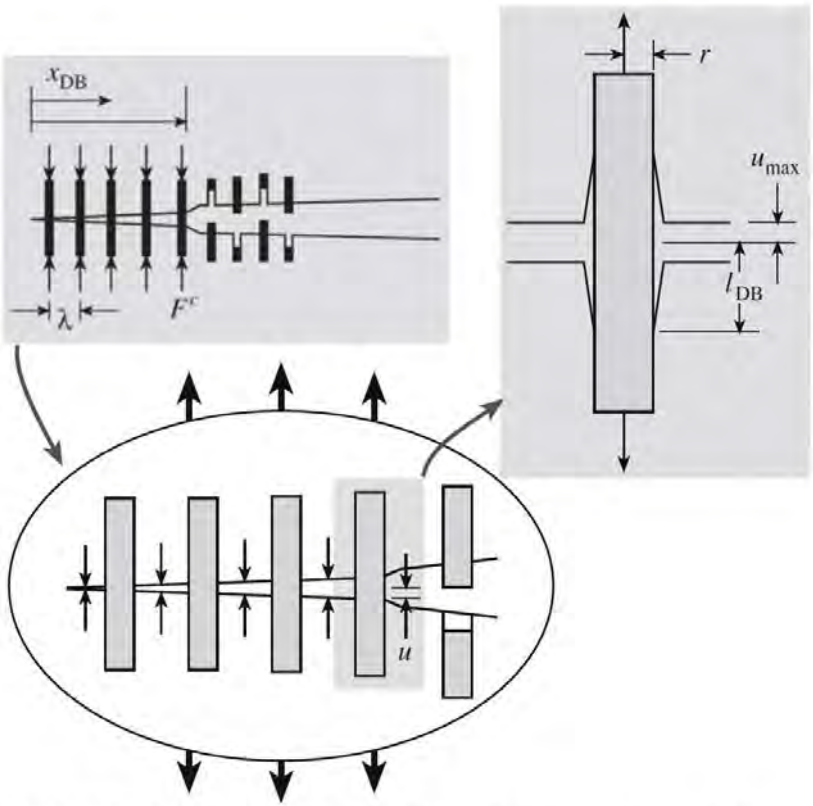

FIGURE 18.19 Illustration of a crack bridging mechanism with debonding and fiber pullout.

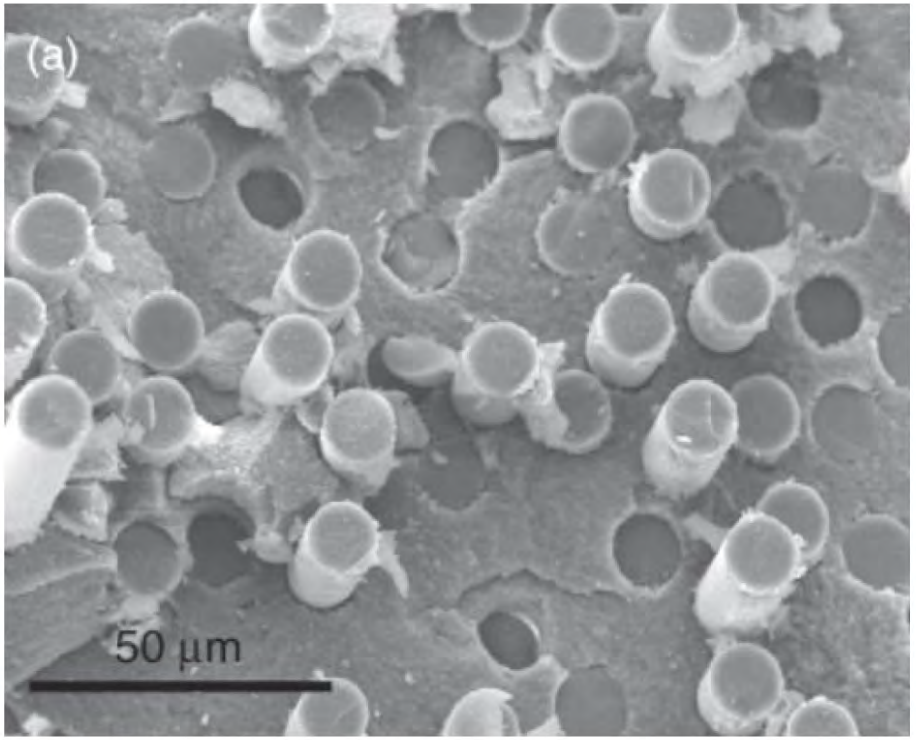

FIGURE 18.18 SEM image showing fiber pullout on the fracture surface of $AlPO_4$-coated alumina/mullite fiber/Al_2O_3 CMC, hot pressed at 1250°C for 1 h.

SiC Whiskers

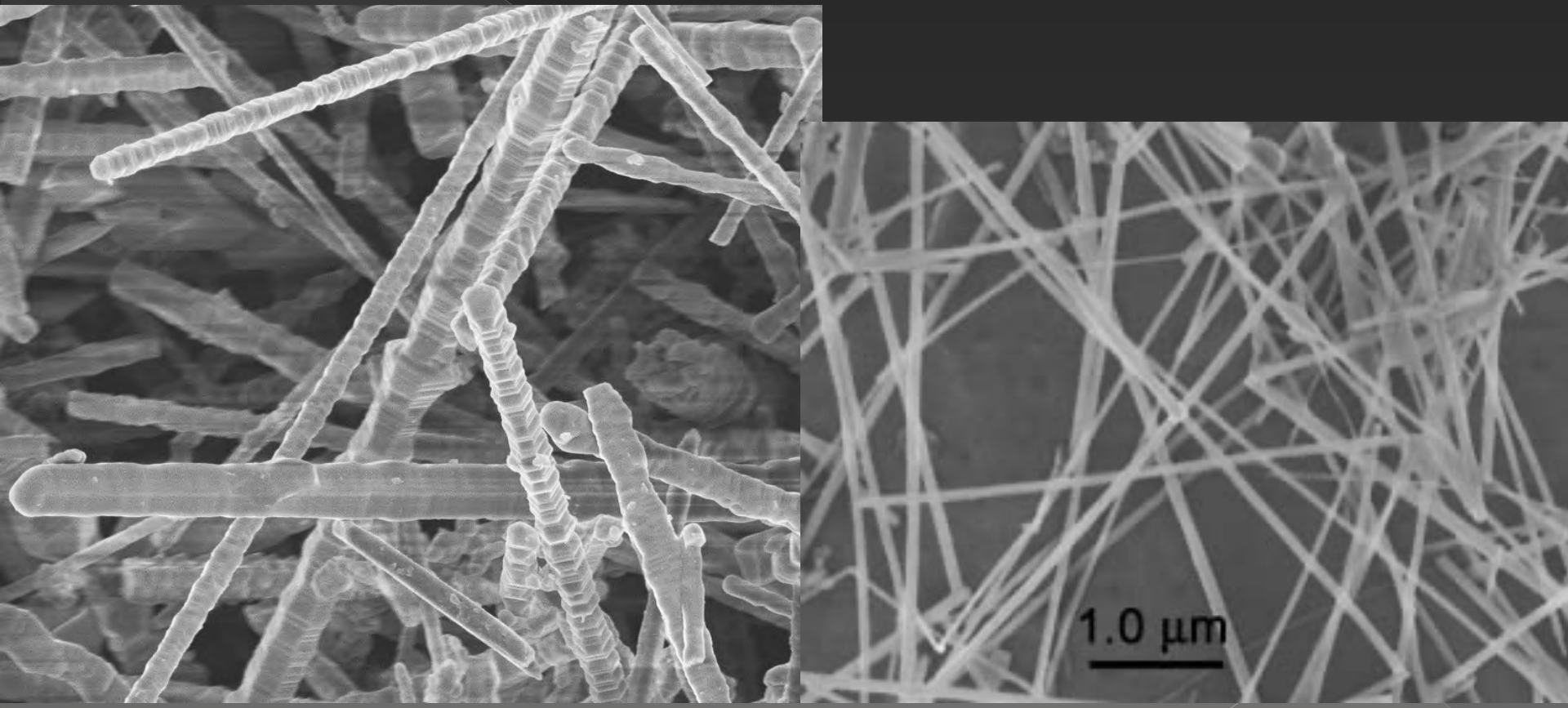

Ni-Co CERMETS (CERamic-METal) with TiC

From: Effect of Co and Ni Contents on the Sintering Behavior, Microstructure Evolution, and Mechanical Properties of (Ti,M)C-Based Cermets

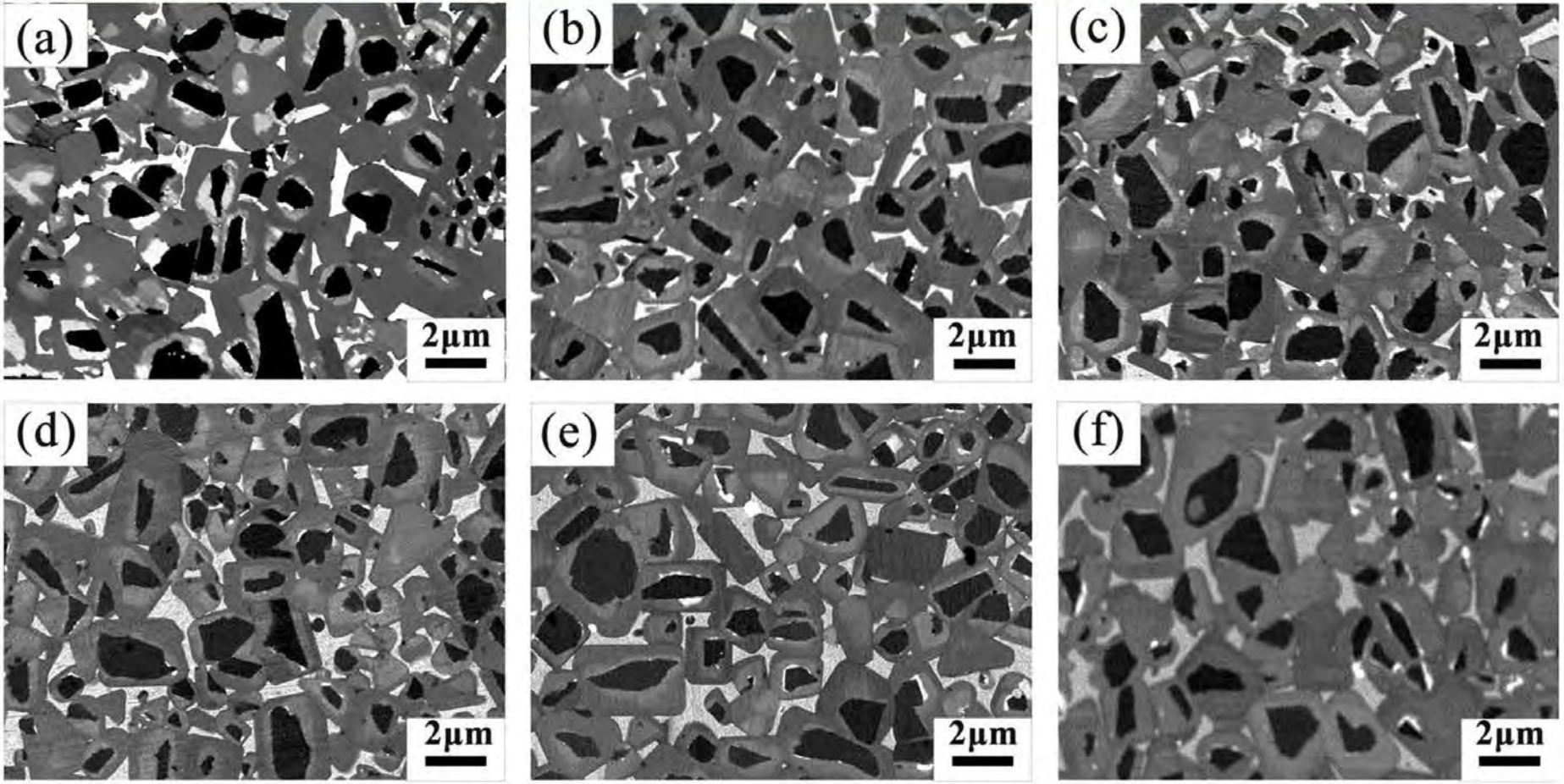

BSE microstructures of (Ti,M)C-based cermets. (a) Cermet A, (b) Cermet B, (c) Cermet C, (d) Cermet D, (e) Cermet E, (f) Cermet F.

NB: The material is ZIRCONIUM OXIDE, ZrO_2.

100 cm^3 of tetragonal ZrO_2 expand to give 105 cm^3 of monoclinic- ZrO_2 (5% transformation strain)

CUBIC
2100°C>T>2800°C (T.F.)

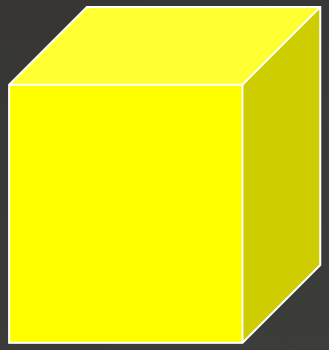

TETRAGONAL
1100°C>T>2100°C (T.F.)

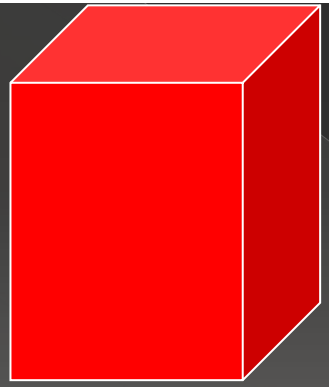

MONOCLINIC
1100°C>T> Room Temp.

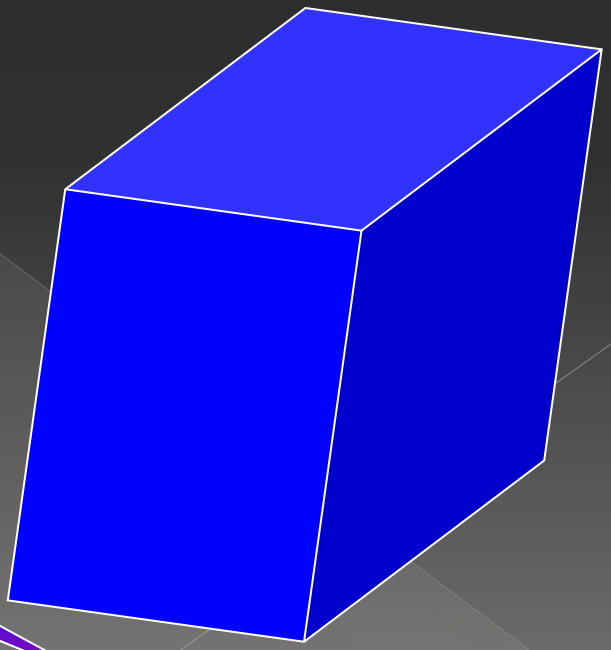

Transformation toughening: Zirconia

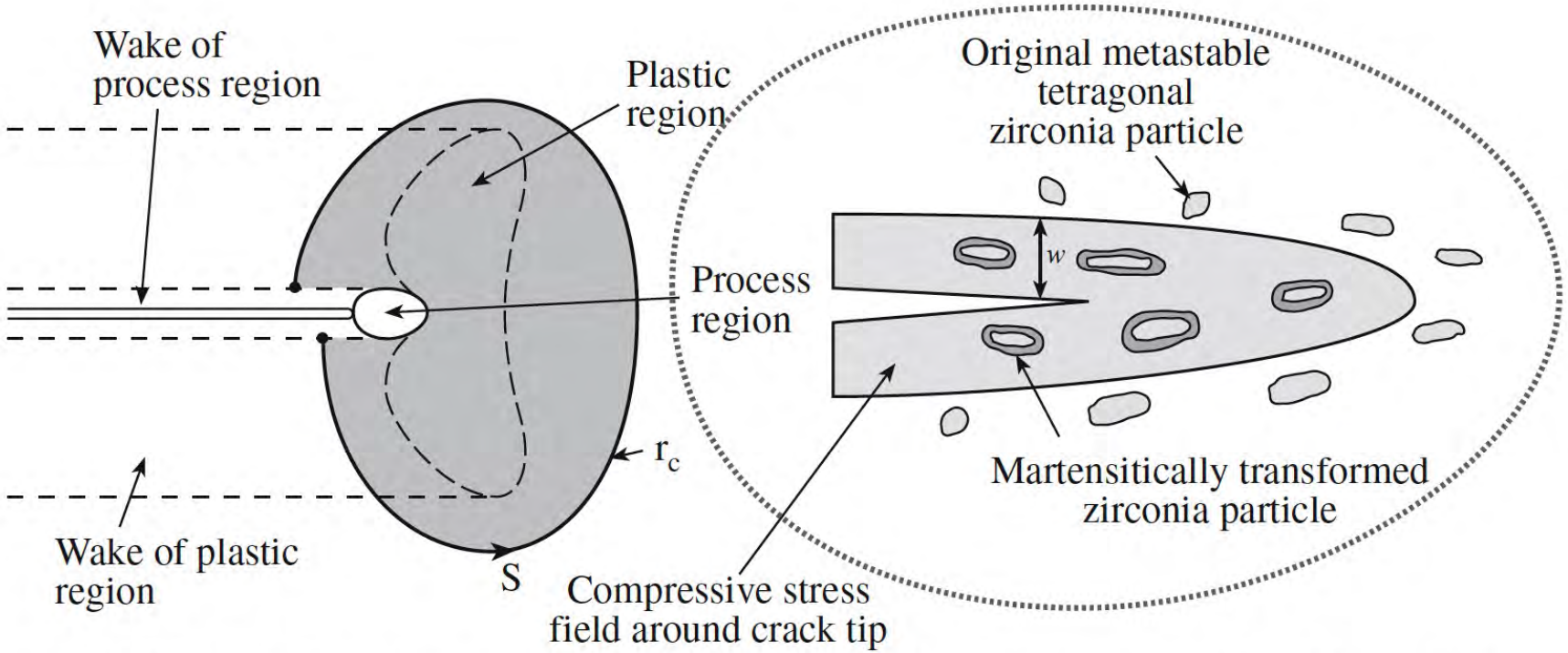

FIGURE 18.22 Illustration of transformation toughening in a ceramic matrix containing ZrO_2 particles.

The transformation toughening of ZrO_2

At the crack tip, tetragonal ZrO_2 particles transform to monoclinic; they try to expand and, consequently,

EXERT A CLOSING PRESSURE ON THE ADVANCING CRACK!!

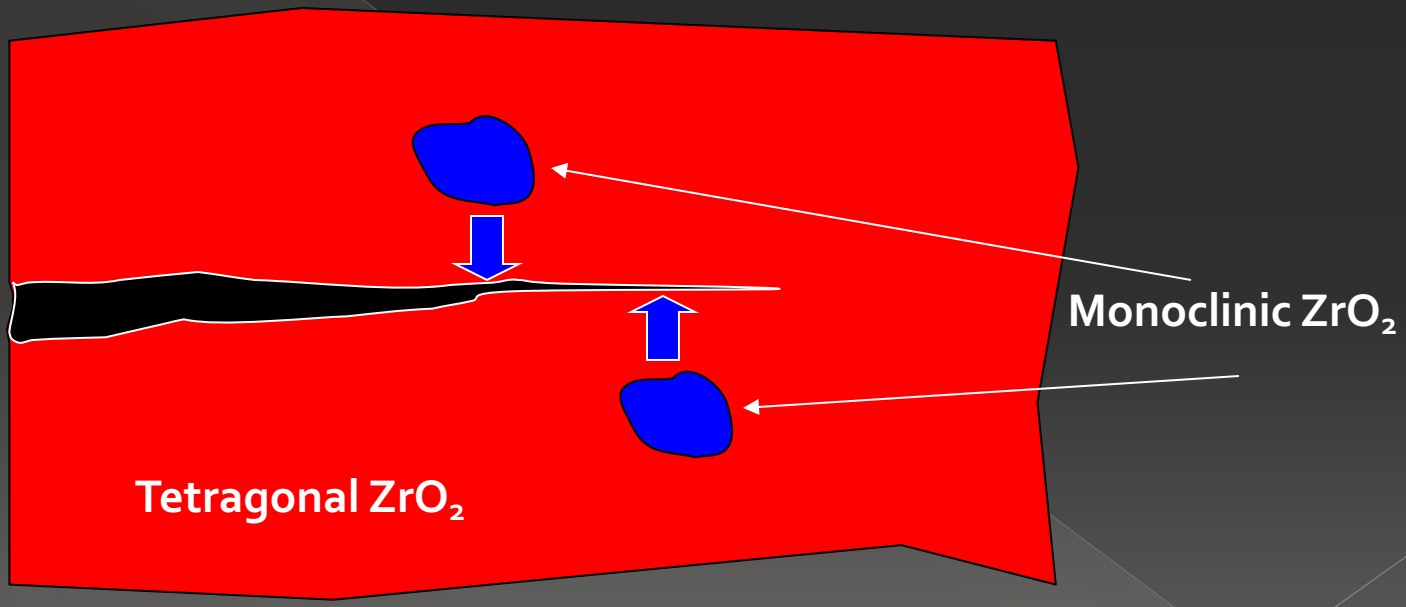

2nd consequence: pseudo-plasticity

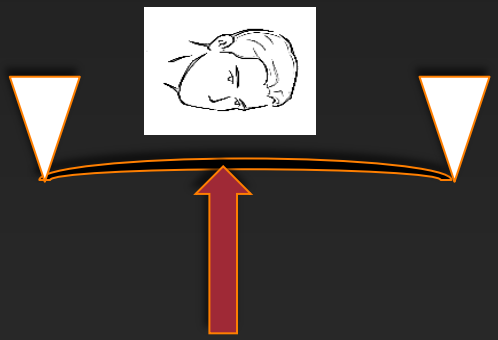

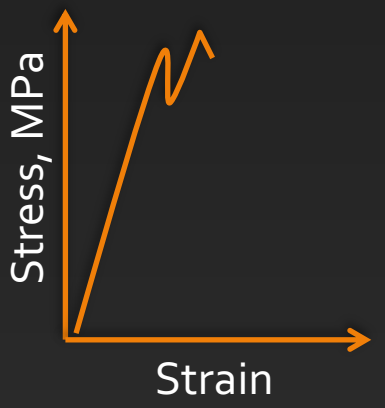

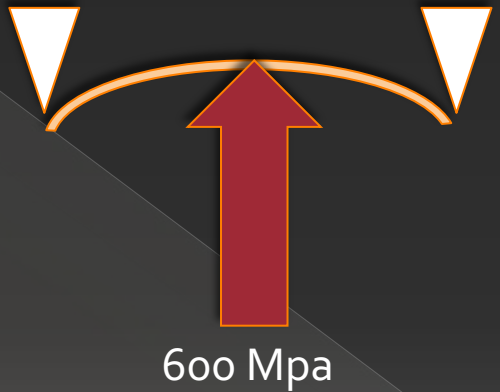

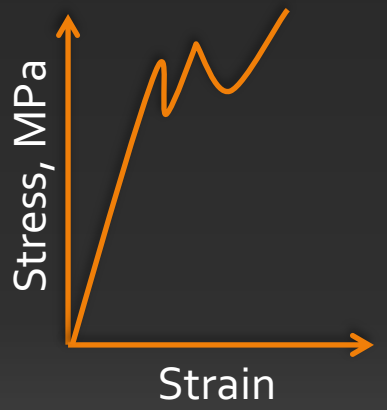

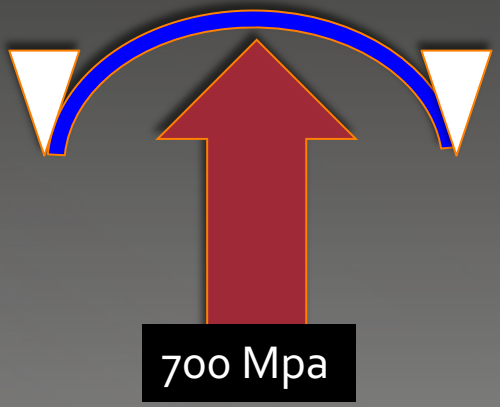

Alumina-zirconia composite fro hip joint prostheses

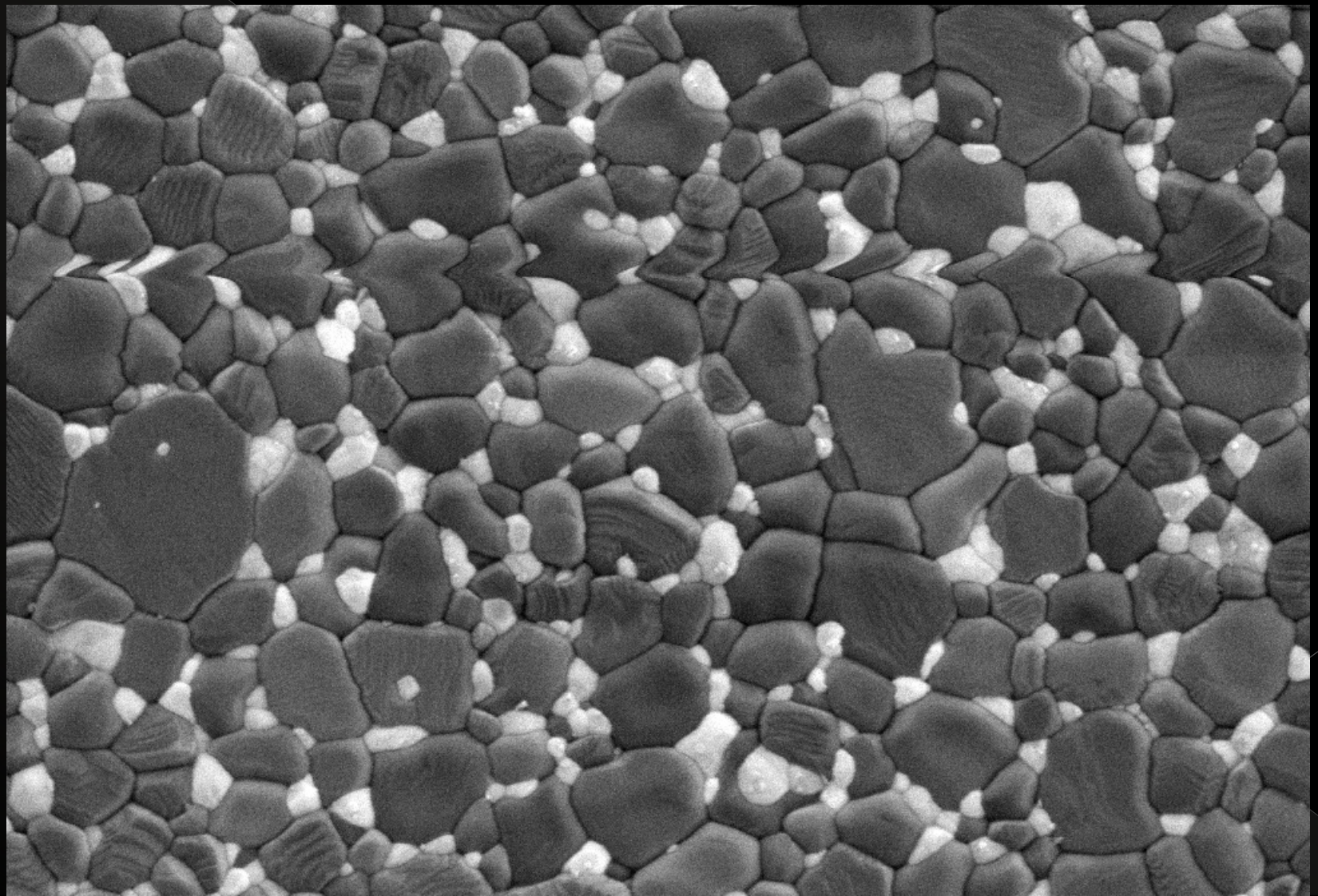

Increase of toughness usually leads to increase in weibull modulus

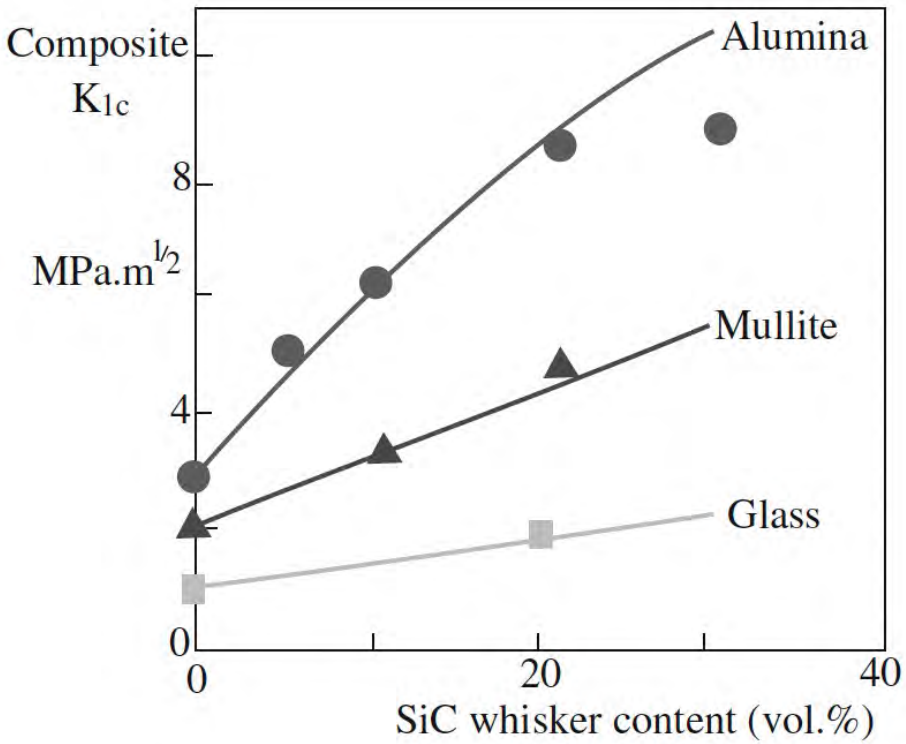

FIGURE 18.20 The effect of SiC whisker content on toughness enhancement in different matrices.

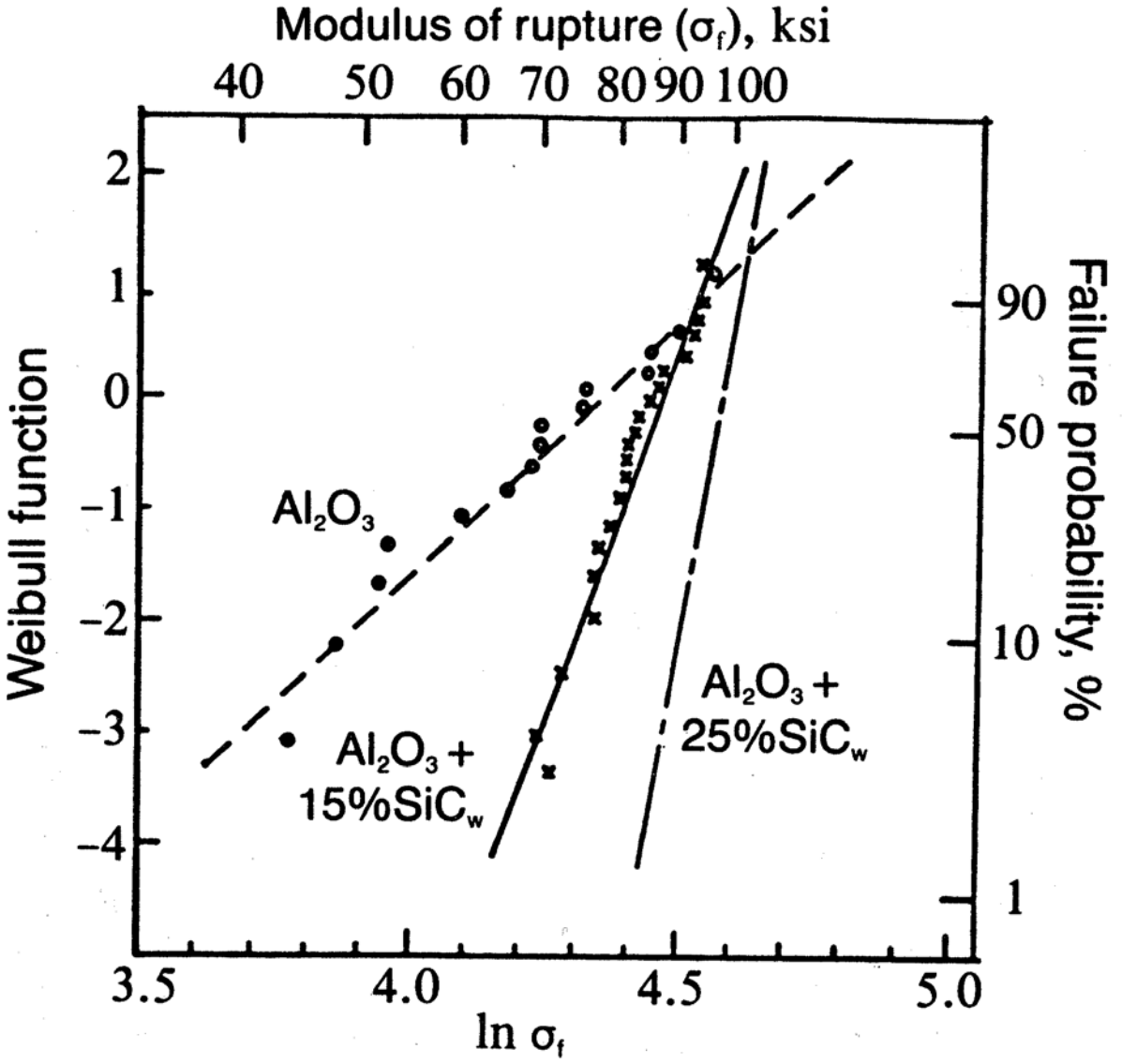

Figure 15.8 Example of the use of Weibull plots to compare material. (Adapted from J.F. Rhodes, H.M. Rootare, C.A. Springs, and J.E. Peters, data presented at the 88th Annual Meeting of the American Ceramic Society, Chicago, Ill. April 28, 1986.)

Raw materials for traditional ceramics

- Halloysite $Al_2Si_2O_5(OH)_4 \cdot 2H_2O$
- Montmorillonite $(Na,Ca)_{0,3}(Al,Mg)_2Si_4O_{10}(OH)_2 \cdot n(H_2O)$

- In genere prodotto di dilavamento feldspatico:
- Feldspati $(Ba,Ca,Na,K,NH_4)(Al,B,Si)_4O_8$

Clay Mineral Structure

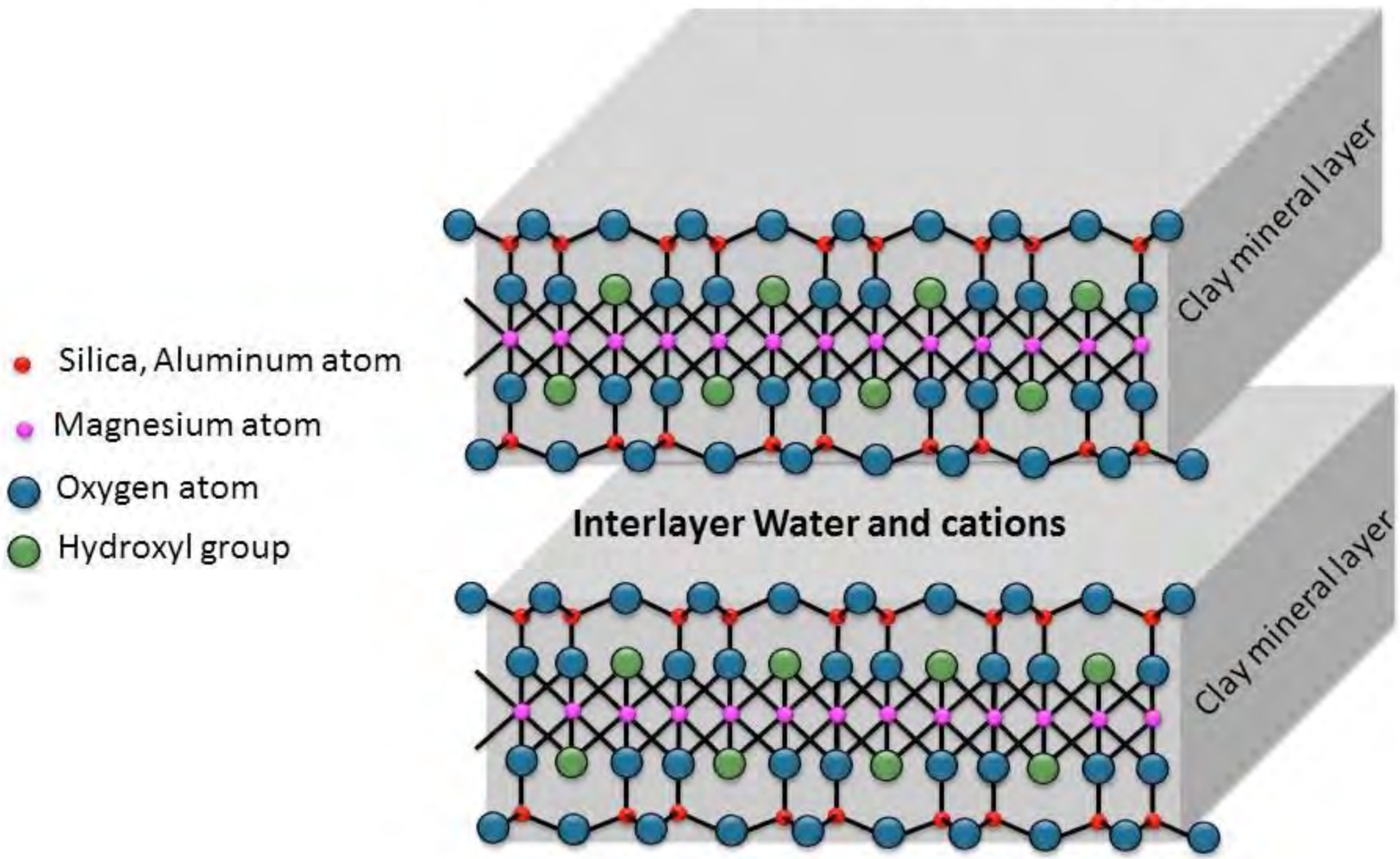

Montmorillonite

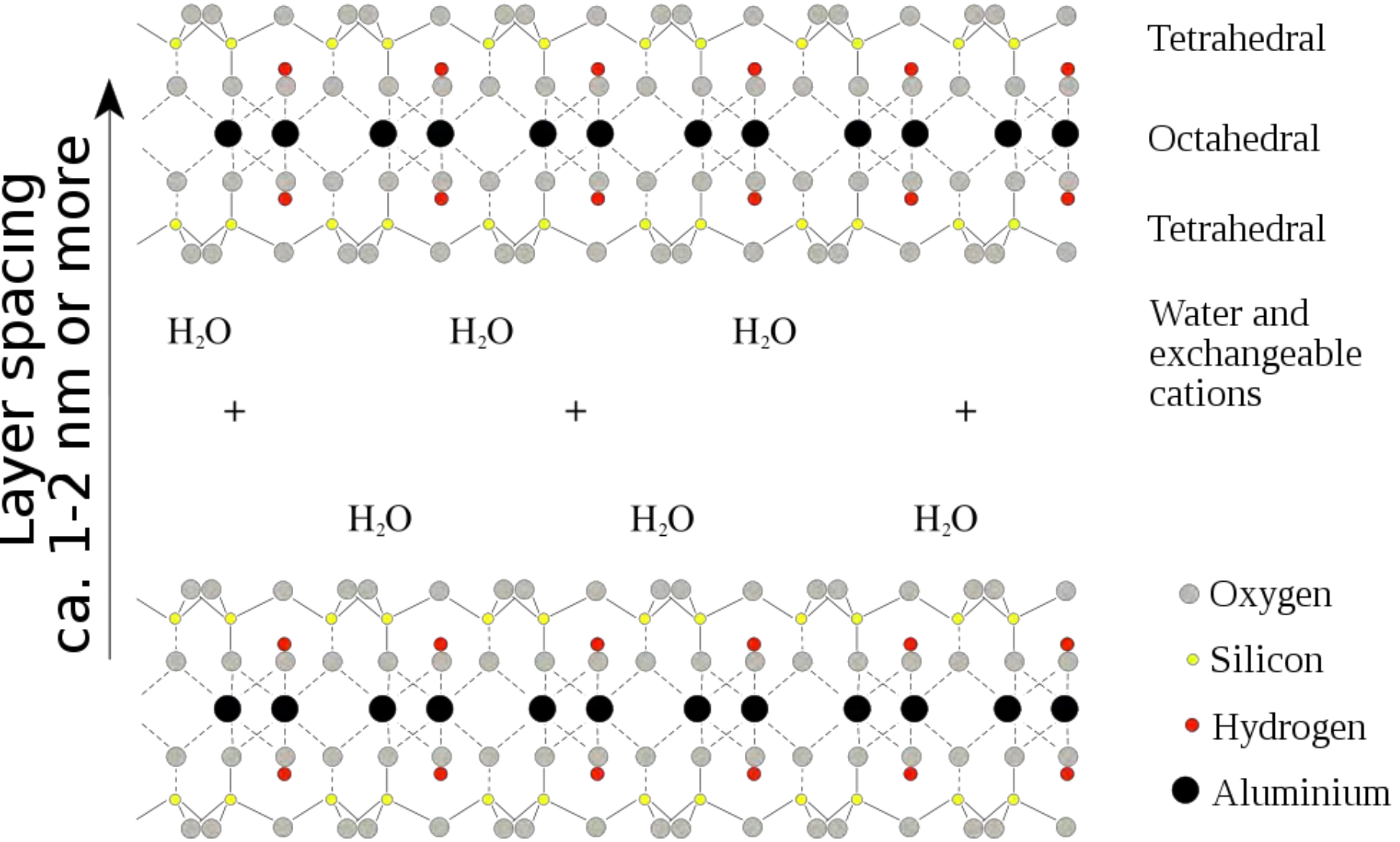

Clay quarry

Bayer Process: Al_2O_3 production

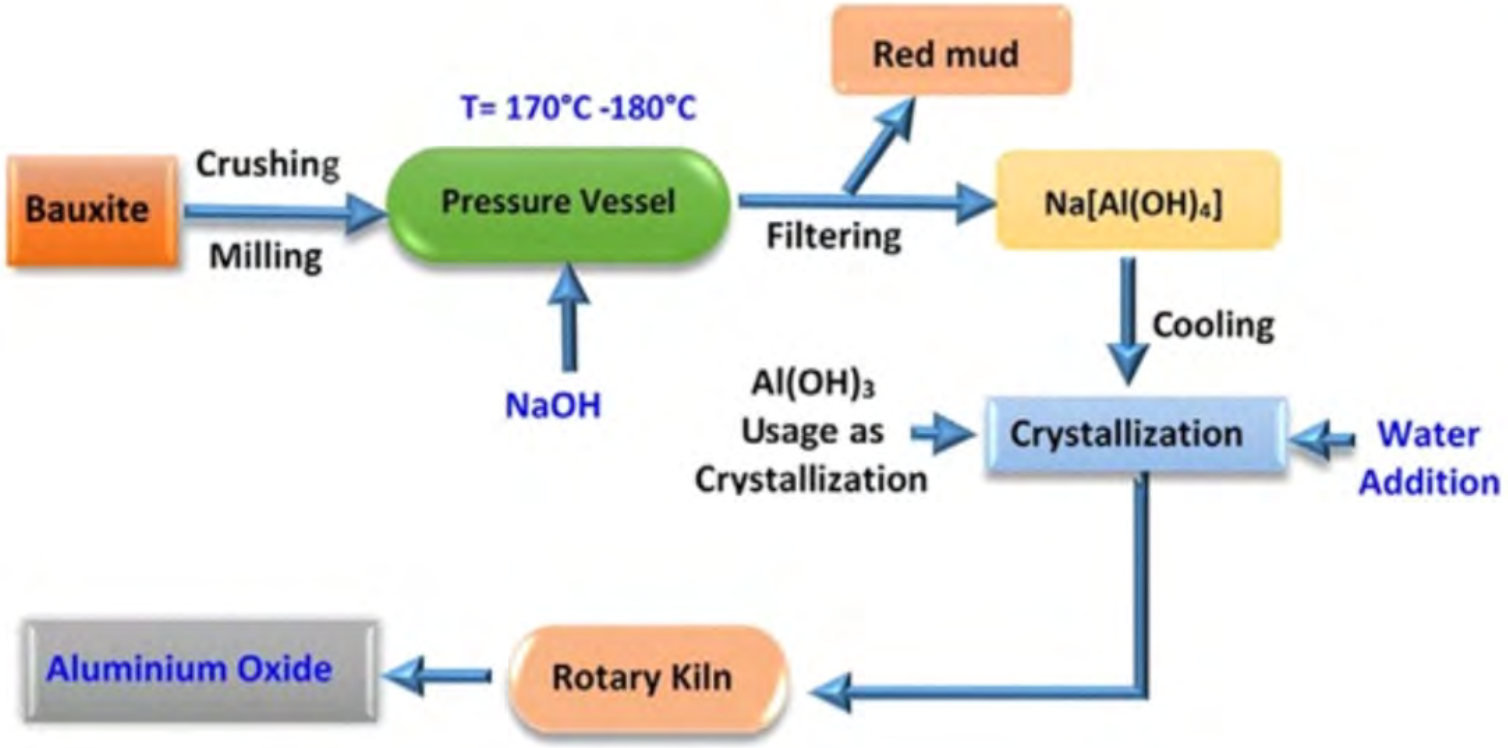

Bayer Process

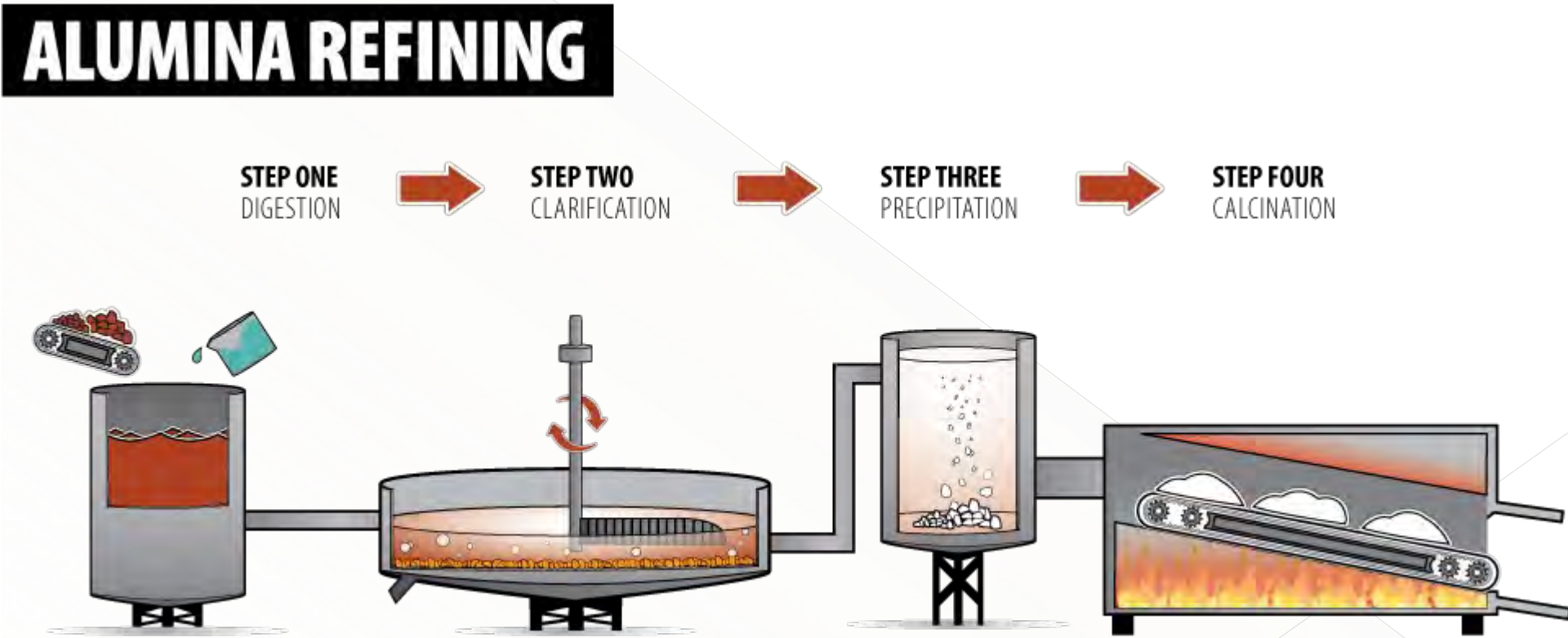

Zirconia powder preparation

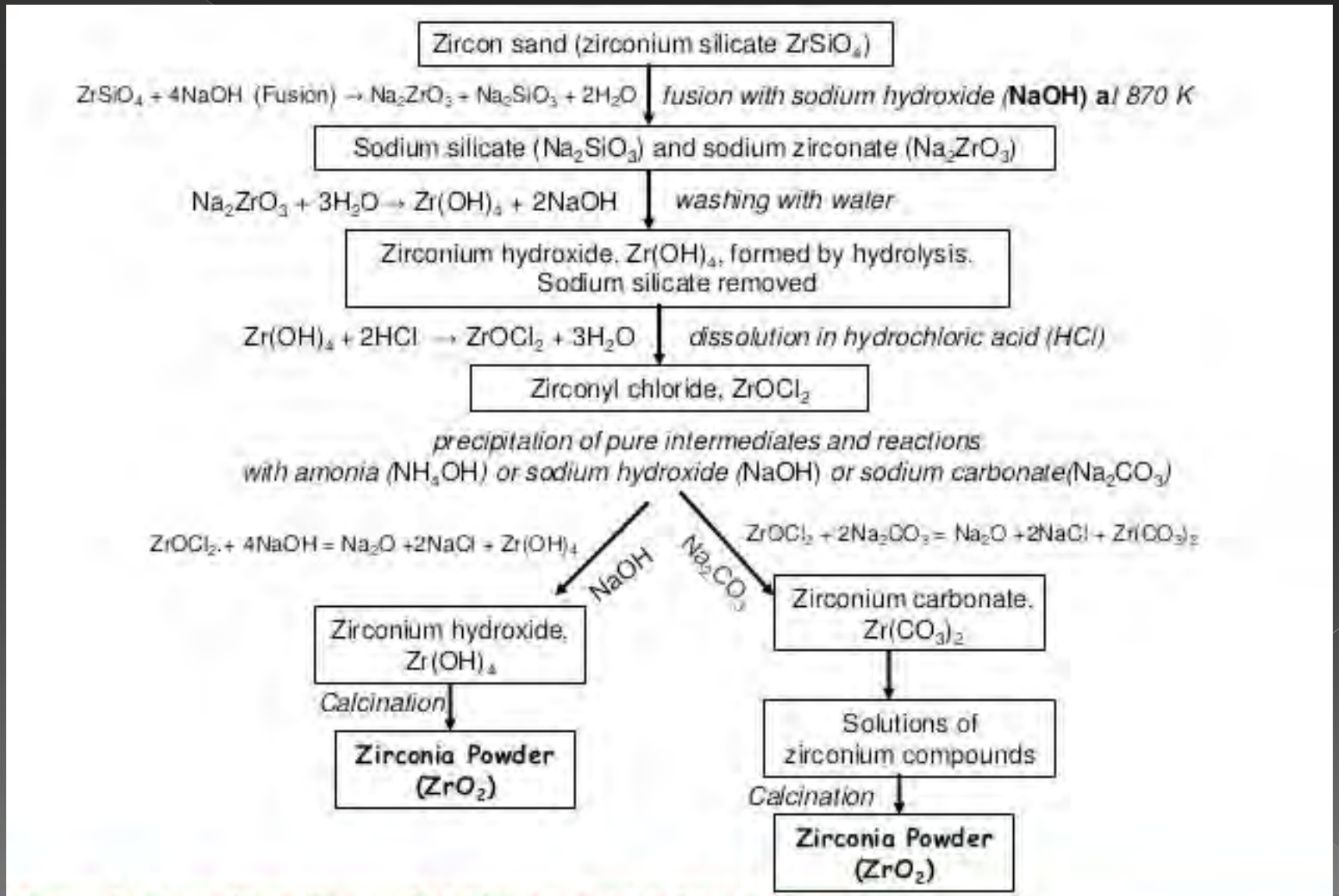

Mullite preparation

Raw Kaolin ($Al_2O_3.2SiO_2.2H_2O$)

I. Calcination

Metakaolin ($Al_2O_3.2SiO_2$)

Metakaolin($Al_2O_3.2SiO_2$)

II. Mixing

Alumina by combustion route

Alumina by solgel route

Commercial Alumina

III. Sintering

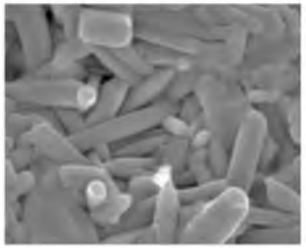

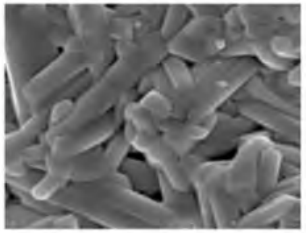

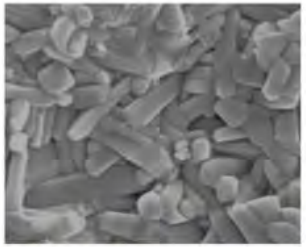

Mullite ($3Al_2O_3.2SiO_2$)

Acheson process: $3C + SiO_2 => SiC + 2CO$

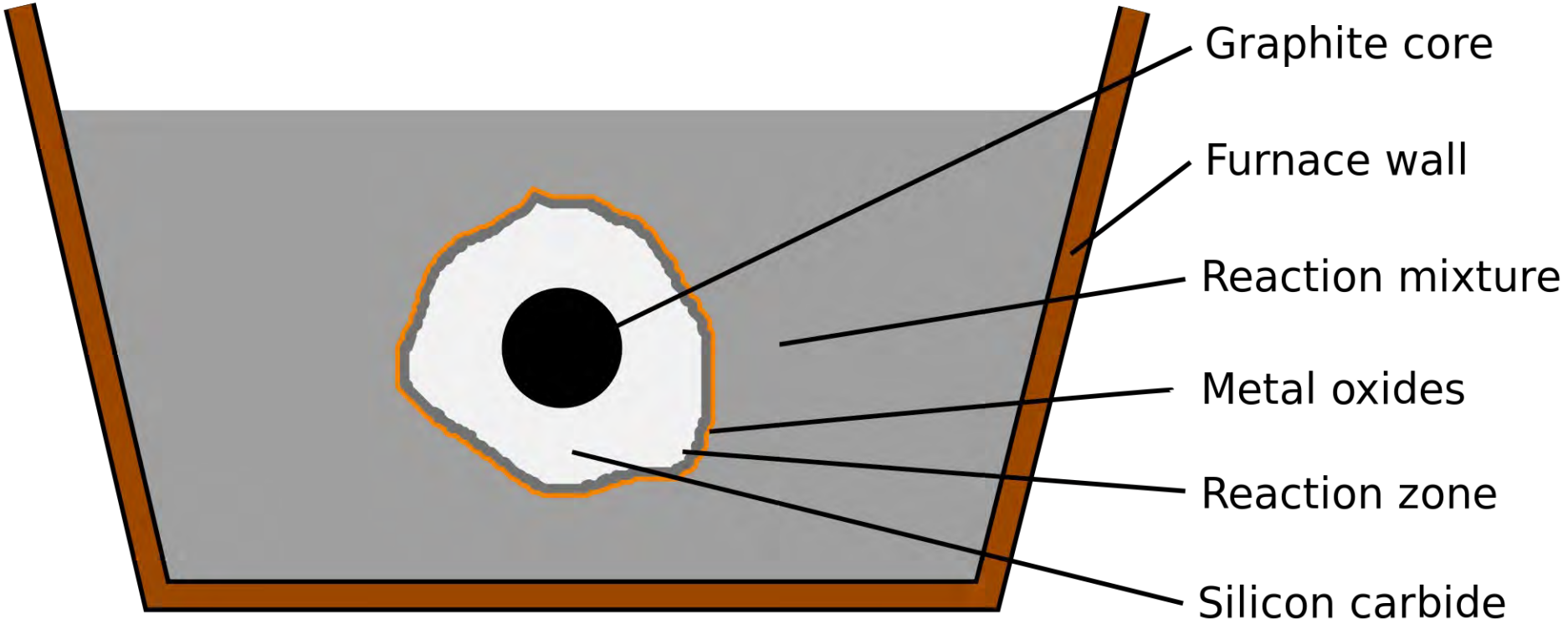

Sol-gel process outline

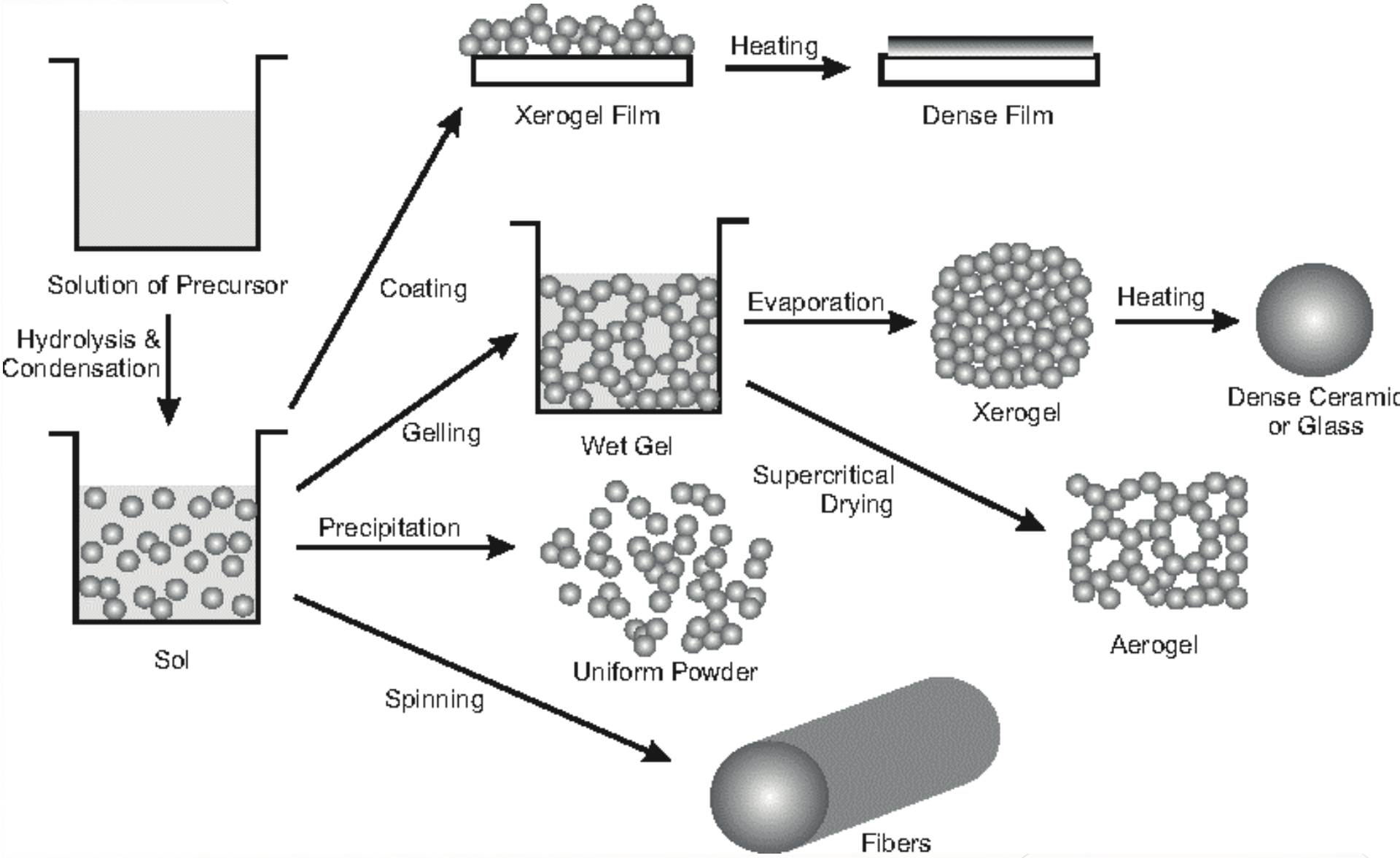

Sol-gel approach for ZnO coatings

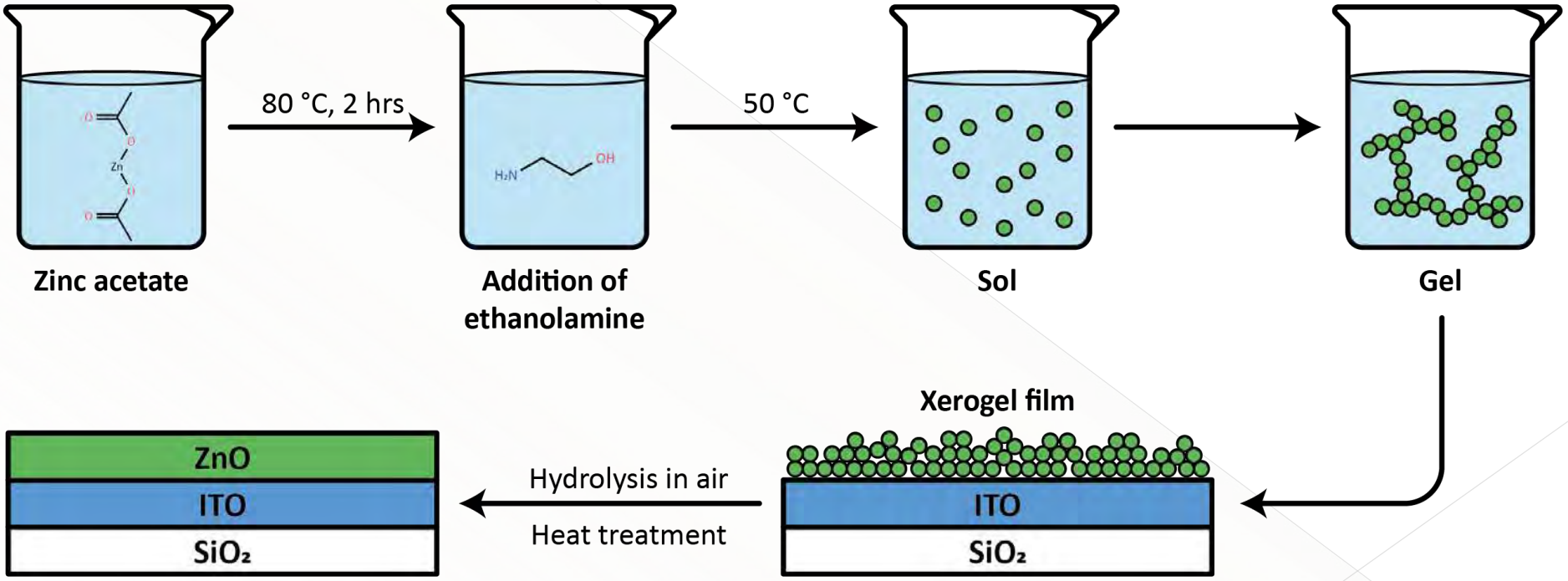

Measuring Particle Size

- Most common method uses screens of different mesh sizes
- *Mesh count* - refers to the number of openings per linear inch of screen
  - A mesh count of 200 means there are 200 openings per linear inch
  - Since the mesh is square, the count is equal in both directions, and the total number of openings per square inch is $200^2 = 40{,}000$
  - Higher mesh count = smaller particle size

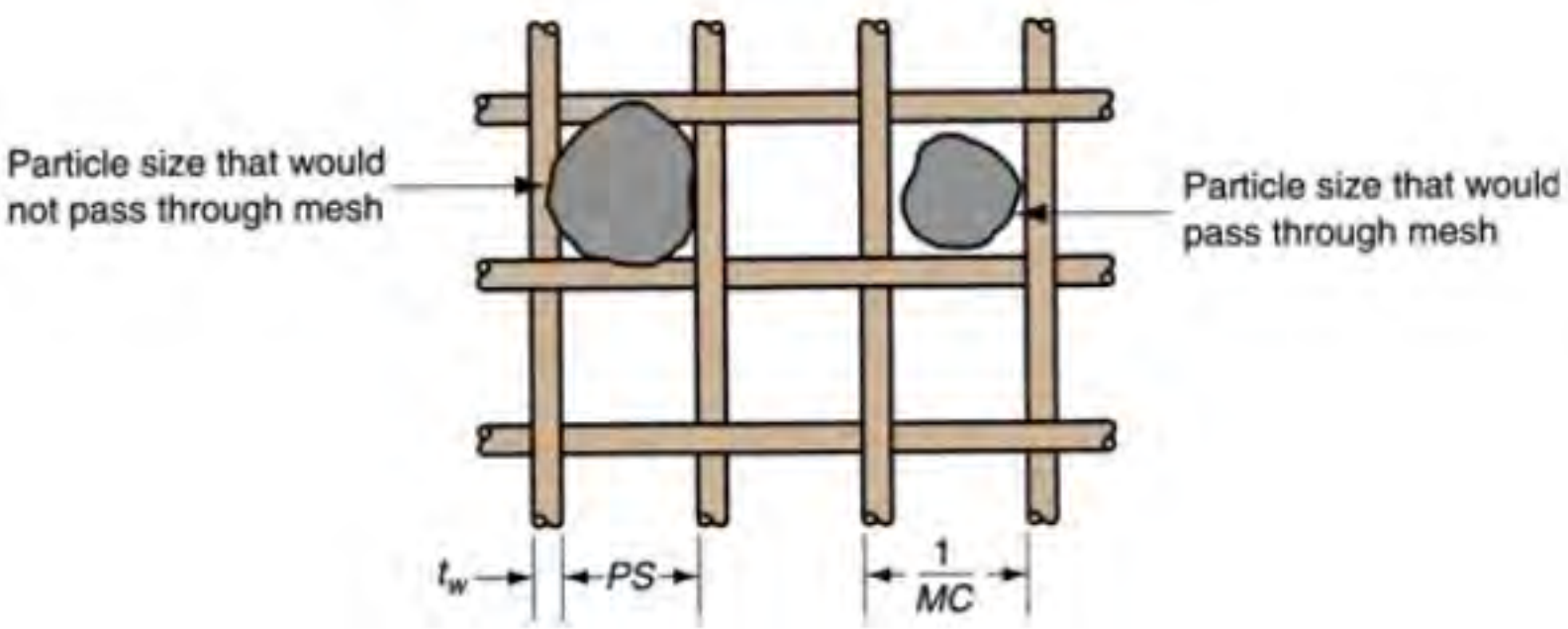
Particle size that would not pass through mesh
Particle size that would pass through mesh
t_w
PS
1
MC